Molecular orbital studies of chemisorption: hydrogen on nickel surfaces

Fassaert, D.J.M.

1976, Dissertation

Note:

To cite this publication please use the final published version (if applicable).

MOLECULAR ORBITAL STUDIES
OF CHEMISORPTION
hydrogen on nickel surfaces

D.J.M.Fassaert

MOLECULAR ORBITAL STUDIES
OF CHEMISORPTION

hydrogen on nickel surfaces

MOLECULAR ORBITAL STUDIES OF CHEMISORPTION

hydrogen on nickel surfaces

DOOR

DÉSIRÉ JOHANNES MARIA FASSAERT

GEBOREN TE NIJMEGEN

Aan mijn ouders

CONTENTS

Chapter IV

LCAO STUDIES FOR HYDROGEN CHEMISORPTION ON

Chapter I

INTRODUCTION

In the last few decades an increasing amount of research
on surface and adsorption phenomena, experimental as well as theoretical, has been published. The main motives for these studies can be
found in the development of semiconductor technology and in the
importance of heterogeneous catalysis for many chemical processes.
Recently, the so-called energy crisis has given a strong stimulus
to the fundamental research on surface phenomena in order to obtain
a better understanding of heterogeneous catalysis. For instance,
considerable interest exists in catalysts for the gasification or
liquefaction of coal, with simultaneous removal of sulfur and
nitrogen. The exploitation of oil shale and tar sands involves similar
problems. Also the environmental legislation in the USA has caused
an important impact on the research of catalysts suitable for
(automobile) emission control devices.

The understanding of processes which take place at solid
surfaces, has been hampered for a long time by the lack of accurate
and reproducible experimental data. The situation was much improved
by the advance of vacuum technology, which provided the possibility
of studying clean surfaces. Even more important was the development
of various photon, electron and ion spectroscopies, which are able to
elucidate the atomic and electronic structure of the surface layers
and to characterize atoms or molecules adsorbed on the surface. For
example, low-energy electron diffraction (LEED) is used to investigate the crystallographic structure of surfaces. The theory of LEED
has reached the stage where it is possible to deduce the position
of adsorbed atoms at the surface as well as the shape of the unit cell.

By Auger electron spectroscopy (AES) the chemical composition of clean or contaminated surfaces may be investigated. AES is often employed to check surface cleanliness. Recently, ion scattering has been used to analyze the surface layer and to determine the position of adsorbed atoms. Photoelectron spectroscopy (PES) provides information about the electronic band structure. Especially ultraviolet photoelectron spectroscopy (UPS) is sensitive to surface properties, such as the existence of surface states (see Chapter II) at clean surfaces. Another important application of UPS to surface studies lies in the detection of chemisorption (see below) levels. Similar information can be obtained from ion-neutralization spectroscopy (INS), which method is even more sensitive to the existence of chemisorption induced "resonance" levels. With these and many other techniques (electron energy loss spectroscopy, field emission or field ionization, work function measurements, ellipsometry, reflectance spectroscopy, flash, thermal or electron impact desorption) an increasing amount of data becomes available on (adsorbate-covered) single crystal surfaces which are structurally well-defined.

The theoretical approach to the surface problem has shown a similar evolution. For a long time, due to the loss of three-dimensional periodicity, theoretical models for surfaces had to remain much more primitive than the solid-state models used in studying bulk properties. The application of computational methods for molecules was not feasible, because of the need to use rather large clusters for describing the substrate effects appropriately. Rough concepts, such as the percentage of d-character in transition metals, or the use of rigid-band models, did not provide much more insight into the reasons for catalytic activity. The last few years have also shown a rapid increase in the number and quality of theoretical studies. The application of both solid-state techniques and molecular methods to the more complex surface problems has become possible by the development of advanced electronic computers. Also the availability of reliable and detailed experimental information from the techniques mentioned above, has stimulated the development of the theory. In conclusion, we can certainly state that, by the interaction between

theory and experiment, surface science has grown into a mature science by now.

In discussions concerning the relevance of surface science for a better understanding of heterogeneous catalysis, it is often pointed out that an important gap exists between these two fields of research: Surface scientists generally study adsorption or simple reactions on the surfaces of clean single crystals at low temperatures and pressures, while industrial catalysis is an enormously complex process involving high temperatures and pressures, many simultaneous reactions each consisting of many steps, and quite a number of impurities and additives. On the other hand, it may be argued that the investigation of adsorption and the simplest cases of catalysis on well-defined clean surfaces, can provide us with the necessary insight to identify those substrate properties which are important to heterogeneous catalysis, also under real reaction conditions. In this development of concepts applicable to catalytic processes theoretical tools are indispensable, since, in many cases, the experimental material does not yield direct information about the surface structure, adsorption bonding, etc., but requires the aid of some theoretical model. Moreover, the interpretation of the experimental data is often rather difficult so that qualitative discussions are not conclusive but rather extensive calculations are needed. Therefore, the strong increase in the theoretical interest in surface and adsorption phenomena, which appears from the large number of recent papers on these subjects (see the list of references in Chapter II) seems, to a large extent, justified.

In studying adsorption one may distinguish between <u>physical adsorption</u>, which results from Van der Waals forces and shows no transfer or "sharing" of electrons between the admolecule and the solid, and <u>chemical adsorption</u> or <u>chemisorption</u>, which arises from the transfer or sharing of electrons between the adsorbate and the adsorbent. The latter type of adsorption generally causes a significant

modification in the adsorbed species, which may even result in the breaking of some adsorbate bonds; the chemisorption bond has all characteristics of a common chemical bond. Physical adsorption is usually weaker than chemisorption and experimentally determined heats of adsorption are often used to distinguish between the two types. There are systems, however, in which this distinction is not clear.

In this thesis we describe some linear combination of atomic orbital (LCAO) studies on chemisorption, in particular models for (atomic) hydrogen adsorbed on different sites of the low index surfaces of nickel crystals. We intend to obtain a better under-standing of the adsorption binding with transition metals by this research.

The thesis is composed as follows. In Chapter II we review the various theoretical techniques used to investigate surface and chemisorption phenomena. We discuss most extensively the more recently developed methods which are suited to study adsorption energies, (local) densities of states, etc., employing models for real crystals. We show how the surface and chemisorption problem is being tackled from two sides, by solid-state physicists and by quantumchemists. The approximations inherent to the various approaches and their conse-quences are discussed. Furthermore, the practical feasibility, merits and drawbacks of the various techniques are indicated and a direct comparison of some methods is discussed. At the end of Chapter II, we pay attention to a few important concepts and interesting physical phenomena, such as virtual and split-off states, indirect interactions between adsorbed particles and dissociative chemisorption.

In surface and chemisorption theory one often employs a so-called resolvent or Green's-function technique. In most cases simple model crystals, for which the crystal problem can be solved analytical-ly, are studied. We present in Chapter III a numerical procedure developed in our group for applying the resolvent method to more com-plicated systems. Thus, it is possible to deal with more realistic models for transition-metal substrates, considering complete d-bands

as well as sp-bands. A few other recent (numerical) methods are also developing along these lines. Chapter IV contains our results from Extended Hückel molecular orbital calculations on finite periodic crystals and clusters. For further concise information we refer to the summaries of the reprinted articles and the introductory remarks with Chapter IV.

Finally, in the Appendix we give some model Hamiltonians originating from solid-state physics and expressed in second-quantized form, which are often employed in chemisorption theory, and we indicate which approximations are implicit in these Hamiltonians.

Chapter II

THEORETICAL MODELS FOR
SURFACES AND CHEMISORPTION

1. Introduction

Theoretical studies on surface phenomena began with the investigation of so-called surface states, which are one-electron states localized close to the surface with energies lying outside the band of the delocalized bulk states. Although the earliest model calculations were performed in the 1930's, the interest in these results was rather small, because there was a negligible technological motivation or experimental confirmation. The first major technological impetus for a more thorough investigation of surface states was provided by the rise of transistor technology during the late 1940's, since the presence of one-electron states in the forbidden band gaps may strongly modify the optical and electrical properties of semiconductors. Moreover, it has been suggested that the surface states play an important rôle in chemical adsorption by allowing the formation of chemisorption states, which are constructed from adsorbate and localized substrate levels. However, the current view is that a chemisorptive bond and chemisorption states may also be formed without the pre-existence of surface states.

Since the problems regarding the occurrence of localized states caused by impurities in the solid and by foreign atoms adsorbed on the solid resemble each other, the development in the theoretical research of impurity states of interest for properties of semiconductors and metals, and the study of chemisorption states important for chemical adsorption and heterogeneous catalysis, have run parallel. We shall restrict ourselves in this chapter, however, to a discussion of the theoretical research on surface and chemisorption phenomena.

6

One-dimensional crystals (chains)

In the earliest investigations the conditions for the occurrence of surface and chemisorption states in strongly parametrized one-dimensional semi-infinite or finite model crystals have been examined. Tamm [1] was the first to show that, under certain conditions, surface states appear. He used a Kronig-Penney model potential (a linear array of δ-function repulsive potentials) which was terminated at a free surface by a step discontinuity, and he matched the wave function and its derivative across the discontinuity. Shockley [2] examined the properties of a general one-dimensional periodic potential, terminated at its potential maximum by a step. He matched the wave functions across the discontinuity and showed that if the bulk bands were "crossed", surface states appeared in the forbidden band gaps when the surface perturbation was sufficiently small. These surface states came to be called "Shockley states" in contrast to the ones found in previous studies, which appeared above or below the bulk band (provided that the surface perturbation was sufficiently large) and which were afterwards called "Tamm states".

Many calculations of surface states have been performed by the tight-binding (TB) method*, which was used for the first time by Goodwin [3]. Various studies investigating the existence conditions and number of surface or chemisorption states, were performed on linear chains which represented mono-atomic and mixed crystals, with and without an adsorbed atom. A survey of these calculations until 1970 can be found in reference [4]. Also the effect of electron

---

* In its original concept, this linear combination of atomic orbitals (LCAO) procedure used an orthogonal set of orbitals with only one orbital per atom, considering merely nearest-neighbour interactions. In this way it is equivalent to the Hückel method known from molecular calculations. The definition has gradually evolved, however, employing more orbitals per atom and taking into account nonorthogonality and more extensive interactions.

correlation [5,6,7] has been examined by means of chain models, as well as adatom-adatom interaction [8,9,10] and chemisorption on supported metals [11].

Three-dimensional crystals

A very common procedure for studying the surface properties of three-dimensional crystals within the LCAO formalism is known as the Green's-function or resolvent technique [4,12]. The method was initially developed to investigate the influence of impurities and defects on the one-electron states in periodic crystal lattices and has been applied by Koutecký [13] to establish the existence conditions of localized states on the (ideal) surfaces of three-dimensional crystals. The properties of chemisorption states, due to the interaction of a foreign atom with a crystal, have also been studied [8,14]. Koutecký and Tomášek [15-19] examined the surface and chemisorption (for the case of adsorption of a complete hydrogen layer) states for the low index planes of semi-infinite diamond- and sphalerite-type crystals. Furthermore, Tomášek [20,21] investigated the effect of electron correlation in diamond-like crystals by using an alternant molecular orbital (AMO) approach. A survey of these semiconductor calculations, which could be performed analytically by introducing several simplifications, such as interactions between specific hybrids only, may be found in reference [22]. Later, Freeman [23] showed how the resolvent method can be applied to more sophisticated models by performing numerical calculations. Levine and Freeman [24] studied by this technique the effect of surface reconstruction upon the energies of the surface states of zinc blende. Recently, Tomášek and Mikušík [25] have obtained Shockley surface states for the (110), (010) and (111) planes of bcc iron.

A second technique which has often been used to investigate surface states in three-dimensional crystals, was developed by Heine [26-28]. In this method the one-electron wave functions (and their normal derivatives) inside the crystal are matched to the solutions of the one-electron Schrödinger equation in the vacuum outside the

surface. The surface plane is defined by an abrupt potential change be-
tween the perfectly periodic potential inside and a constant potential
outside the crystal. Since the energies of the (Shockley) surface
states lie inside the band gaps, the (real) eigenvalues of the crystal
Hamiltonian must also be determined for complex wave vector $\vec{k}$; these
are the so-called evanescent solutions which possess a purely imaginary
$k_{\perp}$, the component of $\vec{k}$ perpendicular to the surface. For each $\vec{k}_{//}$, the
(unchanged) component of the wave vector parallel to the surface plane,
localized states exist when a match of these eigenfunctions and their
normal derivatives to the appropriate vacuum wave functions is possible.
The method described here has been used to study surface states on low
index planes of semiconductors [29-34], simple metals [35] and d-band
metals [36,37]. It is very difficult to investigate surface recon-
struction or chemisorption by the direct matching procedure, since this
would require an interface region in which the potential varies
gradually instead of abruptly at the surface plane.

Many other calculations on surface states have been per-
formed, using a large variety of different techniques; an excellent
review may be found in reference [4]. In all the earlier approaches
only existence conditions and energies of pure surface or chemisorption
states with wave functions localized at the surface and energies out-
side the crystal bulk bands have been calculated. However, most one-
electron states remain within the crystal bands and do not become
localized, but they are nevertheless affected by surface formation and
adsorption. As Koutecký [12] pointed out, these bulk or volume states
should be included in order to obtain surface or adsorption energies
and many other important properties.

Recent developments

In the last few years rapid development in the direction of
more quantitative calculations on more realistic models, for example
the transition metals, have become possible by the availability of
high-speed and large-memory computers. From two sides the surface and
chemisorption problem is being attacked now: by a "solid-state"

approach and by a "molecular" approach. The first group of techniques generally starts from solid-state band calculations on infinite periodic crystals, which are subsequently reduced to semi-infinite crystals with a surface at which adsorption can take place. The second class of methods is of the molecular type. Assuming that the effects of surface and adsorption are rather localized, one applies molecular orbital methods to a finite cluster of atoms, possibly interacting with one or more adsorbed atoms.

Since no encompassing review is available, we shall discuss in the following sections the more recently developed methods which are suitable to calculate (local) densities of states, work functions, and cohesion, surface and chemisorption energies. A survey of the previous calculations can be found in references $[4,9,12,22,38,39]$. We shall not deal with physical adsorption and only in passing discuss ionic adsorption, where the atomic structure of the solid is less important and where continuum models are often used, but we shall chiefly pay attention to theoretical treatments of chemisorption with mainly covalent bonding.

In the next sections, the solid-state and molecular approaches will be discussed successively. Further, we shall concisely consider calculations on thin films or slabs, which are infinite in two directions but consist of a limited number of layers.

2. Semi-infinite crystal models

Several "solid-state" methods have been developed to study the surface and adsorption effects on the electronic properties of substrate and adsorbate. In all cases semi-infinite crystal models are used, but the way in which the solid is actually taken into account differs strongly. In the classical image force model, the solid is considered as a continuous polarizable medium in which image charges are induced by adsorbed particles. This model is often used for the investigation of alkali atoms adsorbed on metals (section 2.1). In the "jellium" model the (continuous) solid is explicitly taken into ac-

count. It is represented by an inhomogeneous electron gas in a uniform
background of positive charge. The atomic structure is sometimes intro-
duced by means of some lattice pseudopotential which is dealt with
perturbationally (section 2.2). It is preferable, however, to consider
directly the effects of the pseudopotential. This may be done in two
ways. Firstly, the wave equation can be solved directly in the
field of the pseudopotential, either by the surface-Green's-function
method (section 2.3) or by a self-consistent scattered wave method
(section 2.4). Secondly, one can employ an expansion of the wave
function into localized basis functions. Some of the most powerful
methods to deal with the surface and chemisorption problem rest on this
technique and we shall especially pay attention to them.

In the LCAO formalism the one-electron wave functions are ex-
panded in localized basis orbitals, while the valence-bond (VB) method
constructs N-electron states from these localized orbitals. It is very
easy to incorporate local potential perturbations in both procedures.
For example, the LCAO method often works with the one-electron Green's
function, taking optimally advantage of the solution of the unperturbed
problem (e.g. the infinite crystal). In general, one may discern three
levels of approximation in the expansion technique: (i) The tight-
binding methods (section 2.5). These do not explicitly take into ac-
count electron repulsion or correlation[*] effects. (ii) The effective
one-electron Hartree-Fock type of methods (section 2.6). Allowance is
made in a self-consistent manner for electron repulsions on one or a

---

[*] It should be noted that in solid-state physics correlation is mostly
understood as any effect that originates from an explicit considera-
tion of the electron-electron repulsions. This departs from the custom
in quantumchemistry or molecular physics, where the correlation energy
is defined as the difference between the experimental energy (corrected
for rotational, vibrational and relativistic terms) and the independent-
particle (usually Hartree-Fock) energy. We shall employ the definition
common to quantumchemists.

few atoms only, which are directly involved in the chemisorption bond. (iii) Many-body approaches, based on a Heitler-London (valence-bond) kind of scheme (section 2.7). Here, also correlation effects are taken into account. In section 2.8 we shall compare the various expansion techniques and discuss their respective merits. Finally, in the last two sections attention is paid to some phenomena which play an important rôle in chemisorption studies, namely the occurrence of virtual and split-off states and the indirect interaction between adsorbed atoms.

2.1 The image force model

An approach to chemisorption, which is especially suited to investigate the (mainly ionic) alkali atom adsorption, stems from Gurney [40]. He pointed out that the valence level of an atom experiences a natural broadening as a result of the uncertainty principle and the finite lifetime of the atomic state, when the atom is allowed to interact with a metal surface. The degree of ionization and hence the strength of the dipole moment per adatom, is determined by the fractional occupation of this broadened level, which in turn depends upon the position of the state relative to the Fermi energy of the solid.

This effect of the interaction of an alkali atom with a metal on the originally sharp atomic ns-level, resulting in a so-called virtual level (see section 2.9), has been calculated by Gadzuk [41]. The interaction of the alkali atom with the metal was represented by the classical image potential. So, the effective one-electron Hamiltonian contained an attractive interaction between the electron and its image charge and a repulsive interaction with the image of the positive ion core, besides the direct electron-ion attraction. First-order Rayleigh-Schrödinger perturbation theory was applied to obtain the shift of the discrete ns-level, while the natural broadening of the level was calculated by time-dependent perturbation theory. Later, Gadzuk et al. [42] examined the alkali level broadening and shift by

Anderson's model [43] which has also been used to study covalent ad-
sorption (see section 2.6). They checked for the occurrence of magnetic
effects by investigating the occupancy of and the splitting between the
virtual spin-up and spin-down levels. Although they found a nonmagnetic
solution, spin correlations did have a definite effect on the position
of the energy levels and thus on the charge of the adsorbed atom.
Gadzuk et al. assumed that the chemisorption energy consisted of two
separate parts: a covalent and an ionic component. The adatom charge
and the covalent portion of the binding energy were obtained from
Anderson's model, while the major (ionic) contribution to the adsorp-
tion bond was calculated by the image force method. Recently, Cini [44]
has shown that both the covalent and ionic energies may be found by
the solution of a single Hamiltonian of the Anderson form. The electro-
static terms are included by redefining the adatom level position and
the electron repulsion term.

Muscat and Newns [45] studied the changes in work function
with surface coverage of adsorbed alkali atoms on a (transition-)metal
substrate. They considered a single atom, taking into account the other
adatoms through their electrostatic field only. Coupling between the
ns and np_z alkali valence orbitals and the eigenstates of the semi-infi-
nite metal introduced lifetime broadening and hybridization of the ad-
sorbate valence levels. The electrostatic interaction between the dif-
ferent atoms and their images pushed down the adatom orbitals as the
coverage increased, and polarized the adatom valence shell.

2.2 The jellium model

In solid-state physics the jellium model is commonly used to
study the (surface) properties of simple metals. Many of the semi-in-
finite crystal methods which are reviewed below, are chiefly concerned
with the interactions between the electrons and the ionic lattice,
rather than those among the electrons. However, the present method is
based on an electron gas type of analysis and disregards details of
the interaction between the (conduction) electrons and the lattice,

focusing instead on the electron-electron interaction. In this so-
called "jellium" model, introduced by Bardeen [46], the solid is re-
presented by a system of free electrons in a semi-infinite uniformly
smeared-out background of positive charge, which replaces the three-
dimensional lattice of ions and terminates abruptly at the surface.
The electronic charge distribution and the potential may then be
obtained self-consistently by applying the theory of an inhomogeneous
electron gas, which has been introduced by Hohenberg, Kohn and Sham
[47,48] and is called the density-functional formalism. The central
quantity in this theory is the electron density, whose basic rôle is
established by the theorem that the properties of the system, in
particular the ground state energy, are functionals of this density
only. The theory includes exchange and correlation effects. Recently,
a review of the formalism has been given by Lang [49].

Using the jellium model and the density-functional formalism,
Bennett and Duke [50] and Smith [51] have performed approximately
self-consistent calculations in order to obtain electronic charge
distributions, work functions and surface potentials for several
metals. These kind of studies yield for the work function good quali-
tative agreement with experiment over a wide range of densities. The
calculated surface energy, however, is completely wrong for higher-
density metals [52]. Lang and Kohn [52,53] reintroduced in the uni-
form-background model the actual ionic structure by using perturbation
theory. They calculated the first-order contributions of the lattice
pseudopotential to the surface energy and the work function. The
results were found to be in rather good agreement with experiments
over the entire range of metallic densities.

Lang [54] used the density-functional formalism to investi-
gate changes in the work function due to the adsorption of alkali
atoms. Representing the substrate ionic lattice by a semi-infinite
uniform positive background, he replaced the array of adsorbate ions
by an adjoining uniform positive slab. Changes in coverage were
treated as changes in the density or thickness of the adsorbate slab.
So, his model was not appropriate to treat low coverages. Recently,

14

a few calculations have been performed which deal with single atom
adsorption. The adatom was represented by an external point charge,
which disturbed the metallic surface. Ying et al. [55] investigated
H chemisorption, while Huntington et al. [56] studied the adsorption
of a Na atom. In both cases some approximations were introduced in the
density-functional formalism. A self-consistent, exact calculation for
single atom chemisorption of H, Li and O on a uniform-background sub-
strate has been carried out by Lang and Williams [57]. Gunnarsson et
al. [58] were able to compare various adsorption sites for the chemi-
sorption of H on an Al(100) surface by reintroducing the effects of
the lattice through a weak pseudopotential.

The previously discussed model for the investigation of
surface and chemisorption phenomena is a reasonable approximation for
the simple metals, i.e., those metals which are known to be free-elec-
tron like in the bulk. However, the model is not very realistic for the
properties of semiconductors or transition metals.

2.3 The surface-Green's-function method

As we have mentioned in the introduction, one of the
methods of calculating surface states is based on matching the wave
functions at the surface boundary. Garcia-Moliner and Rubio [59,60]
developed a new approach to the matching problem, in which the correct
boundary conditions are automatically incorporated into the formalism
and the need to perform a previous calculation of the band structure
for complex wave vectors $\vec{k}$ is eliminated: it is sufficient to know
the band structure of the infinite crystal for real $\vec{k}$ only. Moreover,
it is not necessary to assume an abrupt termination of a perfectly
periodic potential at a geometrical plane.

One starts with a Green's function which contains the
spectrum of the system without a surface and replaces the change in
boundary conditions, which occurs in creating a surface, by an equiv-
alent perturbation. So, the method is conceptually similar to the re-
solvent procedure in the LCAO techniques, where a matrix representa-
tion of the resolvent is used (e.g. section 2.5). It is easy to ob-

tain the surface Green's function (S.G.F.), the restriction of the semi-infinite crystal resolvent to the surface region, from the Green's function for the infinite medium. Knowledge of the S.G.F. makes it possible to calculate the local density of states and the charge density at the surface. The procedure can be applied to all systems consisting of two media which are in contact through an interface. Moreover, it may easily be extended to systems with two interfaces in order to study surface reconstruction, thin films or layers adsorbed on a semi-infinite crystal. The method is rather cumbersome, however, and up to now only a few (simplified) model systems have been calculated [61-65]. Using a simple one-dimensional model, Flores et al. [63] showed that the results of surface state calculations are strongly sensitive to the width of the interface which connects the disturbed periodic crystal potential to the vacuum level. Elices et al. [64,65] applied the surface-Green's-function method to a pseudopotential calculation of the surface band structures of (111) diamond and zinc-blende faces.

2.4 A self-consistent pseudopotential method

As we have seen, the jellium model for metal substrates does not take into account the solid crystallinity. Hence, it is doubtful whether it can properly describe the localized covalent chemisorption bonding which depends on the atomic structure of the surface. Boudreaux [66] has emphasized the importance of considering both the influence of electron-electron exchange and correlation as well as the effect of solid crystallinity in discussing the interaction of a foreign atom with a plane. He gave an expression for the potential felt by an electron near a crystal surface, but did not present a prescription for calculating wave functions which satisfy the relevant boundary conditions. Appelbaum and Hamann [67] developed a procedure for carrying out self-consistent calculations in which the three-dimensional lattice is included nonperturbationally. In this method, a plane is chosen inside the solid at some distance from the surface such that on the inner side of this plane the solid is indistinguish-

able from the bulk. Such a choice can always be made consistent with the degree of over-all accuracy one desires. In the bulk solid, the solutions are appropriate linear combinations of degenerate Bloch functions. These must smoothly join solutions of the wave equation in the region outside the plane, consisting of the last few atomic layers and the vacuum. In this surface region, where the wave functions retain periodic symmetry in the parallel direction, the Schrödinger equation is solved by a numerical integration technique. The core electrons are supposed to undergo essentially no modification. The potential felt by a valence electron consists of a term from the positive-ion cores and a self-consistent potential due to the other valence electrons. The contribution of the ionic cores is approximated by a superposition of identical local model potentials, while the valence-electron contribution is calculated self-consistently using a local approximation for the exchange potential. In order to obtain the (valence-electron) charge density in this procedure, wave functions must be calculated corresponding to a mesh of points in the Brillouin zone.

By this method Appelbaum and Hamann were able to perform self-consistent calculations, for the first time, on the surface properties of semiconductors. They obtained the surface potential, charge density and energy spectrum of the ideal and relaxed or reconstructed Si(111) and (100) surfaces [68-71]. Moreover, they studied the chemisorption of a monolayer of H on the (111) surface of Si and calculated the bulk and local density of states [72]. To determine the charge density they used a two- or four-point surface Brillouin zone (SBZ) scheme.

The method is appropriate for simple metals and semiconductors, but is not directly applicable to transition metals and their compounds [67].

2.5 Tight-binding methods

Many of the solid-state techniques which we have reviewed in the preceding sections, are not very suitable to study the specific properties of transition metals. Since transition metals contain, in

addition to the conduction electrons, a set of rather localized d-electrons, one usually has to resort to different techniques. Some simple models based on the renormalized-atom approach [73] have been used to obtain the bulk and surface densities of states. In this way Levin et al. [74] and Fulde et al. [75,76] have investigated the magnetic properties of nickel surfaces. We shall discuss in this and the next sections some methods which are particularly useful to study surface and chemisorption phenomena in case of transition-metal substrates.

In the tight-binding approximation as applied in this section, one employs usually an orthogonal, localized atomic orbital (AO) or Wannier function basis set. The effective one-electron Hamiltonian H is given by means of a matrix $\underline{H}$, defined with respect to this basis. The matrix elements are the self-energies of the localized orbitals and the hopping or resonance integrals β for nearest-neighbour (sometimes next-nearest-neighbour) interactions. Often, one considers only one orbital per atom and chooses the energy of the free substrate-atom as the energy zero. We may define a one-particle Green's function G corresponding to the effective one-electron Hamiltonian H as follows:

$$G(\varepsilon) = \lim_{s \to 0} \left[(\varepsilon + is) I - H \right]^{-1} , \tag{1}$$

with ε being the energy variable and I the unit operator.

As we have mentioned in the introduction, the Green's-function or resolvent method may be used to obtain the existence conditions and energies of localized surface and chemisorption states. It is also possible to calculate by this technique the surface and chemisorption energies and charge distribution without explicitly solving for the one-electron energies and wave functions. This is due to a direct relationship between the (local) densities of states and the diagonal matrix elements of the Green's function. Considering only one orbital per atom, the average density of states per atom reads:

$$\rho(\epsilon) = -(\pi N)^{-1} \text{ Im Tr } \underline{G}$$

$$= -(\pi N)^{-1} \sum_i \text{Im} \langle \phi(\vec{r} - \vec{R}_i) | G | \phi(\vec{r} - \vec{R}_i) \rangle \tag{2}$$

$$= -(\pi N)^{-1} \sum_n \sum_{\vec{k}_{/\!/}} \text{Im} \langle a(n, \vec{k}_{/\!/}) | G | a(n, \vec{k}_{/\!/}) \rangle \quad ,$$

where N is the total number of atoms. We have given the above expression in terms of an atomic orbital basis $\{\phi(\vec{r} - \vec{R}_i)\}$ and of a layer orbital basis $\{a(n, \vec{k}_{/\!/})\}$ when we have a crystal (with a surface) which is periodic in two directions (see below). The local density of states at a particular lattice site $\vec{R}_i$ is defined by:

$$\rho_i(\epsilon) = -\pi^{-1} \text{Im} \langle \phi(\vec{r} - \vec{R}_i) | G | \phi(\vec{r} - \vec{R}_i) \rangle \quad , \tag{3}$$

and the local density of states per atom for the $N_{/\!/}$ atoms lying in plane n by:

$$\rho_n(\epsilon) = -(\pi N_{/\!/})^{-1} \sum_{\vec{k}_{/\!/}} \text{Im} \langle a(n, \vec{k}_{/\!/}) | G | a(n, \vec{k}_{/\!/}) \rangle \quad . \tag{4}$$

It is straightforward to generalize these expressions in case of more orbitals per atom.

In the following we shall start with a discussion of the Green's-function technique developed by Kalkstein and Soven. Many of the calculations carried out by this method, which requires direct calculation of the Green's function, have employed simplified models like cubium. Next, we shall discuss two related approaches, appropriate for calculations on real transition-metal systems. Both techniques, developed respectively by Cyrot-Lackmann and coworkers (the method of moments), and by Haydock, Heine and Kelly (the recursion method), use a continued-fraction expansion of the Green's function, which is truncated at some level of approximation.

a) The Green's-function technique

We create a semi-infinite crystal by "cleaving" a perfect (infinite) crystal along an imaginary plane in some crystallographic direction. In order to obtain the density of states, the Green's function for the cleaved crystal has to be calculated. Let H_o and H be the effective one-electron Hamiltonians for the perfect and cleaved crystals, respectively, and let G_o and G be the corresponding Green's functions. Then G is given in terms of G_o and the perturbation $V = H - H_o$ by Dyson's equation [77]:

$$G = G_o + G_o V G \quad . \qquad (5)$$

Two different types of terms enter into V. Since H is the Hamiltonian of the cleaved crystal, it can have no matrix elements between localized functions centred on different sides of the cleavage plane. This statement implies that

$$<\phi(\vec{r}-\vec{R}_i)|V|\phi(\vec{r}-\vec{R}_j)> = -<\phi(\vec{r}-\vec{R}_i)|H_o|\phi(\vec{r}-\vec{R}_j)> \quad , \qquad (6)$$

if $\vec{R}_i$ and $\vec{R}_j$ are lattice sites separated by the cleavage plane. The second contribution to the perturbation V is a consequence of the change in the self-consistent field near the surface. If the difference between the potentials in the cleaved and uncleaved crystals is denoted by U, then V will have the additional matrix elements

$$<\phi(\vec{r}-\vec{R}_i)|V|\phi(\vec{r}-\vec{R}_j)> = <\phi(\vec{r}-\vec{R}_i)|U|\phi(\vec{r}-\vec{R}_j)> \quad ., \qquad (7)$$

where $\vec{R}_i$ and $\vec{R}_j$ refer to positions on the same side of the cleavage plane.

The calculations are facilitated by the observation that the cleaved crystal preserves lattice translational symmetry parallel to the surface. Assuming a single (s-like) orbital on each centre, we exploit this fact by transforming the set of localized orbitals $\phi(\vec{r}-\vec{R}_i)$ into a set of layer orbitals $a(n,\vec{k}_{//})$, which are two-dimensional Bloch functions localized near the nth crystallographic plane; $\vec{k}_{//}$ is a

wave vector parallel to the cleavage plane. The conservation of the two-dimensional translation symmetry is reflected in the relation

$$\langle a(m,\vec{k}_{//})|G|a(n,\vec{k}'_{//})\rangle = \delta_{\vec{k}_{//},\vec{k}'_{//}} G(m,n,\vec{k}_{//}) \qquad (8)$$

for the matrix elements of the Green's function in the layer orbital representation. The simplified Dyson equation, which now corresponds to a one-dimensional chain problem, can be solved directly for model crystals which are not too complicated. The (local) density of states can then be calculated according to formula (4) or, instead, one can directly obtain the change in the density of states due to the (surface) perturbation V by the formula [78,79] :

$$\Delta\rho(\varepsilon) = \frac{1}{\pi} \text{ Im } \frac{\partial}{\partial\varepsilon} \ln \det(I-G_o V) \quad . \qquad (9)$$

This procedure may easily be extended to investigate the change in the density of states caused by chemisorption [80,81] .

Kalkstein and Soven [82] calculated for simple cubium (= simple cubic lattice with one s-like orbital per atom, including only nearest-neighbour interactions) the local density of states (LDS) for the surface and the first two interior planes in the (100) and (111) crystallographic direction. It appears that the surface LDS bears little resemblance to the infinite crystal density of states, being a somewhat more sharply peaked function as would be expected from the moment rules (see below). As one proceeds into the crystal the LDS begins to resemble the density of states function for the infinite crystal. Also studying simple cubium, Allan and Lenglart [83] determined directly the change in the density of states at a (100) surface in order to obtain the effect of the surface on the electronic specific heat and the surface entropy. Moreover, they examined the surface pro-erties of various cubic lattices considering single-band crystals [84] . The perturbation potential due to the surface was calculated self-con-sistently in order to satisfy Friedel's sum rule [85] . Einstein and Schrieffer [79] investigated the chemisorption of a single-level atom

on the (100) surface of cubium for A(atop), B(bridge) and C(centred) adsorption. (One, two and four substrate atoms are directly involved in the chemisorption binding, respectively.) They evaluated numerically the chemisorption energies as a function of the filling of the substrate band. A significant dependence on the character of the adsorption site was found. Furthermore, they studied the appearance of virtual and split-off levels (see section 2.9) for different values of the hopping integral between the adatom and the substrate atoms. In order to interpret photoemission spectra Einstein [80,81] examined the change in the electronic (local) density of states due to A-adsorption on the (100) face of cubium. He found that, moving into the bulk, $\Delta\rho_m$ initially decreases fairly rapidly, but remains non-negligible for deeper layers. In many of the above tight-binding calculations the single non-degenerate band was intended to represent the d-band of transition metals.

Recently, Ho et al. [86,87] investigated the electronic properties of the (100) face of a model two-band crystal with the CsCl structure. They calculated directly the change in the density of states due to the creation of the surface and obtained the effect of the surface on the specific heat and the surface entropy. Further, they examined the effect of surface relaxation and reconstruction on the electronic free energy. These studies on two-band crystals can be used to understand the properties of both semiconductor and insulator surfaces, while the one-band calculations are appropriate for metals. Ho et al. [88] also investigated single atom chemisorption on the (100) surface of a one-band bcc "metal". They studied the A- and C-adsorption cases and calculated the changes in the densities of states.

Using a method similar to that proposed by Kalkstein and Soven, Falicov and Yndurain [89,90] have performed two model calculations on the electronic properties of the (111) surface in a diamond-structure solid, with Si as a typical example. Their first model [89] consisted of tetrahedrally coordinated atoms with only one s-orbital per atom. Later [90], they considered four sp^3-hybridized orbitals per atom. They accounted for surface layer relaxation and examined the electronic structure near the surface by calculating the local density

of states at different crystal layers, as well as the bulk density of states. Both models have also been applied to a study of the (111) surface of a binary compound in the zinc-blende structure, with GaAs as a prototype [91].

Pandey and Phillips [92,93] have performed tight-binding calculations of surface energy bands for the unreconstructed, relaxed (111) and (100) surfaces of Si and Ge, and the reconstructed (111) surface of Si. As commonly, they used semi-infinite crystal models, but they did not report their calculation procedure.

b) The method of moments

Although the direct calculation of the Green's function from the Dyson equation (5) provides an elegant procedure to obtain the (local) density of states, it is hardly possible to deal with d-band metals in this way. Therefore, Cyrot-Lackmann et al. [94-98] developed an approximate method to calculate the density of states by using a finite expansion in its moments. For the sake of clearness we shall restrict our description of their approach to crystals with only a single nondegenerate s-band. This treatment may easily be extended to d-band systems.

Let H be the Hamiltonian of an electron that interacts with a lattice of N atoms represented by a superposition of atomic potentials $V(\vec{r}-\vec{R}_i)$:

$$H = T + \sum_{i=1}^{N} V(\vec{r}-\vec{R}_i) \quad . \tag{10}$$

If the eigenvalues of H are written as ε_λ, the density of states per atom reads:

$$\rho(\varepsilon) = \frac{1}{N} \sum_{\lambda} \delta(\varepsilon-\varepsilon_\lambda) = \frac{1}{N} \text{Tr } \delta(\varepsilon-H) \quad . \tag{11}$$

The moment of order p of $\rho(\varepsilon)$ is defined by:

$$\mu_p = \int \varepsilon^p \rho(\varepsilon) \, d\varepsilon = \frac{1}{N} \text{Tr } H^p \quad . \tag{12}$$

The knowledge of the entire set of moments determines uniquely the density of states through the characteristic function $f(x)$:

$$\rho(\epsilon) = \frac{1}{2\pi} \int_{-\infty}^{\infty} e^{ix\epsilon} \, f(x) \, dx \qquad (13)$$

with

$$f(x) = \sum_{p=0}^{\infty} \frac{(-ix)^p}{p!} \, \mu_p \quad . \qquad (14)$$

We assume now that each atom i has only a single s-orbital $\phi_i = \phi(\vec{r} - \vec{R}_i)$ with energy ϵ_o, which satisfies

$$\{T + V(\vec{r} - \vec{R}_i)\} \, \phi(\vec{r} - \vec{R}_i) = \epsilon_o \, \phi(\vec{r} - \vec{R}_i) \quad , \qquad (15)$$

and that the atomic orbitals are mutually orthogonal. The moment μ_p given by (12), can then be written as:

$$\mu_p = \frac{1}{N} \sum_{i_1, \ldots i_p} \langle \phi_{i_1} | H | \phi_{i_2} \rangle \ldots \langle \phi_{i_p} | H | \phi_{i_1} \rangle \quad . \qquad (16)$$

In expression (16) only two types of integrals are retained, the crystal field integrals α and the resonance or transfer integrals β:

$$H_{ii} = \epsilon_o + \sum_{\ell \neq i} \langle \phi_i | V(\vec{r} - \vec{R}_\ell) | \phi_i \rangle = \epsilon_o + \sum_{\ell \neq i} \alpha(\vec{R}_\ell - \vec{R}_i) \quad , \qquad (17)$$

$$H_{ij} = \langle \phi_i | V(\vec{r} - \vec{R}_i) | \phi_j \rangle = \beta(\vec{R}_j - \vec{R}_i) \quad . \qquad (18)$$

For simple cubium it is very easy to obtain exact expressions for the various moments by a walk-counting technique [94]. In case of d-band metals, however, this technique becomes rapidly more complicated for the higher moments, so that one can calculate only a restricted number of moments.

The shape of the density of states curve is determined by the respective moments as follows. The first moment fixes the average shift of the band with respect to the zero level ϵ_o, while the second moment is related to the width of the band. The higher order moments give in-

formation about the asymmetry, extension of the wings and fine struc-
ture. If all the moments are known, existence and uniqueness theorems
guarantee the existence of a positive density of states under certain
conditions [98]. Equations (13) and (14) provide a way to actually
construct the density of states. However, the formulae are useless when
only a finite number of moments are known. With its p first moments, a
density of states curve can be approached by assuming for $\rho(\varepsilon)$ a func-
tion of a given form $f(\lambda_1,..\lambda_p;\varepsilon)$ with p parameters. These parameters
are determined by equating the p moments of $\rho(\varepsilon)$ and those of
$f(\lambda_1,..\lambda_p;\varepsilon)$. To calculate physical properties such as cohesion energy,
surface tension, etc., which are given by an integral over the density
of states, $\rho(\varepsilon)$ may adequately be approximated by a truncated Edgeworth
series, i.e., a gaussian multiplied by a polynomial [94,95,99]. Using
only the first two or four moments, Cyrot-Lackmann and Ducastelle cal-
culated in this way the electronic charge distribution of d-orbitals
[96] and the binding energies of 5d transition-metal atoms adsorbed
on the (100) and (111) planes of 5d transition metals [100]. Allan and
Lannoo [101] investigated the relaxation of transition-metal surfaces.
In these studies only the effect of the d-band was taken into account;
the contribution of the s-band and of s-d mixing was neglected.

The continued-fraction expansion

        In order to calculate the density of states more accurately,
one needs more than four moments. Moreover, the truncated Edgeworth
series is not adequate to uncover details of the density of states
function, such as singularities or band gaps. For this reason, Gaspard
and Cyrot-Lackmann [98] have developed the following procedure to re-
construct the density of states from its moments, which uses a continued-
fraction expansion of the Hilbert transform of $\rho(\varepsilon')$, which is equal to
the Green's function $G(\varepsilon)$:

$$G(\varepsilon) = \int_{-\infty}^{\infty} \frac{\rho(\varepsilon')}{\varepsilon - \varepsilon'} \, d\varepsilon'$$

$$= \cfrac{\alpha_1}{\alpha_2 + \varepsilon - \cfrac{\alpha_2 \, \alpha_3}{\alpha_3 + \alpha_4 + \varepsilon - \cfrac{\alpha_4 \, \alpha_5}{\ddots}}} \quad . \tag{19}$$

The coefficient α_k is a function of the moments $\mu_0, \mu_1, \ldots \mu_{k-1}$. The fraction is truncated at level p and written out as a sum of single fractions:

$$G(\varepsilon) = \sum_{i=1}^{p} \frac{w_1}{\varepsilon - \varepsilon_1} \quad . \tag{20}$$

The parameters w_i and ε_i are obtained by using the fact that approximating the Hilbert transform by a fraction with p levels is equivalent to approximating the integrated density of states $N(\varepsilon)$ by a step function $N_p(\varepsilon)$ with p steps [98]. It can be shown that the exact $N(\varepsilon)$ crosses all the steps of the function $N_p(\varepsilon)$. So, we may write

$$\sum_{\substack{j \\ \varepsilon_j < \varepsilon_1}} w_j \leq N(\varepsilon_1) \leq \sum_{\substack{j \\ \varepsilon_j \leq \varepsilon_1}} w_j \quad , \tag{21}$$

where the ε_i are the positions of the steps in $N_p(\varepsilon)$ and the w_i their values. The 2p unknown quantities ε_i and w_i are determined by assuming that the 2p known moments of the true $\rho(\varepsilon)$, $\mu_0, \ldots \mu_{2p-1}$, are equal to those of the derivative of $N_p(\varepsilon)$, leading to the following set of equations:

$$\sum_{i=1}^{p} w_i \, \varepsilon_i^k = \mu_k \quad , \qquad k = 0, \ldots 2p-1 \quad . \tag{22}$$

Smoothing and subsequently differentiating of the step function $N_p(\varepsilon)$ fixed by the ε_i and w_i, yields $\rho(\varepsilon)$. The coefficients a_n and b_n defined by

$$a_n = \alpha_{2n-1} + \alpha_{2n}$$

$$b_n = \alpha_{2n} \, \alpha_{2n+1} \tag{23}$$

may be used to study precise details of the density of states, such as singularities or gaps. If split-off states occur, there are some isolated poles ε_i outside the band structure, with w_i giving the weight of the corresponding state.

Cyrot-Lackmann et al. [102] studied, by this procedure, the local densities of states at the outer three planes of a (100) and a (111) surface of narrow-band cubium, using 30 moments. Further, they examined 3 adsorption sites (A-, B- and C-adsorption) on a (100) sur- face, calculated the variation of the local densities of states on the adatom as a function of the binding position and the hopping integral between the adatom and its nearest surface atom(s), and gave a detailed discussion on the occurrence of virtual bound states and split-off states (see section 2.9). Very recently, Desjonquères and Cyrot-Lack- mann [103] used the method of moments and continued-fraction analysis to make a detailed study of the local densities of states on clean low index surfaces of fcc Ni, hcp Co and bcc Fe. The d-band degeneracy was fully taken into account and up to 26 moments were calculated. The influence of a surface perturbation potential, determined self-con- sistently by using Friedel's sum rule [85] and the conservation of the total electronic charge, was investigated. Desjonquères and Cyrot- Lackmann [104] also calculated the aspherical charge densities of d-electrons around the atoms at low index surfaces of fcc Ni, hcp Co and bcc Fe in order to achieve a better understanding of adsorption and catalysis phenomena.

c) The recursion method

In the tight-binding model, the effective one-electron Hamiltonian is defined by its matrix elements over a set of localized, orthogonal orbitals $\phi_i = \phi(\vec{r}-\vec{R}_i)$. The recursion method, developed by Haydock et al. [105-107], sets up a new (orthogonal) basis in which the Hamiltonian has a tridiagonal representation $\underline{H}_{TD}$, by generating a unitary transformation U such that

$$\underline{U}^{\dagger} \; \underline{H} \; \underline{U} = \underline{H}_{TD} \quad . \tag{24}$$

The matrix elements of $\underline{H}_{TD}$ are given by:

$$\left[\underline{H}_{TD} \right]_{mn} = \begin{cases} a_m & n = m \\ b_m & n = m+1 \\ b^*_{m-1} & n = m-1 \\ 0 & \text{otherwise} \end{cases} \quad . \tag{25}$$

Thus, the recursion procedure (discussed below) transforms the three-dimensional lattice to a fictitious chain of "atoms" with nearest-neighbour interactions.

From such a tridiagonal matrix $\underline{H}_{TD}$ it is particularly simple to derive various matrix elements of the Green's function. For example, if ϕ_o is a member of the localized orbital basis, we can evaluate the local matrix element

$$G_{oo}(\varepsilon) = <\phi_o | (\varepsilon - H)^{-1} | \phi_o>$$

$$= \left[(\varepsilon \underline{I} - \underline{H}_{TD})^{-1} \right]_{oo} \quad , \tag{26}$$

if we ensure that ϕ_o remains as the first member of the new basis (see below). Let D be the determinant of the matrix $\varepsilon \underline{I} - \underline{H}_{TD}$ and D_n ($n = 0, 1, 2, ..$) be the determinants of the matrices derived from $\varepsilon \underline{I} - \underline{H}_{TD}$ after rows and columns 0 to n have been eliminated. Then we can write:

$$G_{oo}(\varepsilon) = D_o / D \quad . \tag{27}$$

Since the following recursion relation holds among the determinants D_n:

$$D_n = (\varepsilon - a_{n+1}) \, D_{n+1} - \left| b_{n+1} \right|^2 D_{n+2} \quad , \tag{28}$$

we can expand $G_{oo}(\varepsilon)$ in a continued fraction by the repeated application of relation (28):

28

$$G_{oo}(\varepsilon) = \frac{D_o}{(\varepsilon-a_o)\, D_o - |b_o|^2\, D_1} = \frac{1}{\varepsilon-a_o - |b_o|^2\, D_1/D_o} \quad . \qquad (29)$$

The recursion method calculates the (a_i, b_i) from $i = 0$ to N (where N is of the order of 10 to 50). The resolvent is then computed by fixing D_{N+1}/D_N and inserting this ratio at the Nth level of the continued fraction.

The coefficients a_i and b_i

Starting from any normalized state $\tilde{\phi}_o$ (i.e., any normalized linear combination of the localized orbitals ϕ_m) we may construct an ordered orthonormal basis $\{\tilde{\phi}_m\}$ with

$$\tilde{\phi}_m = \sum_n \phi_n\, U_{nm} \quad , \qquad (30)$$

which has $\tilde{\phi}_o$ as its first member and which tridiagonalizes $\underline{H}$. We put $\tilde{\phi}_o = \phi_o$, the orbital considered in eq. (26). The next state $\tilde{\phi}_1$ is given by:

$$b_o^* |\tilde{\phi}_1\rangle = H|\tilde{\phi}_o\rangle - a_o|\tilde{\phi}_o\rangle \quad , \qquad (31)$$

where the coefficients a_o and b_o are chosen so that they orthogonalize $\tilde{\phi}_1$ to $\tilde{\phi}_o$ and normalize $\tilde{\phi}_1$, respectively. The higher $\tilde{\phi}_n$'s are defined similarly by repeated operations with H, orthogonalizing to all previous $\tilde{\phi}_r$ ($r < n$) and normalizing:

$$b_n^* |\tilde{\phi}_{n+1}\rangle = H|\tilde{\phi}_n\rangle - a_n|\tilde{\phi}_n\rangle - b_{n-1}|\tilde{\phi}_{n-1}\rangle \quad . \qquad (32)$$

The fact that $H|\tilde{\phi}_n\rangle$ is automatically orthogonal to all the states $|\tilde{\phi}_m\rangle$ with $m < n-1$, which implies that H is tridiagonal with respect to the basis $\{\tilde{\phi}_m\}$, can be proved easily. Since the matrix elements of $\underline{H}$ (the representation of H in a basis of the localized orbitals) are known, we can obtain the coefficients a_i and b_i by a repeated application of the recursion formula (32).

The recursion relation (28) gives a continued-fraction expansion of the resolvent that is exact to all orders. In practice, one computes only the first (N+1) pairs (a_i, b_i) of coefficients and approximates the remainder of the continued fraction beyond the Nth level. The (a_i, b_i) tend towards asymptotic values denoted by (a_∞, b_∞). By setting $(a_n, b_n) = (a_\infty, b_\infty)$ for $n > N$, which fixes D_{N+1}/D_N, we can evaluate the remainder $t(\varepsilon)$ of the continued fraction analytically:

$$D_{N+1}/D_N = \cfrac{1}{\varepsilon - a_{N+1} - |b_{N+1}|^2 \, D_{N+2}/D_{N+1}}$$

$$= t(\varepsilon) = \cfrac{1}{\varepsilon - a_\infty - |b_\infty|^2 \, t(\varepsilon)} \quad . \tag{33}$$

In this manner we terminate the continued fraction at level N. Since a simple relation exists between the coefficients α_k of Cyrot-Lackmann and the coefficients (a_i, b_i) of Haydock et al., this corresponds to calculating the first 2(N+1) moments of the density of states.

In reference [107] a discussion of the physical and mathematical background of this method, its applications and extensions, and the relation to other similar approaches is presented.

Haydock et al. [108] used this procedure to compare the widths of the d-band at different surfaces of transition metals with that of the bulk density of states in order to explain experimentally (by INS and UPS) determined bandwidths. Haydock and Kelly [106] were the first to obtain local densities of states at atoms on the low index surfaces of real fcc, hcp and bcc d-band metals. They effectively took 8 moments into account. The density of states at atoms in subsurface layers was also calculated and the effect of surface dilation was investigated. Moreover, they examined the density of states of an adatom of the same type placed at a lattice site above the (100) surface of a bcc crystal. The recursion method was used by Bortolani et al. [109] to study the electronic structure of the (111) surface of silicon. They calculated the local density of states of an atom in the surface layer, in the first and second sublayer and in the bulk. Yndurain et al. [110]

calculated the local densities of states of tetrahedrally coordinated solids by a very similar method, which uses a finite cluster of atoms connected to an infinite Bethe lattice [111].

From all these results it may be concluded that the local density of states at a specific lattice site depends mainly on the interaction with a small environment of neighbouring atoms. It should be remarked, however, that taking into account a finite number of moments or setting the higher coefficients a_i and b_i constant, is not entirely equivalent to considering a finite cluster. Apart from the effect of the cluster boundaries (in self-consistent charge calculations), many of the long paths in the walk-counting technique in fact wind around the origin, rather than wander far away. Such paths are contained entirely in a small cluster, but contribute also to the (neglected) higher moments.

2.6 Hartree-Fock type of methods

The tight-binding methods considered in the previous section do not explicitly take into account the electron-electron repulsion. We shall now discuss a model for the chemisorption of a foreign atom on a semi-infinite metal substrate, which allows for the electron-electron repulsion on the adatom in a self-consistent manner by the Hartree-Fock approximation. It has been developed by Grimley [112] and Newns [113] and is based on a method introduced by Anderson [43] for the investigation of localized magnetic impurities.

Anderson's Hamiltonian

We consider a basis set consisting of a single adsorbate orbital ϕ_a and the eigenstates ϕ_k of the unperturbed semi-infinite substrate. The states ϕ_k are supposed to be orthogonal to ϕ_a. (One can make two objections at this point. Firstly, the strong chemisorption binding is due to the overlap between the adatom and substrate orbitals, which may therefore not be neglected. Secondly, the eigenstates of the

semi-infinite crystal form a complete set. So, ϕ_a should be a linear combination of these states and cannot be orthogonal to all of them. We shall return to both points afterwards.) Moreover, we assume that ϕ_a contains one electron in the free atom. It is straightforward to extend the formulae to cases, where the adatom possesses more (degenerate) orbitals and electrons [114]. The Anderson Hamiltonian for the adsorbate-substrate system may now be written in second-quantized form as follows (see Appendix):

$$H = \sum_\sigma \epsilon_a \, n_{a\sigma} + \sum_{k,\sigma} \epsilon_k \, n_{k\sigma}$$
$$+ \sum_{k,\sigma} \left(V_{ak} \, c^{+}_{a\sigma} \, c_{k\sigma} + V_{ka} \, c^{+}_{k\sigma} \, c_{a\sigma} \right) + U \, n_{a\sigma} \, n_{a,-\sigma} \quad , \tag{34}$$

in which σ denotes spin. Here $c^{+}_{a\sigma}$ and $c_{a\sigma}$ are the fermion creation and destruction operators referring to an electron in orbital ϕ_a with spin σ and $n_{a\sigma} = c^{+}_{a\sigma} \, c_{a\sigma}$ is the corresponding number operator; $c^{+}_{k\sigma}$, $c_{k\sigma}$ and $n_{k\sigma}$ have an analogous meaning for the crystal orbitals ϕ_k. The first two terms correspond with that part of the one-electron energy which is due to the (partial) occupation of the unperturbed eigenstates ϕ_a and ϕ_k with eigenvalues ϵ_a and ϵ_k. The third term of H introduces the one-electron hopping integrals coupling these eigenstates, while the last term describes the Coulomb repulsion between electrons of opposite spin in the adatom orbital.

We shall employ the unrestricted Hartree-Fock approximation to expression (34). The two-particle interaction $U \, n_{a\sigma} \, n_{a,-\sigma}$ is replaced by $U \, n_{a\sigma} < n_{a,-\sigma}>$, where the occupation number $<n_{a,-\sigma}>$ has to be calculated self-consistently. Then the Fock Hamiltonian H^σ has the form

$$H^\sigma = \epsilon_\sigma n_{a\sigma} + \sum_k \epsilon_k n_{k\sigma} + \sum_k \left(V_{ak} \, c^{+}_{a\sigma} \, c_{k\sigma} + H.c. \right) \quad , \tag{35a}$$

where

$$\epsilon_\sigma = \epsilon_a + U <n_{a,-\sigma}> \quad . \tag{35b}$$

The adatom local density of states

We introduce the one-electron Green's operator corresponding to the Hamiltonian H^σ:

$$G^\sigma(\varepsilon) = \left[(\varepsilon + is)I - H^\sigma\right]^{-1} \quad , \tag{36}$$

where s is a positive infinitesimal quantity and I the unit operator. The matrix equation for G^σ is

$$(\varepsilon \underline{I} - \underline{H}^\sigma) \underline{G}^\sigma(\varepsilon) = \underline{I} \quad . \tag{37}$$

This equation may easily be solved in the representation of the unperturbed eigenstates ϕ_a and ϕ_k to yield the element $G^\sigma_{aa} = <\phi_a|G^\sigma|\phi_a>$:

$$G^\sigma_{aa}(\varepsilon) = \left[\varepsilon - \varepsilon_\sigma - q(\varepsilon)\right]^{-1}$$

$$= \left[\varepsilon - \varepsilon_\sigma - \alpha(\varepsilon) + i\Gamma(\varepsilon)\right]^{-1} \quad , \tag{38}$$

where the "chemisorption function" $q(\varepsilon)$ is given by:

$$q(\varepsilon) = \sum_k \frac{|V_{ak}|^2}{\varepsilon + is - \varepsilon_k} = \alpha(\varepsilon) - i\Gamma(\varepsilon) \quad . \tag{39}$$

If we define a weighted density of states function $w(\varepsilon)$ by:

$$w(\varepsilon) = \sum_k |V_{ak}|^2 \delta(\varepsilon - \varepsilon_k) \quad , \tag{40}$$

we obtain for the imaginary and real parts of $q(\varepsilon)$:

$$\Gamma(\varepsilon) = \pi w(\varepsilon) \quad , \tag{41}$$

$$\alpha(\varepsilon) = P \int_{-\infty}^{\infty} \frac{w(\varepsilon')}{\varepsilon - \varepsilon'} d\varepsilon' \quad , \tag{42}$$

where P denotes the Cauchy principal value. $\Gamma(\varepsilon)$ and $\alpha(\varepsilon)$ are called

the "level-width" function and "level-shift" function, respectively. The result (38) can be interpreted by saying that the effect of the chemisorptive interaction is to replace ε_a by $\varepsilon_\sigma + \alpha - i\Gamma$, i.e., to shift the level in the free atom by $U\langle n_{a,-\sigma}\rangle + \alpha$ and to broaden it by the imaginary part Γ. Note that the situation is in fact rather complicated, since α and Γ depend on ε!

If the equation

$$\varepsilon - \varepsilon_\sigma - \alpha = 0 \tag{43}$$

has a solution $\varepsilon_{\ell\sigma}$ lying within the substrate band (i.e., the range of energies ε_k), then because Γ does not vanish there, the result of the atom-metal interaction is to change the discrete atomic level into a <u>virtual level</u>[*] at $\varepsilon_{\ell\sigma}$, the width of which is determined by Γ. On the other hand, if the solution $\varepsilon_{\ell\sigma}$ lies outside the band, it is a discrete level, since $\Gamma = 0$. The state which belongs to $\varepsilon_{\ell\sigma}$ is localized in the region of the adatom and is called a <u>split-off state</u>. (The virtual and split-off states are more extensively discussed in section 2.9.)

The local density of states or spectral weight function for the adatom orbital ϕ_a is given by (see formula (3)):

$$\rho_{aa}^\sigma(\varepsilon) = -\pi^{-1}\, \mathrm{Im}\, G_{aa}^\sigma(\varepsilon)$$

$$= \frac{1}{\pi} \frac{\Gamma(\varepsilon)}{\left[\varepsilon - \varepsilon_\sigma - \alpha(\varepsilon)\right]^2 + \Gamma^2(\varepsilon)} \quad . \tag{44}$$

<u>Self-consistency and chemisorption energy</u>

The occupation numbers $\langle n_{a\sigma}\rangle$ can be calculated by integrating the local density of states:

---

[*] Note that the "virtual level" concept, very common in chemisorption theory, has no relationship with the "virtual orbital" concept, known from quantumchemistry.

$$\langle n_{a\sigma} \rangle = \int_{-\infty}^{\varepsilon_F} \rho_{aa}^{\sigma}(\varepsilon) \, d\varepsilon \quad . \tag{45}$$

Substitution of eqs. (44) and (35b) gives $\langle n_{a\sigma} \rangle$ as a function of $\langle n_{a,-\sigma} \rangle$. Similarly, we get $\langle n_{a,-\sigma} \rangle$ as a function of $\langle n_{a\sigma} \rangle$. These coupled equations represent the self-consistency conditions which determine the solutions of the HF eigenvalue equation. For magnetic solutions $\langle n_{a\sigma} \rangle \neq \langle n_{a,-\sigma} \rangle$ and for nonmagnetic solutions $\langle n_{a\sigma} \rangle = \langle n_{a,-\sigma} \rangle$. In the latter case, only one self-consistency condition has to be obeyed.

The chemisorption energy, the difference between the total energies of the perturbed and unperturbed systems, is given by:

$$\Delta E = \left[\sum_{\substack{m,\sigma \\ occ}} \varepsilon_{m\sigma} - U\langle n_{a\sigma} \rangle\langle n_{a,-\sigma} \rangle \right] - \left[2 \sum_{\substack{k \\ occ}} \varepsilon_k + \varepsilon_a \right] \quad , \tag{46}$$

employing the Hartree-Fock expression for the total energy. Usually, one does not solve for the one-electron energies, but one calculates the (local) densities of states from the Green's functions. Therefore, we rewrite eq. (46) as follows:

$$\Delta E = \sum_{\sigma} \int_{-\infty}^{\varepsilon_F} \Delta\rho_{\sigma}(\varepsilon) \, \varepsilon \, d\varepsilon - U\langle n_{a\sigma} \rangle\langle n_{a,-\sigma} \rangle - \varepsilon_a \quad , \tag{47}$$

where

$$\Delta\rho_{\sigma}(\varepsilon) = \rho_{aa}^{\sigma}(\varepsilon) + \Delta\rho_M^{\sigma}(\varepsilon) \quad , \tag{48}$$

with $\Delta\rho_M^{\sigma}$ being the disturbance which the adsorbed atom causes in the density of states for spin σ electrons in the metal. Obtaining eq. (47) from eq. (46) leads to the following difficulty. In general, the Fermi level ε_F changes with chemisorption in order to conserve electrons. However, since self-consistency is only achieved in the adsorbate and not in the adsorbent, it is convenient to keep ε_F fixed during the self-consistent procedure. Consequently, a slight change Δn occurs in

the number of electrons in the system when the chemisorption bond is formed. So, Friedel's sum rule [85] is not obeyed and an extra term, $-\epsilon_F \Delta n$, should be added to the binding energy in order to correct for this deficiency.

Approximations to $w(\epsilon)$; the surface molecule concept

In order to calculate the chemisorption energy and other physical properties one needs an expression for the weighted density of states $w(\epsilon)$. In general, this function cannot be obtained in analytical form. Therefore, Newns [113] used a semi-elliptical, approximate form for $w(\epsilon)$, which is the analytical solution for a chain of atoms with a single atomic orbital each. Via this approximation he calculated the adatom charge and adsorption energy of hydrogen on Ti, Cr, Ni and Cu [113] and also the adsorption energy of "5d atoms" on tungsten [115]. For the latter problem, Thorpe [114] used an expression for $w(\epsilon)$ with maxima above and below the Fermi level. Davison and Huang [116] calculated the chemisorption energy of oxygen on Si, Ge and III-V semiconductors, employing the $w(\epsilon)$ for an AB chain.

The chemisorption model discussed here may considerably be simplified by using the concept of a surface molecule. This concept implies that the adatom interacts strongly with a limited number of atoms in the surface of the metal, thus forming a surface molecule which only weakly interacts with the rest of the metal. The adatom orbital may couple, for example, with a group orbital ϕ_g, which is a linear combination of atomic orbitals on the substrate having the appropriate symmetry for interaction with the adatom on a given site. Since the group orbital is coupled to the rest of the metal, it becomes a virtual resonance in the substrate band with a partial density of states $\rho_g(\epsilon)$, in the same way as the adatom orbital becomes a virtual state in case of a weak chemisorption binding (see section 2.9).

Neglecting the interaction between ϕ_a and the orbitals different from ϕ_g, the weighted density of states function $w(\epsilon)$ can be written as:

$$w(\varepsilon) = \left|\langle\phi_a|V|\phi_g\rangle\right|^2 \rho_g(\varepsilon) \quad . \tag{49}$$

(Note that the $\rho_g(\varepsilon)$ in this equation represents the partial density of states of ϕ_g before the chemisorption interaction is switched on. We shall return to this point.) If the coupling of ϕ_g to the rest of the metal is weak, $\rho_g(\varepsilon)$ has a sharp resonance and the closer it resembles a δ-function the better the surface molecule approximation becomes. Strong coupling results in a broad, featureless group orbital density. The form of the group orbital resonance is therefore the criterion which decides whether the surface molecule concept can be used [114,117].

To illustrate this point, let us replace $w(\varepsilon)$ by a δ-function at ε_g and write $\langle\phi_a|V|\phi_g\rangle = \gamma$. Then:

$$w(\varepsilon) = |\gamma|^2 \delta(\varepsilon-\varepsilon_g) \tag{50}$$

and, using eq. (42):

$$\alpha(\varepsilon) = |\gamma|^2 / (\varepsilon-\varepsilon_g) \quad . \tag{51}$$

Equation (43) for the levels of the system becomes

$$(\varepsilon-\varepsilon_\sigma)(\varepsilon-\varepsilon_g) = |\gamma|^2 \quad . \tag{52}$$

This is simply the secular equation for the energies ε_1 and ε_2 of the bonding and antibonding molecular orbitals formed from two atomic orbitals, one with energy ε_σ, the other with ε_g, and interacting through γ [117,118]. The chemisorption problem now resembles that of a diatomic molecule. This diatomic molecule might be called the surface molecule; the metal is represented by the level ε_g, and the atom-metal coupling by the energy γ. Because of its interaction with the metal, however, the Hartree-Fock theory of the surface molecule is different from that of an ordinary molecule. The surface molecule need not contain an integral number of electrons; it is an open system with the chemical

potential of the electrons (the Fermi level) fixed, not their number. The metal acts as a source or a sink for electrons [114,118].

Using the surface molecule limit, Grimley studied the adsorption of Na and S on nickel [118] and of H on tungsten [117]. Grimley and Thorpe [114,119] calculated the binding energy of 5d transition atoms adsorbed on tungsten. Including overlap between the orbitals of the admolecule and those of the metal Doyen and Ertl [120] investigated the adsorption of CO on some transition metals, represented by a single crystal orbital. Gadzuk [121] calculated the group orbital virtual resonances in the surface molecule picture for some model systems and obtained the resulting adatom density of states.

In a few studies, the applicability of the surface molecule concept has been examined. Penn [122] calculated the metal density of states at the adsorbate site. His opinion is that this level density should resemble that of an atom, i.e., exhibit a small number of well-defined peaks as a function of energy. The width of these peaks must be small compared to the metal band width in order to obtain a surface molecule. Kelly [123], on the other hand, regarded it necessary that the group orbital on the substrate displays atomic-like properties. He calculated [123,124] the group orbital spectrum (density of states) ρ_g for different adsorption geometries, using the recursion method of Haydock et al. [105-107]. If ϕ_a is chosen as $\tilde{\phi}_0$, the orbital $\tilde{\phi}_1$ is precisely ϕ_g (section 2.5). Kelly concluded that the surface molecule picture is of restricted validity and formulated a criterion to decide whether it is applicable to specific cases. According to him, a semi-elliptical group orbital spectrum, instead of the δ-function required for the surface molecule limit, would offer a better assumption for adsorption on a close-packed substrate.

The above criteria for the validity of the surface molecule concept, which are based on the electronic properties of the metal substrate before adsorption, are not completely adequate. Instead of demanding that the group orbital resonances in the substrate band are narrow before chemisorption, it would be better to check whether sharp bonding and antibonding levels, originating from a small adsorbate-

adsorbent complex, occur _after_ chemisorption. This situation, where
one could also speak of a surface molecule, may certainly arise when the
adatom-group orbital coupling is stronger than the interactions inside
the substrate. Actually, this has been confirmed by Grimley and Pisani
[125], who studied the chemisorption of hydrogen on cubium, using the
complete (local) substrate density of states in $w(\varepsilon)$. They found that
the widths of the virtual bonding and antibonding molecular orbitals
of an embedded diatomic molecule H-M were small, although no previous
sharp peaks in the (local) substrate density of states were present.

Overlap effects and overcompleteness

Grimley [126-128] investigated the effect of overlap between
the adsorbate atomic orbital ϕ_a and the crystal orbitals ϕ_k. It
appears that the various formulae obtained by treating Anderson's
Hamiltonian in the Hartree-Fock approximation are easily changed to in-
clude overlap. The chemisorption function has to be redefined. Further-
more, one has to distinguish between net and gross occupations and
level densities, analogously to the definitions of such quantities in
quantumchemistry.

As remarked previously, another problem connected with the
inclusion of overlap effects should now be considered, namely the over-
completeness of the basis set $\{\phi_a, \phi_k\}$. The eigenstates of either the
adsorbate or the semi-infinite metal alone are complete sets. We may
avoid the problem on the admolecule by limiting the set $\{\phi_a\}$ to those
orbitals only which are important in bonding, according to our chemical
experience, but we cannot easily limit the set $\{\phi_k\}$ because they form
a quasi-continuous spectrum going up through the vacuum level. Let us
assume that the one-electron functions ψ for the adsorbate-adsorbent
system can be expanded as follows:

$$\psi = \sum_a c_a \phi_a + \sum_k c_k \phi_k \quad . \tag{53}$$

Now, one can take into account the overcompleteness of the basis set

by imposing the auxiliary conditions

$$\sum_k <\phi_a|\phi_k> c_k = 0 \quad , \qquad \forall \; a \tag{54}$$

which assure uniqueness of the expansion coefficients. These conditions amount to adding a non-Hermitian pseudopotential to the Fock operator [127-129]. Grimley and Newton [130] have performed in this manner some calculations on the chemisorption of hydrogen on free-electron Al.

The problem of overcompleteness may be avoided by introducing a set $\{\phi_m\}$ of atomic orbitals localized on the metal atoms instead of the set $\{\phi_k\}$. The basis set $\{\phi_a,\phi_m\}$ will usually be limited to those orbitals which are important in the chemical bonding, and it will therefore be incomplete as well as nonorthogonal. The overlap effects may be taken into account in a straightforward way [125].

The embedding problem

While the Anderson Hamiltonian restricts the electron-electron interactions to the adatom, some attempts have been undertaken to include the electron repulsions to a larger extent. Grimley and Thorpe [114,131] calculated the binding energy of 5d transition atoms adsorbed on tungsten using Hubbard's Hamiltonian [132] in the Hartree-Fock approximation (see Appendix) to describe the surface molecule. The results were much better than for the Anderson surface molecule and the experimentally observed binding energy trend could be reproduced.

In these calculations [114,131] the diatomic surface molecule was only affected by the underlying metal via an adjustment of the number of electrons so that the proper Fermi level was obtained. However, one can also treat the embedding problem more explicitly in one of the following ways [125,129]:

(i) Start with the noninteracting semi-infinite solid and the adsorbate, so that the adsorbent cluster is already embedded correctly in the surface of the solid, and then switch on the coupling between the adsorbate and the adsorbent cluster, so that the formation of bonds be-

tween the adsorbate and the embedded cluster is studied.

(ii) Start with the adsorbate/adsorbent cluster, and the indented
solid (indented because the adsorbent cluster has been "removed"), and
then switch on the coupling between them so that the cluster becomes
correctly embedded in the solid surface.

Results obtained by the first scheme may easily be re-interpreted
in terms of the second one, and conversely.

The first procedure has been used by Grimley and Pisani
[125] to investigate the adsorption of a hydrogen atom on the (100)
face of simple and face-centred cubium. The adsorbate/adsorbent cluster
consisted of two atoms, A and B, to which the self-consistency problem
was confined, while the solid was handled in the tight-binding approx-
imation. Overlap effects were included and it was assumed that the
perturbation matrix describing the chemisorption interaction, has non-
zero elements over the diatomic molecule AB only. Grimley and Pisani
concluded that, for on-site adsorption of hydrogen, it is hardly satis-
factory to confine the self-consistency problem to the diatomic molec-
ule AB. Further, they compared their results with those of Paulson
and Schrieffer [133], who used a Heitler-London type of scheme (see
next section). The Hartree-Fock calculations gave a significantly
polar bond, so that a stronger chemisorption binding was found than by
the Heitler-London method, which only describes a purely covalent bond.

The second approach to the embedding problem has recently
been discussed by Hyman [134] and Grimley [129]. In his model, Hyman
includes screening effects by metal electrons caused by the induction
of image charges in the metal in response to the excess charge in the
surface complex.

Madhukar [135] has developed a formalism for chemisorption
on transition-metal surfaces, which includes the electronic interac-
tions on both the substrate atoms and the adatom by using a Hubbard
[132] -type of Hamiltonian in the HF approximation. He represented
the narrow d-band of the substrate by a single s-band and accounted
for the nonorthogonality between the adatom and metal wave functions.

The inclusion of the intra-atomic Coulomb repulsion on the substrate atoms leads to an additional self-consistency relation for the substrate levels, which is absent in the Anderson-type approach. The model provides a criterion for the existence of a localized magnetic moment on the chemisorbed atom. Although formal solutions for the (local) densities of states and occupancies have been obtained, practical calculations were difficult to perform without the introduction of simplifying approximations, such as the replacement of the self-consistent substrate levels by a single energy at the centre of the narrow "d-band".

Apart from the calculation of chemisorption energies and local charge and spin distributions, the Hartree-Fock type of model has also been used to study the effect of chemisorption on the field [136] - and photo [137,138] -emission from metal surfaces.

2.7 Many-body approaches

The SCF molecular orbital schemes give a reasonable picture of the chemisorption bond when the bond is very strong, but overestimate the Coulomb interactions between electrons when the bond is weak. There is a competition between the one-electron terms in the Hamiltonian which tend to delocalize the electrons, and the Coulomb repulsion between electrons which leads to localization by keeping them far apart. The importance of correlation effects in bonding is measured by the ratio of the effective Coulomb interaction U (the difference between the intra-atomic and the nearest-neighbour interatomic electron repulsions) and the splitting energy $\Delta\epsilon$ between the bonding and antibonding molecular orbitals. For $U/\Delta\epsilon > 1$ correlation effects are important [139]. In the chemisorption problem the width of the virtual level (weak chemisorption bond) or the separation between the bonding and antibonding virtual or split-off levels (intermediate and strong chemisorption bond) plays the rôle of the molecular splitting energy. Since $U \approx 5 - 10$ eV, correlation effects are likely to be rather important in some chemisorption systems. We shall discuss in this section

a few techniques which have been developed for including correlation effects, with special attention paid to the induced covalent bond method of Schrieffer et al. [140,141,133].

Pollard [142], using a Heitler-London treatment, showed that a single-configuration wave function for the homopolar state M-A, which is composed of the singly occupied orbital of an adatom A and the doubly occupied band states of the metal M, leads to a repulsive exchange interaction. He took account of the nonorthogonality of the adatom and metal states and used a simple free-electron model for the metal. In order to deal with the attractive forces in chemisorption, Toya [143] extended this model by including configurations of the ionic states $M^- - A^+$ and $M^+ - A^-$, as well as excited neutral configurations. Wojciechowski [144,145], studying the adsorption of alkali, Ba and Sr atoms on low index planes of tungsten and copper, improved Toya's model by taking into account the atomic structure of the metal surface. He considered only the ground state configuration for M-A and ionic configurations of the type $M^- - A^+$. Since both Toya and Wojciechowski did not allow for spin polarization in the substrate, they obtained no covalent bonding. Hence, their scheme is similar to Mulliken's theory of donor-acceptor complexes with no electron pair bond being formed.

The induced covalent bond method

We shall now discuss an approach to the theory of non-ionic chemisorption, proposed by Schrieffer and Gomer [140] to treat systems in which the intra-atomic Coulomb interaction U on the adsorbate is large compared to the strength of the interaction between the adsorbate and a metallic substrate. The method proceeds by imitating the Heitler-London (HL) theory for a diatomic molecule, i.e., one atom of the molecule is the adatom, while the other "atom" is the full (N-1)-atom solid, including the free surface. For simplicity, it is assumed that the solid in the absence of the adatom is well described by the tight-binding one-electron scheme.

In the conventional HL scheme one must couple the spin of the adatom electron to an unpaired spin in the solid to form the singlet state which is characteristic for a covalent bond. In zero order no unpaired spins are present in the solid, however, except when localized spin waves occur near the free surface. So, the framework of the HL theory must be enlarged in order to allow for the induction of spin density in the surface region of the solid; the induced spin is then coupled to the adatom spin forming a bond. Schrieffer and Gomer [140] called this an induced covalent bond (ICB). The induced spin density has to be sufficiently large to generate an exchange attraction which overcomes the exchange repulsion. The formal theory of the method, which is appropriate for free radical adsorption, has been worked out by Paulson and Schrieffer [133,141].

The ICB method for H chemisorption is developed by constructing Slater determinants from the orbitals localized on the subsystems, which are used as many-electron basis states. Because of the large value of the adatom intra-atomic Coulomb interaction U charge fluctuations on the adsorbate are small so that only neutral adsorbate states are included; if necessary, ad-ion states may be added by means of perturbation theory. Thus each Slater determinant contains one electron in the adatom orbital ϕ_a with spin σ and N-1 electrons distributed over the substrate states ϕ_k with spin σ_k. Except for the doubly occupied singlet ground state, excited configurations on the substrate, corresponding to various higher spin states (due to spin flips), must be included to account for the induced spin density. The many-electron basis states are labeled by the index $\alpha \equiv (\sigma; n_{k\sigma_k})$ where $n_{k\sigma_k}$ are the occupation numbers (= 0,1) of the substrate spin orbitals. Now, the ground state wave function is formed as a linear combination of the basis states $|\alpha\rangle$:

$$|\Psi_o\rangle = \sum_\alpha c_\alpha |\alpha\rangle \quad . \tag{55}$$

As for H_2, it is very important to include the overlap between ϕ_a and the ϕ_k, the latter being mutually orthogonal. The dominant term in the

adatom-surface binding is the anti-ferromagnetic exchange interaction

$$H_{exch} = \sum_{k,k'} \sum_{\sigma,\sigma'} J_{kk',a} c^+_{k'\sigma} c_{k\sigma'} c^+_{a\sigma'} c_{a\sigma} \qquad (56)$$

between the adatom spin and the spin density in the metal, which contains an exchange integral $J_{kk',a}$ analogous to the exchange interaction J_{ab} for H_2.

Two limiting cases can be discerned [133]. If the adatom-solid interaction is weak, one can treat this coupling as a perturbation. This, in second-order perturbation theory, leads to the following expression for the interaction energy, the so-called weak interaction limit:

$$\Delta E_{WL} = E_{rep} + E^{(2)}_{WL} \quad . \qquad (57)$$

Here, E_{rep} is the exchange repulsion between the adatom and the substrate, which in zero order contains only doubly occupied orbitals. So, in first order of energy the adsorbate is repelled by the metal, just as would occur for H interacting with He. The exchange attraction comes from the second-order energy $E^{(2)}_{WL}$, originating from the admixture of excited "spin flip" configurations. Paulson and Schrieffer show that $E^{(2)}_{WL}$ is proportional to χ_{loc}, the local spin susceptibility at the surface.

The second limit, which is analogous to the surface molecule concept in the Hartree-Fock treatments of the previous section, occurs when the adatom-substrate interaction is stronger than the coupling between substrate atoms near the surface. It is called the strong interaction limit. In this case, one starts with the formation of a surface molecule. An electron is localized in a surface cluster orbital ψ_1 which has a strong overlap with the adatom orbital ϕ_a. Then a Heitler-London bond is formed between ψ_1 and ϕ_a. This surface molecule subsequently rebinds to the remaining "indented solid" via the hopping of electrons from the indented solid to ψ_1 and vice versa, which is again treated in second-order perturbation theory. The chemisorption energy in the strong coupling limit reads:

$$\Delta E_{SL} = \Delta \varepsilon_2 + \varepsilon_{loc} + E_{SL}^{(2)} \quad , \tag{58}$$

where $\Delta \varepsilon_2$ is the HL binding energy of the surface molecule; ε_{loc} is the energy required to localize an electron in the surface orbital ψ_1 on the clean surface and $E_{SL}^{(2)}$ is the "rebinding energy" up to second-order perturbation theory.

Paulson and Schrieffer [133] have employed the ICB formalism to study the adsorption of a H atom on the (100) surface of simple cubium, which was treated in the tight-binding approximation. Atomic orbitals of a simple gaussian form were used and the effect of the "size" of the metal atoms was examined by varying the exponents of the substrate atomic orbitals. The binding energy for chemisorption above two symmetric sites of the surface layer, viz. over a single substrate atom and on a bridge site between two surface atoms, was calculated as a function of the adatom-surface separation for both the weak and strong interaction limits. From the results, it was concluded that the surface molecule point of view is a good starting point in the vicinity of the binding curve minimum.

Finally, one remark about the importance of ionic states: When the intra-atomic Coulomb interactions on the adsorbate are screened by the metal, the admixture of ionic states into the HL scheme may become necessary. Therefore, in case of sufficiently strong coupling, the molecular orbital method might be more appropriate.

Some other approaches

Newns [146] has studied electron correlation effects in the chemisorption of 5d atoms on a tungsten substrate, using a two-centre Hubbard model. One atom was chosen to represent the tungsten surface and the binding energy was calculated as a function of the number of d-electrons on the other atom for a range of values of the intra-atomic Coulomb interaction. It appeared that the electron correlations tended to make the adsorption energy vary as the triangular peaked curve

which is observed experimentally.

Bagchi and Cohen [147] have set up a formalism to deal with the problem of hydrogen chemisorption on the surface of a metal, which takes overcompleteness and nonorthogonality of the wave functions as well as electron correlation into account. The atom-metal system was described in terms of an overcomplete basis set consisting of the eigenstates (both occupied and unoccupied) of the metal and the occupied electronic state on the adatom. The theory was applied to the situation where the intra-atomic Coulomb repulsion is small so that hydrogen chemisorbs in a nonmagnetic configuration and the ground state is nondegenerate in the spin. Newns' model for hydrogen chemisorption [113] could be derived as a limiting case of the present formalism when the Hartree-Fock approximation is used, the overlap of the adsorbate orbital with the metallic wave functions vanishes and certain simplifying assumptions are made about the various matrix elements.

Madhukar and Bell [148] have investigated the screening and polarization effects which occur in case of chemisorption on transition-metal surfaces, using the Anderson model without introducing the Hartree-Fock approximation. They have demonstrated that the Green's function matrix element $G_{aa}^{\sigma}(\varepsilon)$ in this case possesses two different poles, associated with the adatom ionization and electron-affinity levels respectively, in contrast to the single-pole HF approximation (see eq. (38)). However, when the intra-adsorbate Coulomb interaction U becomes small with respect to the adsorbate-substrate coupling V_{ai}, the two peaks merge into a single peak at some intermediate energy – just the situation described by Hartree-Fock. Further, Madhukar and Bell have shown that the free-adatom ionization level ε_a must be shifted upwards due to screening and polarization effects in order to explain the experimentally (by photoemission and ion-neutralization spectroscopy) determined bonding levels.

Van Santen [149] has discussed the changes in the heat of chemisorption of a hydrogen atom upon alloying a group VIII metal with a group IB metal, using the Anderson model and considering one orbital

per atom. The ensemble effect which ascribes changes in the heat of chemisorption exclusively to changes in the geometry of the adsorption complex (e.g. the number of neighbours), as well as the ligand effect which takes into account variations in bond strength due to a different intrinsic activity of the binding metal atoms, have been investigated. Simple models have been used to calculate the effect of alloying, which is represented by changes in the d-band width and in the electron concentration in the orbital on the atom(s) involved in the chemisorption bonding.

2.8 Comparison of the methods

Up to now, calculations for the adsorption on real d-band systems have only been performed by means of tight-binding methods. The more advanced Hartree-Fock and Heitler-London like approaches have only progressed to the study of cubium-like systems or had to make drastic assumptions, for example about the structure of the d-band. Moreover, the embedding of a self-consistent cluster into a tight-binding substrate causes a number of problems, while in the ICB scheme the intermediate case between the weak and strong limits waits for a direct approach.

In order to compare the different methods a few calculations have been performed on simple linear model systems. Blyholder and Coulson [150] have examined a six-atom linear chain, where one of the end atoms represented a chemisorbed atom. Each atom contributed one valence electron in a s-type orbital. A simple tight-binding (Hückel) model of the chain showed both the localized Tamm state and the main bonding features of a semi-infinite chain. A more elaborate SCF-LCAO-MO calculation for a linear chain of six hydrogen atoms yielded results so similar to those obtained by the simple tight-binding technique that Blyholder and Coulson concluded that the latter method is semi-quantitatively adequate for the prediction of localized states and the changes in such properties as charge and bond order.

Einstein [151] has applied the Anderson model to a chain of four atoms, one representing the adatom, the other three the substrate, to compare the methods of Grimley/Newns and Schrieffer with the exact solution. Each site possessed a spherical orbital and the band was taken to be half-filled. The total spin state was assumed to be a singlet. The following Anderson-type Hamiltonian was considered:

$$H = \epsilon_a \sum_\sigma n_{a\sigma} + U n_{a\sigma} n_{a,-\sigma} - V \sum_\sigma (c_{1\sigma}^\dagger c_{a\sigma} + H.c.)$$
$$- T \sum_{i=1}^{2} \sum_\sigma (c_{1\sigma}^\dagger c_{i+1,\sigma} + H.c.) \quad ; \tag{59}$$

ϵ_a is the energy level of the singly occupied adatom, U the intra-atomic Coulomb repulsion on the adatom, T the tight-binding hopping parameter for the three-atom substrate chain and V the hopping integral between the adatom and the first atom of the chain. The diagonal energies of the chain atoms were taken as zero, thus fixing the zero level at the centre of the "bulk" states. The calculations were restricted to the so-called Anderson symmetric model, in which $\epsilon_a = -\frac{1}{2}U$. For the half-filled band case considered here, this ensures the occupation numbers of all atoms to be equal to one and the adsorption bond to be purely covalent.

In this model, the eigenstates of the Hamiltonian (59) can be found analytically, so that Einstein could calculate the exact chemisorption energy as a function of adatom Coulomb repulsion, adatom-substrate hopping and substrate band width. He has also performed calculations by four approximate methods, which are here summarized.

When the chemisorption interaction is weak, the binding energy is approximated by the second-order perturbation contribution of

$$H_V = - V \sum_\sigma (c_{1\sigma}^\dagger c_{a\sigma} + H.c.) \tag{60}$$

to the eigenstate of the V = 0 Hamiltonian. For strong V, the rebonded-surface-complex (RSC) picture is more appropriate. In this case, the end atom separates from the substrate chain to form essentially a

diatomic molecule with the adatom. The dimer then rebinds to the in-
dented chain. The diatomic surface complex and the indented chain are
treated exactly. The subsequent rebonding of the surface complex to
the chain is described by:

$$H_T = - T \sum_\sigma (c_{1\sigma}^\dagger c_{2\sigma} + H.c.) \quad , \tag{61}$$

which is again handled by second-order perturbation theory.

In the Hartree-Fock approximation the Hamiltonian given by
formula (59) is transformed into a one-electron operator, which is to
be determined self-consistently:

$$H_{HF}^\sigma = \epsilon_{a\sigma} n_{a\sigma} - V (c_{1\sigma}^\dagger c_{a\sigma} + H.c.) - T \sum_{i=1}^{2} (c_{i\sigma}^\dagger c_{i+1,\sigma} + H.c.) \tag{62}$$

with

$$\epsilon_{a\sigma} = \epsilon_a + U \langle n_{a,-\sigma} \rangle \quad . \tag{35b}$$

In the Anderson symmetric model, the adatom stays neutral and the
self-consistency condition becomes

$$\langle n_{a\sigma} \rangle + \langle n_{a,-\sigma} \rangle = 1 \quad . \tag{63}$$

Calculations have been performed for the restricted (RHF),
$\langle n_{a\sigma} \rangle = \langle n_{a,-\sigma} \rangle = \frac{1}{2}$, as well as for the unrestricted (UHF) case.

Exact and approximate results have been obtained for three
values of the adatom Coulomb repulsion U. In all these cases it has
been found that there is a smooth transition from the regime where the
weak limit holds to that where the rebonded surface complex (RSC) is
valid. The interpolated curve for the interaction energy versus hopping
parameter V is nearly equal to the exact curve and more accurate than
the UHF one. The UHF solution underestimates the binding energy.
Nonetheless, it gives a reasonable account of the interaction energy,
as RHF does for strong hopping parameter V. For small V RHF fails com-

pletely, however, as can be expected.

So, from the model calculations of Einstein it may be con-
cluded that for purely covalent bonding the valence-bond type of
approach of Schrieffer yields better results than the (un)restricted
Hartree-Fock approximation. Furthermore, HF requires an iterative
solution, whereas the weak limit and RSC results can be obtained
directly.

2.9 Virtual and split-off states

In this section we shall delve in detail into the possible
effects of the chemisorption interaction on the originally discrete
level ε_a of the adatom and on the total density of states. As we
have seen in section 2.6, the local density of states for the
single adatom orbital ϕ_a can be expressed (using an Anderson type
of model) as:

$$\rho_{aa}^{\sigma}(\varepsilon) = \frac{1}{\pi} \frac{\Gamma(\varepsilon)}{\left[\varepsilon - \varepsilon_{\sigma} - \alpha(\varepsilon)\right]^2 + \Gamma^2(\varepsilon)} \quad , \tag{44}$$

with ε_{σ} being defined by eq. (35b), while $\Gamma(\varepsilon)$ and $\alpha(\varepsilon)$ are given
by eqs. (40), (41) and (42). One can qualitatively understand the
local density of states by looking at two limiting cases [139].
Suppose the solid has a single energy band of width W and centred
at ε_c. If V_{ak} is weak , then $\Gamma(\varepsilon)$ and $\alpha(\varepsilon)$ are small compared
with W and $\rho_{aa}^{\sigma}(\varepsilon)$ has a narrow peak near ε_{σ} which is well approxi-
mated by evaluating Γ and α at $\varepsilon = \varepsilon_{\sigma}$. If ε_{σ} lies within the band,
$\rho_{aa}^{\sigma}(\varepsilon)$ is a Lorentzian function of half-width $\Gamma(\varepsilon_{\sigma})$ centred at
$\varepsilon_{\sigma} + \alpha(\varepsilon_{\sigma})$, i.e., a virtual state or resonance level occurs. If ε_{σ}
is outside the band, we see from eq. (41) that $\Gamma(\varepsilon_{\sigma}) = 0$. So, $\rho_{aa}^{\sigma}(\varepsilon)$
is a δ-function, a sharp bound state which differs little from the
adatom orbital itself and occurs at an energy slightly shifted
from ε_{σ}.

If V_{ak} is sufficiently strong, so that $\Gamma(\varepsilon)$ over most of the
band is large compared with both W and the difference between ε_{σ} and

51

ϵ_c, the level shift function $\alpha(\epsilon)$ is large near the band. For ϵ above the top of the band the level shift is positive, while for ϵ below the bottom of the band $\alpha(\epsilon)$ is negative [113,139]. This feature leads to two sharp peaks of $\rho^\sigma_{aa}(\epsilon)$, one below the bottom of the band and one above the top. The eigenvalues are just the bonding and antibonding levels arising from the adatom orbital ϕ_a mixing with a linear combination of localized orbitals on the solid. Thus, one has a surface complex formed from the adatom and a cluster of surface atoms with the bonding state of the complex below the band and the antibonding state above the band [113,139]. These localized levels are called split-off levels.

As we shall see below, these limit cases are not the only possibilities. For intermediate V_{ak} slightly broadened bonding and antibonding levels can appear inside the band.

Some quantitative calculations have been performed. Cyrot-Lackmann et al. [102] have examined the adatom local density of states for a single-level atom adsorbed on the (100) surface of narrow-band cubium, using the method of moments. They first investigated the case for which the adatom and the substrate possess the same atomic energy level. For atop adsorption the local density of states is symmetric since the odd moments are zero. It is not symmetric for adsorption at a bridge or centred site. The asymmetry is stronger for the centred site than for the bridge site because the number of paths (see section 2.5) with an odd number of steps is greater. For a weak adatom-substrate atom hopping integral β' the local density of states has the shape of a broadened δ-peak. When β' is increased with respect to the substrate hopping parameter β (or the band width) two virtual states with increasingly sharp maxima appear. These maxima approach the band edges and for some critical value of β'/β, strongly depending on the adsorption position, split-off states with a finite weight, which are strictly localized near the adatom, appear: the adatom and its nearest neighbours form a surface molecule. The weights of the split-off states asymptotically converge to 0.5 for all three adsorption

sites. Cyrot-Lackmann et al. [102] have also considered an atom adsorbed in the on-site position with an atomic energy level ε_a different from the substrate level. The local density of states is no longer symmetrical. When β'/β increases and ε_a is in the lower half of the band, then first one split-off state appears below the band and finally a second state emerges above the band. If ε_a lies below the band, there is always a split-off state below the band, the second one appearing above the band for a sufficiently large value of β'/β. If ε_a is positive with respect to ε_c, the behaviour is reversed.

Einstein [80,81] has examined the changes in the total density of states

$$\Delta\rho = \Delta\rho_M + \rho_{aa} \tag{64}$$

caused by chemisorption of an atom in the atop position above a (100) cubium surface, using the model of Einstein and Schrieffer [79]. The behaviour of $\Delta\rho$ for different strengths of the adatom-substrate coupling appeared to be very similar to that found by Cyrot-Lackmann et al. for ρ_{aa}. The split-off states which correspond to bonding and antibonding states have now unit weight. In order to satisfy the electron-conservation sum rule

$$\int_{-\infty}^{\infty} \Delta\rho(\varepsilon) \, d\varepsilon = 1 \quad , \tag{65}$$

there must be a region of negative $\Delta\rho$. Indeed, it is found that in forming an indented solid, density of states is removed from (the centre of) the band region.

A concept which is directly related to all these findings, namely the model of a "virtual surface molecule", was introduced by Gadzuk [121] in order to explain the structure observed in electron spectroscopy of chemisorbed atoms. The basic idea is that the adsorbate interacts strongly with the localized group orbital in the tight-binding d-band of a transition metal. If the interaction is sufficiently strong,

localized states are formed outside the narrow d-band. These states correspond to a bonding and antibonding molecular orbital on the adsorbate and the nearest-neighbour substrate atoms. The discrete surface molecule states interact with the remaining indented solid. Since these states lie outside the d-band, the most likely interaction is a weak decay into the broad s-band. This converts the discrete surface molecule states into narrow virtual molecular states. While the binding energy is supplied in the surface molecule formation, the level width is thus acquired in the weak residual interaction with the s-band. By this model, Gadzuk explained how it is possible to have simultaneously narrow virtual levels, which implies weak chemisorption, and also high binding energies as observed experimentally.

With regard to the assumption of Gadzuk and many others concerning a weak coupling with the s-band for chemisorption on a transition-metal substrate, it should be noted that the interaction with the s-band appears to be strong (see Chapter IV).

2.10 Indirect interactions between adsorbed particles

The interactions between chemisorbed atoms or molecules may be classified as either direct (through-space) or indirect (through-bond) interactions. The former includes the short range interaction which appears when the adsorbates are close enough together for their electron clouds to overlap and the long range Coulomb interaction between the surface dipoles formed as a consequence of charge transfer in chemisorption. As Koutecký [8] has shown, an important indirect interaction occurs due to the sharing of the same electrons between the chemisorbed particles and the substrate: one adsorbate distorts the electron distribution in the metal, another one interacts with this distorted substrate. The direct interactions are of particular interest for ionic adsorption. For instance, Bennett [152] has calculated the effect of direct adatom-adatom interactions on the net charge of an alkali atom on a metal substrate, using the semiclassical image force model. Since we are especially interested in the covalent

54

adsorption of small particles (e.g. hydrogen atoms), we shall further discuss the phenomena of indirect interaction.

Grimley [112] has studied the long range indirect interaction between two adsorbed atoms A and B in the restricted HF approximation, using a generalization of the Anderson Hamiltonian, which accounts for the intra-atomic Coulomb repulsions on the two adatoms. With ϕ_a and ϕ_b being the atomic orbitals on A and B, respectively, and ϕ_k the one-electron wave functions of the semi-infinite substrate, the matrix element $G_{aa}(\varepsilon)$ of the Green's function reads:

$$G_{aa}(\varepsilon) = \left\{ \varepsilon - \varepsilon_a - q_a - \frac{q_{ab} \, q_{ba}}{\varepsilon - \varepsilon_b - q_b} \right\}^{-1} \quad , \tag{66}$$

where

$$q_a = q_b = \sum_k \frac{|V_{ak}|^2}{\varepsilon + is - \varepsilon_k} \quad , \tag{67}$$

$$q_{ab} = q_{ba} = \sum_k \frac{V_{ak} \, V_{kb}}{\varepsilon + is - \varepsilon_k} \quad , \tag{68}$$

$$\varepsilon_a = \varepsilon_b = \varepsilon_f + U \langle n \rangle \quad , \tag{69}$$

with ε_f being the orbital energy of an electron in the free atom. The other quantities have their usual meaning. The last term in eq. (66) is due to the presence of a second atom on the metal surface. If atom B were absent, or if A and B were infinitely far apart, G_{aa} would be given by eq. (38). To examine the influence of atom B on the level density ρ_{aa} associated with atom A, we separate q_{ab} into real and imaginary parts:

$$q_{ab} = \beta - i \Delta \tag{70}$$

with

$$u(\varepsilon) = \sum_k V_{ak} \, V_{kb} \, \delta(\varepsilon - \varepsilon_k) \tag{71}$$

$$\Delta(\epsilon) = \pi u(\epsilon) \tag{72}$$

$$\beta(\epsilon) = P \int_{-\infty}^{\infty} \frac{u(\epsilon')}{\epsilon - \epsilon'} d\epsilon' \quad ; \tag{73}$$

P indicates the Cauchy principal value. Equation (66) can now be written as

$$G_{aa}(\epsilon) = \frac{1}{2} \left\{ \frac{1}{\epsilon - \epsilon_a - \alpha - \beta + i(\Gamma + \Delta)} + \frac{1}{\epsilon - \epsilon_a - \alpha + \beta + i(\Gamma - \Delta)} \right\} \quad . \tag{74}$$

Since $G_{aa} = G_{bb}$, this equation can be interpreted as the splitting into two virtual levels

$$\epsilon_a + \alpha - i\Gamma \pm (\beta - i\Delta) \tag{75}$$

of two chemisorbed atoms with degenerate atomic levels at ϵ_f. Two atoms chemisorbed without mutual interaction would produce a twofold degenerate virtual level at $\epsilon_a + \alpha - i\Gamma$ (see section 2.6). The level density associated with eq. (74) is given by:

$$\rho_{aa}(\epsilon) = \frac{1}{2\pi} \left\{ \frac{\Gamma + \Delta}{(\epsilon - \epsilon_a - \alpha - \beta)^2 + (\Gamma + \Delta)^2} + \frac{\Gamma - \Delta}{(\epsilon - \epsilon_a - \alpha + \beta)^2 + (\Gamma - \Delta)^2} \right\} \tag{76}$$

and it is quite clear that two virtual levels have now been produced.

The interaction energy of the adatoms is approximately given by:

$$\Delta W = 2 \int_{-\infty}^{\epsilon_F} \left(\rho(\epsilon) - \rho_{\infty}(\epsilon) \right) \epsilon \, d\epsilon \quad , \tag{77}$$

with $\rho(\epsilon)$ being the density of states for the total system (substrate plus mutually interacting adatoms) and $\rho_{\infty}(\epsilon)$ being the total density of states when the two chemisorbed atoms are far apart. In expression (77) it is assumed that the Fermi level ϵ_F and the occupation number $<n>$ do not change when the indirect interaction is switched on. In this way Grimley [112] has investigated the long range behaviour of the indirect interaction, which he found to oscillate with the distance R between the

adatoms, the amplitude being proportional to R^{-2}. This value has been corrected afterwards (see next paragraph).

In order to study the effect of the interactions between adatoms on the heat of adsorption at low surface coverage, Grimley and Walker [153] have extended the model to a system of N adatoms, still retaining only the two-body contribution to ΔW, however, which determines the initial slope of the Q (differential heat of adsorption) versus θ (surface coverage) curve. Calculations have been performed for chemisorption on tungsten, using a free-electron model for the substrate. For the case where the adsorption of a single atom results in the formation of a virtual level close to the Fermi energy, an oscillatory interaction (attractive or repulsive, depending on distance) was obtained, which at long range falls off as R^{-3}.

Einstein and Schrieffer [79] have studied the indirect pair interaction at nearby binding sites, using their tight-binding model for the (100) surface of cubium discussed earlier. The calculations have been performed for the cases that both adatoms select the same binding site, directly above a surface atom, at a bridge site or at a centred position. So, the present model includes crystal structure effects, as distinct from the one of Grimley and Walker. Since the calculations were carried out numerically, the interaction energy ΔW could be obtained as a function of adsorbate separation, even for closely spaced adatoms. In their calculations Einstein and Schrieffer observed that split-off states occur for weaker interaction potentials than in the single atom case: a downward-shifted state and an upward-shifted one are found (cf. Grimley [112]). Further, the strength of the pair interaction at nearest-neighbour separation appeared to be about an order of magnitude smaller than the adsorption energy of a single adatom. The interaction energy showed an oscillatory behaviour and fell off exponentially for the first few lattice spacings while its asymptotic form appeared to decrease as R^{-5} rather than as R^{-3}. According to Einstein and Schrieffer, this may be explained by the fact that the virtual level approximation of Grimley and Walker is probably not valid for the parameter values which correspond to the observed

binding energies, since split-off states occur in this range of coupling.

Using the method of moments, Cyrot-Lackmann et al. [102] have investigated the adatom local density of states, when two adatoms are adsorbed at nearest-neighbour distance in the on-site position on the (100) surface of cubium. For a small adsorbate-substrate interaction β' (relative to the substrate-substrate interaction β) a splitted virtual state appeared which for increasing β'/β passed into two pairs of split-off states. The first pair occurred for a smaller value of β'/β and the second for a larger ratio than in the single atom case. This result agrees very well with the findings of Grimley and Walker and of Einstein and Schrieffer.

3. Cluster models

In recent years, cluster calculations have become of increasing interest in dealing with the surface and chemisorption problem. This has been promoted by the rapid development of quantummechanical methods for molecular calculations, which are made practicable by the fast and large electronic computers becoming available. One may now perform similar calculations on rather large clusters intended to represent the (metal) substrate with or without an adsorbate. Herewith it is assumed that local effects, which thus may be computed more accurately than by the solid-state methods, play a more important rôle in chemisorption phenomena than the collective properties of the bulk crystal. A justification for this assumption may be found in theoretical (the surface molecule concept) as well as experimental (e.g. ion-neutralization spectroscopy [154,155]) results.

A difficulty arising in cluster calculations is the appearance of undesirable boundary effects caused by the limited size of the cluster. Usually these have been ignored; in some cases one has tried to meet this problem by saturating the border atoms with hydrogen [156,157], by introducing periodically connected boundary conditions [158], or by considering the cluster as an open system whose electron

content is determined by a fixed Fermi level or chemical potential [159]. Actually, the latter type of calculations have also been made [114,118] based on a semi-infinite crystal model and, in general, one may remark that many of the "solid-state" techniques can in fact be conceived as cluster methods with some kind of boundary conditions. The method of moments (section 2.5), for instance, takes into account only interactions within a distinct cluster, the range being determined by the highest moment. In the embedding procedure (section 2.6) a small cluster is calculated self-consistently and subsequently embedded into a semi-infinite crystal by a Green's-function technique.

Altogether, we have given less space to the cluster methods, since the computational techniques are standard for molecules and have extensively been described in (text)books and review articles. Some of the results and also the problem of boundary conditions are discussed in more detail in the articles reprinted in Chapter IV.

The calculation methods

As remarked previously, the methods which are used to investigate surface and chemisorption phenomena by cluster calculations, are similar to those employed to study the properties of organic molecules and transition-metal complexes. However, the application of the more advanced methods is somewhat retarded by the large number of electrons present in (transition-metal) clusters, which demands the use of large basis sets.

In order to study the adsorption of hydrogen atoms and unsaturated hydrocarbons on transition-metal surfaces, Bond [160,161] has outlined a qualitative molecular orbital picture, based on the model of Goodenough [162] for the behaviour of the metal atom d-orbitals under influence of the crystal field. In the octahedral environment of a fcc crystal the d-orbitals split into two separate groups, the e_g and t_{2g} orbitals. The direction of emergence of these orbitals at the (100), (110) and (111) planes is established and the chemisorption bond is described in terms of the overlap with these directional surface or-

bitals. A similar model has been used by Knor and Müller [163] to describe the field-ionization process. Semi-empirical calculations have been performed based on Bonds model [164]. Other studies have examined its correctness [165]. Weinberg and Merrill [166] developed an empirical model to study the dissociative chemisorption of small molecules, based on the crystal field surface orbital (CFSO) description of Bond and the bond-energy bond-order (BEBO) relationships of gas phase kinetics and spectroscopy.

While the older molecular orbital calculations on clusters [167-171] used the simple Hückel scheme, the larger part of the more recent studies have been performed by the Extended Hückel [172] or the CNDO [173] method, the so-called semi-empirical LCAO-MO methods. Both consider all the valence electrons. The Extended Hückel Theory (EHT) does not explicitly take into account the electronic repulsions, but replaces the exact Hamiltonian by a sum of effective one-electron Hamiltonians, the matrix elements of which are obtained from experimental ionization potentials and calculated overlap integrals. The CNDO method is an approximation of the SCF-LCAO-MO or Hartree-Fock-Roothaan method. Many of the two-electron integrals are neglected or calculated approximately, while the one-electron integrals are parametrized with the help of experimental data.

Up to now, only a few SCF-LCAO-MO or ab initio calculations [174] have been performed on clusters. Sometimes electron correlation is taken into account in such computations.

During the last few years an increasing number of calculations are being done by the Hartree-Fock-Slater (HFS) method. The one-electron Schrödinger equation, which contains a kinetic energy, electrostatic potential and exchange/correlation term, is solved numerically. Slaters $X\alpha$ statistical approximation to the exchange/correlation [175] is used. In the self-consistent-field $X\alpha$ scattered wave (SCF-$X\alpha$-SW) formalism the potentials in the cluster are determined by the "muffin-tin" approximation [176]. Very recently, a few calculations have been reported which employ the discrete variational method (DVM) [177] and single site orbital (SSO) scheme [178]. In this procedure

the multiple scattering formalism is replaced by a numerical LCAO method. This allows one a greater flexibility in the choice of the potential function, which is important at the surface.

Since correlation effects are assumed to play an important rôle in the process of dissociative chemisorption, valence-bond like and multi-configurational methods have been used to study that problem.

The methods shortly described above, have been employed for cluster calculations in order to examine the electronic properties of pure solids and the chemisorption on semiconductors, simple metals and transition metals. In the following, we shall give a concise, but rather complete review of the various problems which have been investigated.

Pure (substrate) clusters

With various goals in mind, the electronic properties of pure clusters have been examined. On the one hand, one has attempted to simulate the bulk metal properties by considering a finite cluster as an approximate model for the infinite crystal. The electronic structure and binding energy per atom for lithium with varying cluster size has been investigated by EHT [179], Xα-SW [180] and ab initio [181] calculations to determine whether the cohesion energy approaches that of bulk lithium. Beryllium clusters were also examined [181]. Further, by a Hückel-like method the relative stability of different crystalline lattices (fcc, bcc and pentagonal) has been studied on very large lithium clusters [182]. (I)EHT and INDO calculations on finite and periodic two-dimensional hexagonal boron nitride clusters have been performed to examine whether the electronic properties of cluster sizes, such as band gap, valence band width and bond energy, converge to those of the infinite crystal and to check the effect of the boundary conditions [156,183]. The electronic properties of transition-metal clusters have been calculated by multiple scattering techniques in order to compare them with the crystal properties

[184,185]. Computations on cubo-octahedral Cu_{13}, Ni_{13}, Pd_{13} and Pt_{13} clusters gave electronic structures which are remarkably similar to the band structures and densities of states for the bulk solids [185]. CNDO studies on nickel clusters have been used to fit parameters for further calculations [186].

On the other hand, computations have been carried out on the specific electronic properties (ionization energy, electron affinity, d-orbital occupancy, charge and level densities, etc.) of metal clusters, which may differ from the corresponding bulk properties because of the large surface to volume ratio. In this manner, there have been attempts to find active sites and to explain the catalytic behaviour of metal aggregates, which for example play a rôle in supported catalysts. (It should be remarked, however, that these particles actually contain 100 – 100,000 metal atoms and, therefore, are not small in the sense used here.) Thus, calculations by the Xα-SW [180] and EHT or CNDO [186-189] schemes have been used to determine: (i) what cluster geometry is the most stable, (ii) what is the possible significance of this geometry and the cluster size to the surface and catalytic properties of small (transition-)metal particles. Painter et al. [190] have investigated by the Xα-SW method to what extent trends in the bulk densities of states in a series can be used in a discussion of surface effects. They found a correlation between the observed catalytic activities of surfaces of the iron series transition metals (Fe, Ni and Cu) and the calculated electronic distributions and densities of states near the Fermi energy. It was also checked how the charge density at a surface is modified by the presence of steps.

Finally, some semi-empirical cluster calculations have been performed on the properties of alloys [188,189], supported catalysts [191] and the metal-semiconductor interface [192].

While the preceding references have tried to clear up catalytic behaviour by studying the electronic properties of pure substrate clusters, the following investigations have looked at chemi-

sorption phenomena directly, by comparing clusters without and with an adsorbed species.

Adsorbate-substrate clusters

In the older calculations the Hückel method has been used to study the adsorption of unsaturated hydrocarbons and other π-system molecules on a small cluster of metal atoms [167-171]. More recently, one has obtained (semi)quantitative results for the adsorption of a single atom or a small molecule by the EHT, CNDO, Xα and ab initio methods. In a few cases the substrate has been represented only by a single atom [193-205]. For instance, studies by EHT have been done on the interaction of CO and H_2 on transition metals [195], the adsorption of CO on NiO [196], the difference between the catalytic activities of palladium metal and its salts [197], and the transition-metal catalysis of olefin isomerizations [198]. The transition metal-hydrogen bond was investigated in detail by LCAO-SCF (+CI) calculations [199-205]. In most models, however, the local environment and symmetry of the adsorption site was taken into account, more or less completely. Moreover, in several calculations it was examined how strongly the adsorption energy varies for different positions in order to explain the surface (im)mobility of adsorbates or to predict the most favourable adsorption sites. In this manner, one has investigated the adsorption of H, C, N, O and F on graphite by EHT and CNDO [206,158], O and H_2O on graphite by CNDO [157], H and O on boron nitride by CNDO [207], H on lithium by EHT [208] and ab initio [209], O on lithium by Xα-SW [159], H on beryllium ab initio [210], substituted methanes on lead by EHT [211], H on nickel by EHT [164,165,212], CNDO [213] and Xα-DVM [214], H on copper by EHT [165], O on nickel by Xα-SW [215,216], CO on nickel by EHT [217], Xα-DVM [218] and CNDO [219], H and N on tungsten by EHT [220,221], O on various transition metals by EHT [222], and ethylene on nickel by Xα-SW [223].

In nearly all the calculations enumerated up to now, the adsorption of a single particle was studied. However, in a few cases the

surface coverage was varied [211,217] or models for chemisorption under high coverage conditions were used [159,215]. Further, Grimley and Torrini [224] have examined the indirect interaction between two bridge-bonded nearest-neighbour H atoms adsorbed on (100) tungsten.

Dissociative chemisorption

One of the most important functions of several solid catalysts is the dissociative adsorption of some molecule as the first step of a reaction on the surface of the catalyst. This process is much harder to study than the chemisorption of a single atom or molecule and only few semiquantitative calculations are available at the moment. Weinberg et al. [166,225-227] have used the CFSO-BEBO method to examine the dissociative adsorption of H_2, CO, O_2, CO_2, N_2O and ethylene on platinum and of O_2 on nickel surfaces.

In many dissociative chemisorption studies the Extended Hückel method has been employed. Moffat [228] has examined the dissociative chemisorption of H_2 on several boron clusters. For some configurations the total energy was less than the combined energies of a hydrogen molecule and the boron cluster. Further, an activation energy barrier was found. Anderson and Hoffmann [229] have performed calculations on the adsorption of first row diatomic molecules (Li_2, B_2, C_2, N_2, O_2, F_2, CO, NO) and ethylene on the (100) surface of tungsten and nickel. The distance to the surface plane and the internuclear separation were kept constant and in most cases the diatomic molecules were placed perpendicularly to the surface. The dissociation was analyzed in terms of charge transfer between adsorbate and substrate, adsorbate bond-weakening and bond-formation with the metal atoms. These authors have also looked for active sites. Recently, Baetzold [230] has studied the dissociative adsorption of H_2 on various transition-metal substrates (Co, Ni, Cu, Pd and Ag), pure metals as well as alloys. The metal-H distance was kept constant, but the H-H bond was stretched from its equilibrium position. It appeared that the adsorption energy depends more strongly on cluster shape and on the orientation of the

H$_2$ molecule, than on cluster size. Baetzold analyzed the dissociation in terms of binding energies and found a lower-energy path for H$_2$ dissociation on group VIII than on group IB metals. He has also investigated the dissociative adsorption of BH$_3$-NH$_3$. It should be noted that the Extended Hückel method, as most MO methods, cannot be used to calculate interaction energies over a wide range of interatomic distances and gives a wrong dissociation limit, since it does not explicitly take into account electron repulsion and correlation effects. So, this technique is not very suited to study the dissociative chemisorption of molecules.

Deuss and Van der Avoird [231] have examined the dissociative chemisorption of H$_2$ by a simple effective 4-electron Ni$_2$H$_2$ model, in which the interaction energy was calculated by a perturbation method which took exchange forces into account and is comparable with the valence-bond method. They investigated the activity of the 3d and 4s electrons separately and suggested a possible rôle of the 3d component in the chemisorption binding in lowering the activation barrier for H$_2$ dissociation. This would explain, for instance, the different behaviour of nickel and copper. A similar approximate valence-bond model has been used by McCreery and Wolken [232] to study the chemisorption of H$_2$ on W(100). Very recently, Melius et al. [233] have investigated the chemisorption of H$_2$ on nickel, also using a Ni$_2$H$_2$ model. The electronic structure was calculated by ab initio methods which included electron correlation, the core electrons of Ni being replaced by an effective potential. As to the rôle of the 3d electrons in the dissociative chemisorption process, they suggested that the partly filled d-orbitals in the transition metal provide those symmetry states which according to the Woodward-Hoffmann rules could lead to dissociation without too high an activation barrier. The low activation energy reaction path would not be accessible for copper because of its completely filled d-band, which prevents the formation of such symmetry states. We refer to Chapter IV for a further discussion of these results.

In concluding this review of the various theoretical approaches to the surface and chemisorption problem we shall briefly discuss the relatively few attempts to tackle these problems by considering thin films or finite slabs. These films consist of a finite number of, generally infinite, atomic layers in which the two-dimensional translation symmetry parallel to the surfaces is preserved. They are used to study the electronic band structure, as compared to that of bulk solids, and the physical properties of thin films per se. Further, they provide a procedure to investigate specific surface properties (e.g. surface states) and chemisorption phenomena.

Many of the calculations have employed the tight-binding or LCAO method, by which particularly the surface bands of several semiconductors have been studied. Using an orthogonal next-nearest-neighbour as well as a nonorthogonal third-nearest-neighbour LCAO scheme, Alstrup [234,235] has extensively examined the occurrence of surface states on ideal, non-reconstructed Si (111) and (110) surfaces. Pandey and Phillips [236] have reported computations for Si (111) surfaces where relaxation of the surface layer was incorporated. In other tight-binding calculations the surface states on the (111) surface of diamond [237], the (111) and (100) surfaces of diamond-type semiconductors (C, Si, Ge and α-Sn) [238], and the (110) and (111) surfaces of Ge, GaAs and ZnSe [239,240] have been investigated. Cooper and Bennett [241] have examined the changes in the nature of d-band states in crystals of fcc transition and noble metals as the crystals become very thin. They studied the size and surface effects for (100) and (111) films by performing calculations for the Γ_{12} bands (i.e., the bands corresponding to the d atomic states of e_g-symmetry).

Messmer et al. [242] have used the EHT to calculate the band structure of a two-dimensional graphite sheet. To investigate the chemisorption of hydrogen, they introduced the concept of a molecular unit cell, consisting of a set of primitive unit cells of graphite and an adsorbate atom above the surface. They examined the changes in

the density of states caused by the adsorbate-surface interactions, by performing band structure calculations for an infinite, periodic array of molecular unit cells. We have studied by the EHT the hydrogen mono-layer adsorption on layer crystals of nickel and copper (see Chapter IV).

Alldredge and Kleinman [243,244] have developed a pseudo-potential method to calculate both surface and bulk states in thin films, which may be used for nearly-free-electron (NFE) metals. The crystal potential is described in terms of a nonlocal pseudopotential, which contains a superposition of nonlocal atomic pseudopotentials and an exchange/correlation term treated by the local approximation used in jellium studies [52,53]. By this method Alldredge and Kleinman [244] have carried out a self-consistent energy band calculation for a 13-layer (100) lithium film to study the charge density and surface electronic states. Caruthers et al. [245-248] have performed (non self-consistent) energy band calculations on 13-layer films of (100), (110) and (111) aluminum. The results were compared with a projection of the three-dimensional energy bands along the appropriate direction in order to examine the effects of both the surface and the finite thick-ness of the film. Caruthers and Kleinman [249] have extended the method to transition metals by supplementing the basis set of plane waves orthogonalized to the core wave functions, with a set of d-like functions defined within a "muffin-tin" radius of each atomic site. From their calculations on a 13-layer (100) iron film it appeared that the existence and symmetry of transition-metal surface states depend strongly on details of the potential, so that self-consistent calcula-tions are necessary for this study.

A similar self-consistent pseudopotential method has been developed by Cohen et al. [250]. It has been used to perform self-con-sistent calculations on Si (111) unrelaxed, relaxed and reconstructed surfaces [251]. Density of states curves for a 12-layer slab were ob-tained. Also the electronic structure of a metal-semiconductor inter-face has been investigated, considering a slab of Si with the (111) surfaces being exposed to a jellium of Al density on both sides [252].

A third formalism [253-256] to study crystal films follows a Green's-function procedure and can be considered as a generalization of the Korringa-Kohn-Rostoker (KKR) method [257,258] for band calculations of infinite systems or of the scattered wave formalism [176] for molecular calculations. An application to a monolayer film of copper has been presented by Kar and Soven [256].

References

[1] I. Tamm, Z. Physik 76, 849 (1932).

[2] W. Shockley, Phys. Rev. 56, 317 (1939).

[3] E.T. Goodwin, Proc. Cambridge Phil. Soc. 35, 221,232 (1939).

[4] S.G. Davison and J.D. Levine, in: *Solid State Physics*, edited by H. Ehrenreich, F. Seitz and D. Turnbull (Academic Press, New York, 1970), Vol. 25, p. 1.

[5] S.G. Davison and A.T. Amos, J. Chem. Phys. 43, 2223 (1965).

[6] S.G. Davison and H.T. Ho, Trans. Faraday Soc. 63, 812 (1967).

[7] J. Koutecký, J. Chem. Phys. 47, 5215 (1967).

[8] J. Koutecký, Trans. Faraday Soc. 54, 1038 (1958).

[9] T.B. Grimley, Advan. Catalysis 12, 1 (1960).

[10] S.G. Davison and Y.S. Huang, Surface Sci. 13, 337 (1969).

[11] E. Ruckenstein and Y.S. Huang, J. Catalysis 30, 309 (1973).

[12] J. Koutecký, Advan. Chem. Phys. 9, 85 (1965).
(Different resolvent formalisms are compared in a more recent paper: J. Koutecký, "Quantum theory of surface phenomena", to be published.)

[13] J. Koutecký, Phys. Rev. 108, 13 (1957).

[14] J. Koutecký and A. Fingerland, Collection Czech. Chem. Commun. 25, 1 (1960).

[15] J. Koutecký and M. Tomášek, Phys. Rev. 120, 1212 (1960).

[16] J. Koutecký, Surface Sci. 1, 280 (1964).

[17] J. Koutecký and M. Tomášek, Surface Sci. 3, 333 (1965).

[18] M. Tomášek, Czech. J. Phys. B 16, 828 (1966).

[19] M. Tomášek, in: *The Structure and Chemistry of Solid Surfaces*, edited by G.A. Somorjai (John Wiley and Sons, New York, 1969), p. 15-1.

[20] M. Tomášek, Surface Sci. 4, 471 (1966).

[21] M. Tomášek, Phys. Stat. Solidi (b) 16, 389 (1966).

[22] M. Tomášek and J. Koutecký, Intern. J. Quantum Chem. 3, 249 (1969).

[23] S. Freeman, Phys. Rev. B 2, 3272 (1970).

[24] J.D. Levine and S. Freeman, Phys. Rev. B 2, 3255 (1970).

[25] M. Tomášek and P. Mikušík, Phys. Rev. B 8, 410 (1973).

[26] V. Heine, Proc. Phys. Soc. 81, 300 (1963).

[27] V. Heine, Surface Sci. 2, 1 (1964).

[28] V. Heine, Proc. R. Soc. Lond. A 331, 307 (1972).

[29] R.O. Jones, Phys. Rev. Lett. 20, 992 (1968).

[30] I. Bartoš, Surface Sci. 15, 94 (1969).

[31] R.O. Jones, in ref. [19], p. 14-1.

[32] R.O. Jones, J. Phys. C: Solid State Phys. 5, 1615 (1972).

[33] F. Yndurain and M. Elices, Surface Sci. 29, 540 (1972).

[34] F. Flores and J. Rubio, J. Phys. C: Solid State Phys. 6, L258 (1973).

[35] D.S. Boudreaux, Surface Sci. 28, 344 (1971).

[36] F. Forstmann and J.B. Pendry, Z. Physik 235, 75 (1970).

[37] F. Forstmann and V. Heine, Phys. Rev. Lett. 24, 1419 (1970).

[38] J.D. Levine and P. Mark, Phys. Rev. 182, 926 (1969).

[39] A. van der Avoird, Thesis, Eindhoven, 1968.

[40] R.W. Gurney, Phys. Rev. 47, 479 (1935).

[41] J.W. Gadzuk, Surface Sci. 6, 133 (1967).

[42] J.W. Gadzuk, J.K. Hartman and T.N. Rhodin, Phys. Rev. B 4, 241 (1971).

[43] P.W. Anderson, Phys. Rev. 124, 41 (1961).

[44] M. Cini, Surface Sci. 52, 75 (1975).

[45] J.W. Muscat and D.M. Newns, J. Phys. C: Solid State Phys. 7, 2630 (1974).

[46] J. Bardeen, Phys. Rev. 49, 653 (1936).

[47] P. Hohenberg and W. Kohn, Phys. Rev. 136, B864 (1964).

[48] W. Kohn and L.J. Sham, Phys. Rev. 140, A1133 (1965).

[49] N.D. Lang, in: *Solid State Physics*, edited by H. Ehrenreich, F. Seitz and D. Turnbull (Academic Press, New York, 1973), Vol. 28, p. 225.

[50] A.J. Bennett and C.B. Duke, Phys. Rev. 160, 541 (1967).

[51] J.R. Smith, Phys. Rev. 181, 522 (1969).

[52] N.D. Lang and W. Kohn, Phys. Rev. B $\underline{1}$, 4555 (1970).

[53] N.D. Lang and W. Kohn, Phys. Rev. B $\underline{3}$, 1215 (1971).

[54] N.D. Lang, Phys. Rev. B $\underline{4}$, 4234 (1971).

[55] S.C. Ying, J.R. Smith and W. Kohn, Phys. Rev. B $\underline{11}$, 1483 (1975).

[56] H.B. Huntington, L.A. Turk and W.W. White III, Surface Sci. $\underline{48}$, 187 (1975).

[57] N.D. Lang and A.R. Williams, Phys. Rev. Lett. $\underline{34}$, 531 (1975).

[58] O. Gunnarsson, H. Hjelmberg and B.I. Lundquist, to be published.

[59] F. Garcia-Moliner and J. Rubio, J. Phys. C: Solid State Phys. $\underline{2}$, 1789 (1969).

[60] F. Garcia-Moliner and J. Rubio, Proc. R. Soc. Lond. A $\underline{324}$, 257 (1971).

[61] F. Yndurain and J. Rubio, Phys. Rev. Lett. $\underline{26}$, 138 (1971).

[62] I. Bartoš and B. Velický, Czech. J. Phys. B $\underline{24}$, 981 (1974).

[63] F. Flores, E. Louis and J. Rubio, J. Phys. C: Solid State Phys. $\underline{5}$, 3469 (1972).

[64] M. Elices, F. Flores, E. Louis and J. Rubio, J. Phys. C: Solid State Phys. $\underline{7}$, 3020 (1974).

[65] E. Louis and M. Elices, Phys. Rev. B $\underline{12}$, 618 (1975).

[66] D.S. Boudreaux, Phys. Rev. B $\underline{1}$, 4551 (1970).

[67] J.A. Appelbaum and D.R. Hamann, Phys. Rev. B $\underline{6}$, 2166 (1972).

[68] J.A. Appelbaum and D.R. Hamann, Phys. Rev. Lett. $\underline{31}$, 106 (1973); $\underline{32}$, 225 (1974).

[69] J.A. Appelbaum, G.A. Baraff and D.R. Hamann, Phys. Rev. B $\underline{11}$, 3822 (1975).

[70] J.A. Appelbaum, G.A. Baraff and D.R. Hamann, Phys. Rev. Lett. $\underline{35}$, 729 (1975).

[71] J.A. Appelbaum and D.R. Hamann, Phys. Rev. B $\underline{12}$, 1410 (1975).

[72] J.A. Appelbaum and D.R. Hamann, Phys. Rev. Lett. $\underline{34}$, 806 (1975).

[73] L. Hodges, R.E. Watson and H. Ehrenreich, Phys. Rev. B $\underline{5}$, 3953 (1972).

[74] K. Levin, A. Liebsch and K.H. Bennemann, Phys. Rev. B $\underline{7}$, 3066 (1973).

[75] P. Fulde, A. Luther and R.E. Watson, Phys. Rev. B $\underline{8}$, 440 (1973).

[76] H. Takayama, K. Baker and P. Fulde, Phys. Rev. B $\underline{10}$, 2022 (1974).

[77] F.J. Dyson, Phys. Rev. $\underline{75}$, 1736 (1949).

[78] G. Allan, Ann. Phys. (Paris) $\underline{5}$, 169 (1970).

[79] T.L. Einstein and J.R. Schrieffer, Phys. Rev. B $\underline{7}$, 3629 (1973).

[80] T.L. Einstein, Surface Sci. $\underline{45}$, 713 (1974).

[81] T.L. Einstein, Phys. Rev. B $\underline{12}$, 1262 (1975).

[82] D. Kalkstein and P. Soven, Surface Sci. $\underline{26}$, 85 (1971).

[83] G. Allan and P. Lenglart, Surface Sci. $\underline{15}$, 101 (1969).

[84] G. Allan and P. Lenglart, Surface Sci. $\underline{30}$, 641 (1972).

[85] J. Friedel, Nuovo Cimento, Suppl. $\underline{7}$, 287 (1958).

[86] W. Ho, S.L. Cunningham, W.H. Weinberg and L. Dobrzynski,
      Phys. Rev. B $\underline{12}$, 3027 (1975).

[87] W. Ho, S.L. Cunningham, W.H. Weinberg and L. Dobrzynski, to
      be published .

[88] W. Ho, S.L. Cunningham and W.H. Weinberg, Surface Sci.
      $\underline{54}$, 139 (1976).

[89] L.M. Falicov and F. Yndurain, J. Phys. C: Solid State Phys.
      $\underline{8}$, 147 (1975).

[90] L.M. Falicov and F. Yndurain, J. Phys. C: Solid State Phys.
      $\underline{8}$, 1563 (1975).

[91] F. Yndurain and L.M. Falicov, J. Phys. C: Solid State Phys.
      $\underline{8}$, 1571 (1975).

[92] K.C. Pandey and J.C. Phillips, Phys. Rev. Lett. $\underline{32}$, 1433 (1974).

[93] K.C. Pandey and J.C. Phillips, Phys. Rev. Lett. $\underline{34}$, 1450 (1975).

[94] F. Cyrot-Lackmann, J. Phys. Chem. Solids $\underline{29}$, 1235 (1968).

[95] F. Cyrot-Lackmann, J. Phys. (Paris) $\underline{31}$, Suppl. C 1, 67 (1970).

[96] F. Ducastelle and F. Cyrot-Lackmann, J. Phys. Chem. Solids
      $\underline{31}$, 1295 (1970).

[97] J.P. Gaspard and F. Cyrot-Lackmann, J. Phys. (Paris) $\underline{33}$, Suppl.
      C 3, 175 (1972).

[98] J.P. Gaspard and F. Cyrot-Lackmann, J. Phys. C: Solid State
      Phys. $\underline{6}$, 3077 (1973).

[99] F. Cyrot-Lackmann, Surface Sci. $\underline{15}$, 535 (1969).

[100] F. Cyrot-Lackmann and F. Ducastelle, Phys. Rev. B $\underline{4}$, 2406 (1971).

[101] G. Allan and M. Lannoo, Surface Sci. $\underline{40}$, 375 (1973).

[102] F. Cyrot-Lackmann, M.C. Desjonquères and J.P. Gaspard, J. Phys.
      C: Solid State Phys. $\underline{7}$, 925 (1974).

[103] M.C. Desjonquères and F. Cyrot-Lackmann, J. Phys. F: Metal
      Phys. $\underline{5}$, 1368 (1975).

[104] M.C. Desjonquères and F. Cyrot-Lackmann, to be published.

[105] R. Haydock, V. Heine and M.J. Kelly, J. Phys. C: Solid State Phys. **5**, 2845 (1972).

[106] R. Haydock and M.J. Kelly, Surface Sci. **38**, 139 (1973).

[107] R. Haydock, V. Heine and M.J. Kelly, J. Phys. C: Solid State Phys. **8**, 2591 (1975).

[108] R. Haydock, V. Heine, M.J. Kelly and J.B. Pendry, Phys. Rev. Lett. **29**, 868 (1972).

[109] V. Bortolani, C. Calandra and M.J. Kelly, J. Phys. C: Solid State Phys. **6**, L349 (1973).

[110] F. Yndurain, J.D. Joannopoulos, M.L. Cohen and L.M. Falicov, Solid St. Commun. **15**, 617 (1974).

[111] J.D. Joannopoulos and F. Yndurain, Phys. Rev. B **10**, 5164 (1974).

[112] T.B. Grimley, Proc. Phys. Soc. **90**, 751 (1967).

[113] D.M. Newns, Phys. Rev. **178**, 1123 (1969).

[114] B.J. Thorpe, Surface Sci. **33**, 306 (1972).

[115] D.M. Newns, Phys. Lett. **33A**, 43 (1970).

[116] S.G. Davison and Y.S. Huang, International Symposium on Characterization of Adsorbed Species in Catalytic Reactions, Ottawa, June 1974.

[117] T.B. Grimley, in: *Adsorption-Desorption Phenomena*, edited by F. Ricca (Academic Press, New York, 1972), p. 215.

[118] T.B. Grimley, J. Vac. Sci. Technol. **8**, 31 (1971).

[119] T.B. Grimley and B.J. Thorpe, J. Phys. F: Metal Phys. **1**, L4 (1971).

[120] G. Doyen and G. Ertl, Surface Sci. **43**, 197 (1974).

[121] J.W. Gadzuk, Surface Sci. **43**, 44 (1974).

[122] D.R. Penn, Surface Sci. **39**, 333 (1973).

[123] M.J. Kelly, J. Phys. C: Solid State Phys. **7**, L157 (1974).

[124] M.J. Kelly, Surface Sci. **43**, 587 (1974).

[125] T.B. Grimley and C. Pisani, J. Phys. C: Solid State Phys. **7**, 2831 (1974).

[126] T.B. Grimley, J. Phys. C: Solid State Phys. **3**, 1934 (1970).

[127] T.B. Grimley, in: *Proc. Int. School of Physics 'Enrico Fermi' Course LVIII*, edited by F.O. Goodman (Editrice Compositori, Bologna, 1974), p. 298.

[128] T.B. Grimley, Progr. Surface and Membrane Sci. **9**, 71 (1975).

[129] T.B. Grimley, Advanced Study Institute on Electronic Structure and Reactivity of Metal Surfaces, Namur (Belgium), Sept. 1975, to be published in the NATO Advanced Study Institute Series.

[130] T.B. Grimley and C.J.P. Newton, Phys. Lett. **51A**, 267 (1975).

[131] T.B. Grimley and B.J. Thorpe, Phys. Lett. **37A**, 459 (1971).

[132] J. Hubbard, Proc. R. Soc. Lond. A **276**, 238 (1963).

[133] R.H. Paulson and J.R. Schrieffer, Surface Sci. **48**, 329 (1975).

[134] E.A. Hyman, Phys. Rev. B **11**, 3739 (1975).

[135] A. Madhukar, Phys. Rev. B **8**, 4458 (1973).

[136] D. Penn, R. Gomer and M.H. Cohen, Phys. Rev. B **5**, 768 (1972).

[137] J.W. Gadzuk, Phys. Rev. B **10**, 5030 (1974).

[138] T.B. Grimley and G.F. Bernasconi, J. Phys. C: Solid State Phys. **8**, 2423 (1975).

[139] J.R. Schrieffer, J. Vac. Sci. Technol. **9**, 561 (1972).

[140] J.R. Schrieffer and R. Gomer, Surface Sci. **25**, 315 (1971).

[141] J.R. Schrieffer, in ref. [127], p. 250.

[142] W.G. Pollard, Phys. Rev. **60**, 578 (1941).

[143] T. Toya, J. Res. Inst. Catalysis (Japan) **6**, 308 (1958).

[144] K.F. Wojciechowski, Acta Phys. Polon. **29**, 119 (1966).

[145] K.F. Wojciechowski, Acta Phys. Polon. **33**, 363 (1968).

[146] D.M. Newns, Phys. Rev. Lett. **25**, 1575 (1970).

[147] A. Bagchi and M.H. Cohen, Phys. Rev. B **9**, 4103 (1974).

[148] A. Madhukar and B. Bell, Phys. Rev. Lett. **34**, 1631 (1975).

[149] R.A. van Santen, Surface Sci. **53**, 35 (1975).

[150] G. Blyholder and C.A. Coulson, Trans. Faraday Soc. **63**, 1782 (1967).

[151] T.L. Einstein, Phys. Rev. B **11**, 577 (1975).

[152] A.J. Bennett, J. Chem. Phys. **49**, 1340 (1968).

[153] T.B. Grimley and S.M. Walker, Surface Sci. **14**, 395 (1969).

[154] H.D. Hagstrum and G.E. Becker, J. Chem. Phys. **54**, 1015 (1971).

[155] G.E. Becker and H.D. Hagstrum, Surface Sci. **30**, 505 (1972).

[156] A. Zunger, J. Phys. C: Solid State Phys. **7**, 76 (1974).

[157] M.R. Hayns, Theoret. Chim. Acta (Berl.) **39**, 61 (1975).

[158] A.J. Bennett, B. McCarroll and R.P. Messmer, Phys. Rev. B **3**, 1397 (1971).

[159] C.M. Quinn and N.V. Richardson, J. Phys. C: Solid State Phys. **8**, L236 (1975).

[160] G.C. Bond, Platinum Metals Rev. **10**, 87 (1966).

[161] G.C. Bond, Disc. Faraday Soc. **41**, 200 (1966).

[162] J.B. Goodenough, Phys. Rev. 120, 67 (1960).

[163] Z. Knor and E.W. Müller, Surface Sci. 10, 21 (1968).

[164] D. Shopov, A. Andreev and D. Petkov, J. Catalysis
13, 123 (1969).

[165] D.J.M. Fassaert, H. Verbeek and A. van der Avoird, Surface Sci.
29, 501 (1972); reprinted in Chapter IV.

[166] W.H. Weinberg and R.P. Merrill, Surface Sci. 33, 493 (1972).

[167] G. Blyholder, J. Phys. Chem. 68, 2772 (1964).

[168] A. Laforgue, J. Rousseau and B. Imelik, Advan. Chem. Phys.
8, 141 (1965).

[169] H.H. Dunken and Ch. Opitz, Z. Physik. Chem. (Leipzig)
239, 161 (1968).

[170] H.H. Dunken and Ch. Opitz, Z. Physik. Chem. NF 60, 25 (1968).

[171] G. Blyholder and M.C. Allen, J. Am. Chem. Soc. 91, 3158 (1969).

[172] R. Hoffmann, J. Chem. Phys. 39, 1397 (1963).

[173] J.A. Pople and D.L. Beveridge, *Approximate Molecular Orbital
Theory* (McGraw-Hill, New York, 1970).

[174] H.F. Schaefer III, *The Electronic Structure of Atoms and
Molecules: A Survey of Rigorous Quantum Mechanical Results*
(Addison-Wesley, Reading, 1972).

[175] J.C. Slater, Advan. Quantum Chem. 6, 1 (1972).

[176] K.H. Johnson, Advan. Quantum Chem. 7, 143 (1973).

[177] D.E. Ellis and G.S. Painter, Phys. Rev. B 2, 2887 (1970).

[178] F.W. Averill and D.E. Ellis, J. Chem. Phys. 59, 6412 (1973).

[179] D. Lazarov and P. Markov, Surface Sci. 14, 320 (1969).

[180] J.G. Fripiat, K.T. Chow, M. Boudart, J.B. Diamond and K.H.
Johnson, to be published.

[181] H. Stoll, Arbeitsbericht des Instituts für Theoretische Chemie
der Universität Stuttgart, nr. 19, p. 101 (1972).

[182] A. Julg, M. Bénard, M. Bourg, M. Gillet and E. Gillet, Phys.
Rev. B 9, 3248 (1974).

[183] A. Zunger, J. Phys. C: Solid State Phys. 7, 96 (1974).

[184] D. House and P.V. Smith, J. Phys. F: Metal Phys. 3, 753 (1973).

[185] R.P. Messmer, S.K. Knudson, J.B. Diamond, C. Yang and K.H.
Johnson, as referred to by [180].

[186] G. Blyholder, Surface Sci. 42, 249 (1974).

[187] R.C. Baetzold, J. Chem. Phys. 55, 4363 (1971).

[188] R.C. Baetzold, J. Catalysis 29, 129 (1973).

[189] R.C. Baetzold and R.E. Mack, J. Chem. Phys. 62, 1513 (1975).

[190] G.S. Painter, P.J. Jennings and R.O. Jones, J. Phys. C: Solid State Phys. 8, L199 (1975).

[191] R.C. Baetzold, Surface Sci. 36, 123 (1973).

[192] R.C. Baetzold, J. Solid State Chem. 6, 352 (1973).

[193] Ch. Opitz and H.H. Dunken, Z. Physik Chem. (Leipzig) 249, 154 (1972).

[194] H. Kölbel and K.D. Tillmetz, Ber. Bunsenges. Phys. Chem. 76, 1156 (1972).

[195] H. Kölbel and K.D. Tillmetz, J. Catalysis 34, 307 (1974).

[196] P. Politzer and S.D. Kasten, Surface Sci. 36, 186 (1973).

[197] H. Arai and T. Kunugi, J. Catalysis 39, 294 (1975).

[198] A.B. Anderson, Chem. Phys. Lett. 35, 498 (1975).

[199] P.S. Bagus and H.F. Schaefer III, J. Chem. Phys. 58, 1844 (1973).

[200] P.R. Scott and W.G. Richards, J. Phys. B: Atom. Molec. Phys. 7, 500 (1974).

[201] P.R. Scott and W.G. Richards, J. Phys. B: Atom. Molec. Phys. 7, 1679 (1974).

[202] P.R. Scott and W.G. Richards, J. Chem. Phys. 63, 1690 (1975).

[203] G.A. Henderson, G. Das and A.C. Wahl, J. Chem. Phys. 63, 2805 (1975).

[204] A.B. Kunz, M.P. Guse and R.J. Blint, J. Phys. B: Atom. Molec. Phys. 8, L358 (1975).

[205] R.J. Blint, A.B. Kunz and M.P. Guse, Chem. Phys. Lett. 36, 191 (1975).

[206] A.J. Bennett, B. McCarroll and R.P. Messmer, Surface Sci. 24, 191 (1971).

[207] B. McCarroll and R.P. Messmer, Surface Sci. 27, 451 (1971).

[208] P. Markov and D. Lazarov, Compt. Rend. Acad. Bulgare Sci. 22, 455 (1969).

[209] A.B. Kunz, D.J. Mickish and P.W. Deutsch, Solid St. Commun. 13, 35 (1973).

[210] C.W. Bauschlicher Jr., D.H. Liskow, C.F. Bender and H.F. Schaefer III, J. Chem. Phys. 62, 4815 (1975).

[211] J.C. Robertson and C.W. Wilmsen, J. Vac. Sci. Technol. 8, 53 (1971).

[212] D.J.M. Fassaert and A. van der Avoird, Surface Sci. 55, 313 (1976); reprinted in Chapter IV.

[213] G. Blyholder, J. Chem. Phys. 62, 3193 (1975).

[214] T. Tanabe, H. Adachi and S. Imoto, to be published.

[215] R.P. Messmer, C.W. Tucker and K.H. Johnson, Surface Sci. 42, 341 (1974).

[216] I.P. Batra and O. Robaux, Surface Sci. 49, 653 (1975).

[217] J.C. Robertson and C.W. Wilmsen, J. Vac. Sci. Technol. 9, 901 (1972).

[218] J.T. Waber, H. Adachi, F.W. Averill and D.E. Ellis, Japan. J. Appl. Phys. Suppl. 2, Pt. 2, 695 (1974).

[219] G. Blyholder, J. Phys. Chem. 79, 756 (1975).

[220] L.W. Anders, R.S. Hansen and L.S. Bartell, J. Chem. Phys. 59, 5277 (1973).

[221] L.W. Anders, R.S. Hansen and L.S. Bartell, J. Chem. Phys. 62, 1641 (1975).

[222] W. Sarholz, D. Baresel and G. Schulz-Ekloff, Surface Sci. 42, 574 (1974).

[223] N. Rösch and T.N. Rhodin, Phys. Rev. Lett. 32, 1189 (1974).

[224] T.B. Grimley and M. Torrini, J. Phys. C: Solid State Phys. 6, 868 (1973).

[225] W.H. Weinberg, J. Catalysis 28, 459 (1973).

[226] W.H. Weinberg and R.P. Merrill, Surface Sci. 39, 206 (1973).

[227] W.H. Weinberg, H.A. Deans and R.P. Merrill, Surface Sci. 41, 312 (1974).

[228] J.B. Moffat, J. Colloid Interface Sci. 44, 415 (1973).

[229] A.B. Anderson and R. Hoffmann, J. Chem. Phys. 61, 4545 (1974).

[230] R.C. Baetzold, Surface Sci. 51, 1 (1975).

[231] H. Deuss and A. van der Avoird, Phys. Rev. B 8, 2441 (1973).

[232] J.H. McCreery and G. Wolken Jr., J. Chem. Phys. 63, 2340 (1975).

[233] C.F. Melius, J.W. Moskowitz, A.P. Mortola, M.B. Baillie and M.A. Ratner, to be published.

[234] I. Alstrup, Surface Sci. 20, 335 (1970).

[235] I. Alstrup, Phys. Stat. Solidi (b) 45, 209 (1971).

[236] K.C. Pandey and J.C. Phillips, Solid St. Commun. 14, 439 (1974).

[237] D. Pugh, Phys. Rev. Lett. 12, 390 (1964).

[238] K. Hirabayashi, J. Phys. Soc. Japan 27, 1475 (1969).

[239] J.D. Joannopoulos and M.L. Cohen, Phys. Lett. 49A, 391 (1974).

[240] D.J. Chadi and M.L. Cohen, Phys. Rev. B 11, 732 (1975).

[241] B.R. Cooper and A.J. Bennett, Phys. Rev. B 1, 4654 (1970).

[242] R.P. Messmer, B. McCarroll and C.M. Singal, J. Vac. Sci. Technol. 9, 891 (1972).

[243] G.P. Alldredge and L. Kleinman, Phys. Rev. Lett. 28, 1264 (1972).

[244] G.P. Alldredge and L. Kleinman, Phys. Rev. B 10, 559 (1974).

[245] E. Caruthers, L. Kleinman and G.P. Alldredge, Phys. Rev. B 8, 4570 (1973).

[246] E. Caruthers, L. Kleinman and G.P. Alldredge, Phys. Rev. B 9, 3325 (1974).

[247] E. Caruthers, L. Kleinman and G.P. Alldredge, Phys. Rev. B 9, 3330 (1974).

[248] E. Caruthers, L. Kleinman and G.P. Alldredge, Phys. Rev. B 10, 1252 (1974).

[249] E. Caruthers and L. Kleinman, Phys. Rev. Lett. 35, 738 (1975).

[250] M.L. Cohen, M. Schlüter, J.R. Chelikowsky and S.G. Louie, Phys. Rev. B 12, 5575 (1975).

[251] M. Schlüter, J.R. Chelikowsky, S.G. Louie and M.L. Cohen, Phys. Rev. Lett. 34, 1385 (1975).

[252] S.G. Louie and M.L. Cohen, Phys. Rev. Lett. 35, 866 (1975).

[253] M. Scherer and P. Phariseau, Surface Sci. 18, 298 (1969).

[254] J.L. Beeby, J. Phys. C: Solid State Phys. 6, 1242 (1973).

[255] W. Kohn, Phys. Rev. B 11, 3756 (1975).

[256] N. Kar and P. Soven, Phys. Rev. B 11, 3761 (1975).

[257] J. Korringa, Physica 13, 392 (1947).

[258] W. Kohn and N. Rostoker, Phys. Rev. 94, 1111 (1954).

Chapter III

**RESOLVENT METHOD FOR QUANTITATIVE CALCULATIONS
ON SURFACE STATES AND ADSORPTION**

Resolvent method for quantitative calculations on surface states and adsorption: General method

A van der Avoird, S P Liebmann,* and D J M Fassaert

Institute of Theoretical Chemistry University of Nijmegen, Nijmegen, The Netherlands

(Received 1 April 1974)

A new method is presented for the calculation of surface and adsorption effects on one-electron states in crystals Conceptually, this method is similar to the Koster-Slater resolvent method for impurity states, which has often been applied to surface states in semi-infinite crystals The elaboration is very different, however The proposed scheme works for finite crystals, the resolvent matrix is calculated numerically instead of analytically, and the applicability of the method depends on a suitable algorithm for the numerical solution of the Koster-Slater equations Such an algorithm is described In comparison with the resolvent method for semi-infinite crystals, this method permits a more quantitative treatment of real crystals, such as transition metals or semiconductors On the other hand, compared with standard molecular-orbital methods on finite clusters, it can handle much larger crystals

I INTRODUCTION

Although many important processes occur on the surfaces of solids, as for instance chemisorption and heterogeneous catalysis on transition metals or semiconductors, the understanding of these processes is far from being complete. Experimentally, more and more data are becoming available for adsorption on well-defined surfaces, [1-11] but the interpretation of these data is very difficult. From this situation arises a considerable need for theoretical calculations on surfaces and adsorption and, in particular, for improvement of the methods to yield more quantitative information on real crystals.

The majority of the quantum-theoretical methods for the study of surface and adsorption states on crystals are based on the linear combination of atomic orbitals (LCAO) or tight-binding [12] formalism. They can be divided into two types: the "solid-state" approach and the "molecular" approach. The first group starts from solid-state band calculations on infinite periodic crystals (satisfying Born–Von Kármán cyclic boundary conditions with an infinite number of unit cells). These infinite crystals are then reduced to semi-infinite crystals with a surface, and the influence of the perturbation which effects this surface formation is mostly taken into account by a resolvent or Green's-function technique. A description of these methods can be found in several review articles. [13,14] The resolvent method applied to this problem is based on Koster-Slater treatment of impurity states in crystals. [15] This type of approach requires the use of an analytical resolvent, to be constructed from the infinite-crystal solutions For this reason one has to introduce various approximations such as neglect of nonorthogonality of the basis orbitals and of many interactions between them. In practice, one often falls back on the use of a model Hamilto-

nian depending only on a few parameters, [16-23] or one calculates model crystals with one orbital per atom, [24-26] or even one-dimensional chains. [13,27] The same type of model crystals have also been studied by different methods, without using the resolvent technique. [28-33] It is doubtful whether such models will yield a valuable description of real crystals such as transition metals, which have rather localized d electrons on the one hand, and diffuse conduction electrons on the other. Moreover, these methods only calculate "pure" surface or adsorption states with wave functions localized at the surface and energies lying outside the crystal bands. Most states, however, remain within the crystal bands and are not completely localized, but are still affected by surface formation or by adsorption. As Koutecký [13] points out, these states must be included when calculating total surface energies or adsorption energies: although they shift only by infinitely small amounts, we have an infinite number of them (in the semi-infinite crystal model).

The second class of methods is of the molecular type Assuming that the effects of the surface or adsorption are localized, which is probably true in many cases and has been confirmed both by theory [34-36] and experiment, [3,4,7,10] one applies molecular-orbital methods to a cluster of crystal atoms, possibly interacting with one or more adsorbed atoms. [37-43] Although this approach takes into account all interactions within a (semiempirical) molecular-orbital (MO) formalism, it suffers from the drawback that the clusters must remain rather small (up to about 15 transition-metal atoms or 30 first- or second-row atoms). This gives rise to undesirable boundary effects. One can try to compensate for such effects, for instance, by saturating the "dangling" bonds with hydrogen atoms or by connecting them to other dangling bonds, [39] but it

would be better to increase also the size of the clusters.

As we are especially interested in chemisorption and catalysis on transition-metal surfaces, in which both the d electrons and the conduction electrons play a role,[40,44] we have developed a method which does not require the simplifying parametrization of the "solid-state" methods and still calculates larger crystals than the "molecular" methods. It avoids unwanted boundary effects and, moreover, it calculates all one-electron states in crystals having a surface, possibly with adsorption, also those states which are not strictly localized at the surface. By application of the presented method one can obtain quantitative information about properties of solid surfaces and about adsorption phenomena. This might also be helpful for the interpretation and correlation of experimental data for adsorbed atoms and molecules.[1-11]

II DESCRIPTION OF THE METHOD

The proposed method works for finite crystals (in practice up to about 1000 atoms) with two surfaces parallel to a chosen crystal plane. This plane is defined by two elementary lattice translations, $\vec{a}_1$ and $\vec{a}_2$, which can be the primitive translations of the bulk crystal or linear combinations of them.[13] The third elementary translation $\vec{a}_3$, which is nonparallel to the surface, carries from one crystal layer to another. The number of layers is finite; the dimensions of the crystal parallel to the surface could be infinite, but we find it advantageous to keep these dimensions finite as well, while still avoiding undesirable boundary effects by imposing Born–Von Kármán cyclic boundary conditions on the finite number of unit cells $(\vec{a}_1, \vec{a}_2)$. This implies that we assume the crystal wave functions to satisfy the relations

$$\psi(\vec{r}) \equiv \psi(\vec{r} - N_1\vec{a}_1) \equiv \psi(\vec{r} - N_2\vec{a}_2) , \qquad (1)$$

N_1 and N_2 being the number of unit cells in the directions $\vec{a}_1$ and $\vec{a}_2$, respectively. Working in an LCAO model, we denote the basis atomic orbitals as

$$| \chi_p(m_1, m_2, m_3) \rangle = \chi_p(\vec{r} - m_1\vec{a}_1 - m_2\vec{a}_2 - m_3\vec{a}_3) , \quad (2)$$

where the index $p = 1, \ldots, \nu$ labels the different atomic orbitals in one unit cell with the origin $(m_1\vec{a}_1 + m_2\vec{a}_2 + m_3\vec{a}_3)$. Now, because of the periodic boundary conditions the crystal wave functions can be expressed as

$$| \psi^{k_1, k_2} \rangle = \sum_{m_3} \sum_{p=1}^{\nu} | a_p^{k_1, k_2}(m_3) \rangle c_{p,m_3}^{k_1, k_2} ,$$

with $\qquad\qquad\qquad\qquad\qquad\qquad\qquad (3)$

$$| a_p^{k_1, k_2}(m_3) \rangle = \sum_{m_1=1}^{N_1} \sum_{m_2=1}^{N_2} | \chi_p(m_1, m_2, m_3) \rangle e^{i(k_1 m_1 + k_2 m_2)}.$$

The summation over m_3 runs over all layers of the crystal. The two-dimensional Bloch orbitals $| a_p^{k_1, k_2}(m_3) \rangle$ are called "layer orbitals"; the components of the wave vector, k_1 and k_2, must satisfy

$$k_1 = 2\pi n_1/N_1 , \qquad k_2 = 2\pi n_2/N_2$$

with

$$n_1 = 1, 2, \ldots, N_1, \quad n_2 = 1, 2, \ldots, N_2.$$

Expression (3) is equivalent to the statement that layer orbitals with different (k_1, k_2) are noninteracting, which is so because they belong to different irreducible representations of the finite cyclic group that is the translation group of this crystal. So we see that the periodic boundary conditions, besides eliminating end effects, result in a considerable simplification of the wave equations, also for finite crystals. Actually, this assumption of finite, but cyclic, crystals is nonphysical, which is probably not very serious, however, as it corresponds exactly to collecting a finite selection from the infinite crystal solutions—namely, those Bloch waves of which the wavelength is a divisor of the total crystal dimensions.

The method for calculating the one-electron states of this crystal now proceeds as follows. We start with a crystal of N_3 layers, which is also periodic in the third ($\vec{a}_3$) direction. This completely periodic crystal is called the "unperturbed" system. The extra periodicity facilitates the solution of the secular equations for this system if we use three-dimensional Bloch orbitals as a basis:

$$| b_p^{k_1, k_2, k_3} \rangle = \sum_{m_3=1}^{N_3} | a_p^{k_1, k_2}(m_3) \rangle e^{i k_3 m_3} ,$$

with $\qquad\qquad\qquad\qquad\qquad\qquad\qquad (4)$

$$k_3 = 2\pi n_3/N_3 , \qquad n_3 = 1, 2, \ldots, N_3$$

We then define a perturbation $V = V^S + V^T$ which has the following effects·

(i) V^S removes so many layers from the periodic crystal that the two surface layers on both sides of the crystal interact only with inside layers. Thus we have created two "Shockley" surfaces,[45] just as the removal of a segment from a circle creates two "ends."

(ii) V^T adds the effect of a surface potential to the atoms near the surface. If this effect is nonzero, we shall speak of "Tamm" surfaces.[46]

This perturbation effects complete layers so that the periodicity parallel to the surface is conserved. The influence of the perturbation is taken into account in an exact way by the resolvent or Green's-function method, the resolvent being constructed from the "unperturbed" periodic crystal solutions. The combination of this method with the LCAO model was first used by Lifshitz[47] and by Baldock[30]

and formulated more generally by Koster and Slater.[15] In our case, we obtain a set of simultaneous equations containing the resolvent matrix and the perturbation matrix over layer orbitals, which we shall call the "Koster-Slater equations." These equations can be regarded as the matrix representation of a homogeneous integral equation.[48] The Koster-Slater treatment of the LCAO problem, which in fact is a way to deal with the effect of "local" changes in the secular matrix, also shows some resemblance to a matrix-partitioning technique by Löwdin.[49]

In case of adsorption, we define an extra unperturbed problem which consists of a set of secular equations for noninteracting adsorbate layers. Adding the interactions between the crystal and the adsorbate layers and the interactions among different adsorbate layers to the perturbation, i. e., $V = V^S + V^T + V^A$, we can also take adsorption effects into account by the resolvent method. As long as the adsorbed layers have the same two-dimensional periodicity as the crystal layers, all equations can be solved for each (k_1, k_2) separately.

Conceptually, this method is similar to the semi-infinite crystal treatments.[13,14] The practical elaboration is very different, however, for the following reasons:

(i) All matrix elements between atomic orbitals are calculated explicitly, within a given (possibly semiempirical) LCAO model. An arbitrary range can be specified, outside which the interactions are neglected. (We have used for this range, for instance, the fourth-nearest-neighbor distance for the fcc crystals nickel and copper.) We work with nonorthogonal basis functions because orthogonal orbitals, even of the localized type such as Löwdin[50] or Wannier[51] orbitals, always involve some amount of delocalization. This effect is usually neglected, but it can be quite large—for instance, in case of conduction electrons.

(ii) We do not require the unperturbed problem to be solved analytically. Instead, we use a numerical method (matrix diagonalization) to obtain these solutions from a set of secular equations.

(iii) The Koster-Slater equations which are constructed from a numerical resolvent matrix (and perturbation matrix) must be solved numerically as well. The dimension of these equations is determined by the number of layers which are directly affected by the surface or by adsorption; so it is smaller than the dimension of the secular problem over all layer orbitals. Since the Koster-Slater equations are nonlinear in the energy, however, the applicability of the method depends on a suitable algorithm for their numerical solution. We have found one in the procedure developed by Williams[52] for solving the Korringa-Kohn-Rostoker (KKR) equations[53,54] in solid-state band calcula-

tions. Although the physical background of these equations is quite different from the surface or adsorption problem, they have almost the same mathematical structure as the Koster-Slater equations occurring in our problem. In the next sections the latter equations will be derived for surfaces and for adsorption, in a manner which is generalized to nonorthogonal basis functions. We bring them into a standard form adapted to the algorithm just mentioned and we show the function of this algorithm. Because of the special character of our problem, where the perturbation has to annihilate interactions between different nonorthogonal orbitals, the perturbation matrix in the resolvent method depends on the (unknown) energy of the perturbed problem, and therefore Williams's algorithm had to be generalized.

III SURFACES

Since the periodicity of the crystal permits the solution of all equations for each two-dimensional wave vector (k_1, k_2) separately, we shall omit these indices in the notation for the layer orbitals

$$|a_p(m)\rangle = |a_p^{k_1, k_2}(m)\rangle ,$$

and for the Bloch orbitals   (5)

$$|b_p^k\rangle = |b_p^{k_1, k_2, k}\rangle .$$

Except for the calculation of the matrix elements, the three-dimensional-crystal problem becomes identical to the calculation of a linear chain.

The "unperturbed" crystal is described in terms of layer orbitals by the following secular equations:

$$\sum_{m'=1}^{N_3} \sum_{p'=1}^{\nu} [\langle a_p(m)|H|a_{p'}(m')\rangle$$
$$- E_i^{(0)}\langle a_p(m)|a_{p'}(m')\rangle]c_{p'i}^{(0)}(m') = 0 ,$$
$$m=1,\ldots,N_3, \quad p=1,\ldots,\nu . \quad (6)$$

The solutions $E_i^{(0)}$ and $c_{pi}^{(0)}(m)$ are numbered by $i = 1, \ldots, N_3\nu$. The explicit form of the one-electron Hamiltonian H depends on the type of LCAO method used. Taking advantage of the periodicity of the unperturbed crystal, one can solve, instead of this $(N_3\nu)$-dimensional secular problem, a set of N_3 secular problems of dimension ν over Bloch orbitals:

$$\sum_{p'=1}^{\nu} [\langle b_p^k|H|b_{p'}^k\rangle - E_j^{(0)}(k)\langle b_p^k|b_{p'}^k\rangle]c_{p'j}^{(0)}(k) = 0 ,$$
$$p=1,\ldots,\nu . \quad (7)$$

The solutions are now labelled by $j = 1, \ldots, \nu$ and $k = 2\pi n_3/N_3$, with $n_3 = 1, \ldots, N_3$. The solutions of Eq. (6) can then be expressed as

$$E_i^{(0)} = E_j^{(0)}(k) ,$$
$$c_{pi}^{(0)}(m) = e^{ikm}c_{pj}^{(0)}(k) , \quad (8)$$

where i, j, and k run as indicated above. The eigenvectors are orthogonal and are assumed to be normalized:

$$\sum_{p=1}^{\nu} \sum_{p'=1}^{\nu} c_{pi}^{(0)}(k)^* \langle b_p^k | b_{p'}^{k'} \rangle c_{p'j}^{(0)}(k') = \delta_{kk'} \delta_{jj'} , \qquad (9)$$

$$\sum_{m=1}^{N_3} \sum_{p=1}^{\nu} \sum_{m'=1}^{N_3} \sum_{p'=1}^{\nu} c_{pi}^{(0)}(m)^* \langle a_p(m) | a_{p'}(m') \rangle c_{p'i}^{(0)}(m') = \delta_{ii'} .$$

From now on, we shall work only in terms of layer orbitals and introduce a compact matrix notation (matrices are denoted by capitals, column vectors by small letters). The indices run both over layers ($m = 1, \ldots, N_3$) and over atomic orbitals ($p = 1, \ldots, \nu$). The unperturbed equations (6) read

$$(\underline{H}^{(0)} - E_i^{(0)} \underline{S}^{(0)}) \underline{c}_i^{(0)} = \underline{0} , \qquad (10)$$

with $E_i^{(0)}$ and $c_i^{(0)}$ given by (8).

For the real system of interest, i.e., a crystal with two surfaces, the energy E and the wave function $\underline{c}$ (in terms of layer orbitals) are to be determined from the equation

$$(\underline{H} - E\underline{S})\underline{c} = \underline{0} . \qquad (11)$$

The matrices $\underline{H}$ and $\underline{S}$ are changed with respect to $\underline{H}^{(0)}$ and $\underline{S}^{(0)}$ only in a few parts. In order to express these changes in mathematical form, it is convenient to distinguish some subsystems in the original crystal of N_3 layers (see Fig. 1).

The subsystem $\Re$ contains the layers which are removed from the periodic crystal by the Shockley perturbation V^S in order to create a crystal with two surfaces. The remaining crystal is denoted by $\mathfrak{C}$. In this crystal a set of outer layers $\mathfrak{O}$ is directly affected by this removal (because they were interacting with $\Re$) and/or by the Tamm perturbation V^T. Projection matrices for these systems ($\underline{P}^R$, $\underline{P}^C$, $\underline{P}^O$, $\underline{P}^{C-O}$) are defined as follows[55]: Let $\underline{P}^m$ be a $(N_3 \nu) \times (N_3 \nu)$ dimensional matrix with a $\nu \times \nu$ unit matrix on the diagonal for layer m and zero otherwise. Then, for a given subsystem $\mathfrak{X}$

$$\underline{P}^X = \sum_{m \in \mathfrak{X}} \underline{P}^m . \qquad (12)$$

These projection matrices are idempotent, mutually exclusive, and form the following resolution of the $(N_3 \nu) \times (N_3 \nu)$ identity matrix:

$$\underline{I} = \underline{P}^R + \underline{P}^C = \underline{P}^R + \underline{P}^O + \underline{P}^{C-O} . \qquad (13)$$

The changes in $\underline{H}$ and $\underline{S}$ can now be written as

by V^S: $\quad \Delta \underline{H}^S = -\underline{P}^R \underline{H}^{(0)} \underline{P}^O - \underline{P}^O \underline{H}^{(0)} \underline{P}^R ,$

$$\Delta \underline{S}^S = -\underline{P}^R \underline{S}^{(0)} \underline{P}^O - \underline{P}^O \underline{S}^{(0)} \underline{P}^R ;$$

by V^T: $\quad \Delta \underline{H}^T = \underline{P}^O \underline{T} \underline{P}^O ,$

$$\Delta \underline{S}^T = \underline{0} \qquad (14)$$

The matrix $\underline{T}$ describes the effects of the surface

potential V^T which are localized in the outer layers $\mathfrak{O}$. If the structure of these outer layers would be changed with respect to the bulk structure, the overlap matrix $\Delta \underline{S}^T$ would be nonzero as well. The fact that $\underline{H}$ and $\underline{S}$ are only locally modified (see Fig. 2) is now expressed by means of projection matrices. Because of this fact, it is advantageous, instead of solving the new secular problem (11), to use the resolvent technique.[13,14] Define the perturbation matrix

$$\begin{aligned}
\underline{V}(E) &= \underline{V}^S(E) + \underline{V}^T , \\
&= \Delta \underline{H} - E \Delta \underline{S} , \\
&= -\underline{P}^R(\underline{H}^{(0)} - E\underline{S}^{(0)})\underline{P}^O \\
&\quad -\underline{P}^O(\underline{H}^{(0)} - E\underline{S}^{(0)})\underline{P}^R + \underline{P}^O \underline{T} \underline{P}^O , \qquad (15)
\end{aligned}$$

and the resolvent matrix

$$\underline{G}(E) = \sum_{i=1}^{N_3 \nu} \underline{c}_i^{(0)} (E - E_i^{(0)})^{-1} \underline{c}_i^{(0)\dagger} , \qquad (16)$$

with $E_i^{(0)}$ and $\underline{c}_i^{(0)}$ being the solutions of the unperturbed problem (10). Both $\underline{V}(E)$ and $\underline{G}(E)$ depend on the energy E of the perturbed system, which must still be determined. Writing the perturbed equations (11) as

$$\underline{V}(E)\underline{c} = -(\underline{H}^{(0)} - E\underline{S}^{(0)})\underline{c} , \qquad (17)$$

multiplying this by $\underline{G}(E)$, and using the relation

$$-\underline{G}(E)(\underline{H}^{(0)} - E\underline{S}^{(0)}) = \underline{I} , \qquad (18)$$

which is proved by substituting (16), (10), and the normalization condition (9), we obtain the Koster-Slater equations

$$\underline{G}(E)\underline{V}(E)\underline{c} = \underline{c} \qquad (19)$$

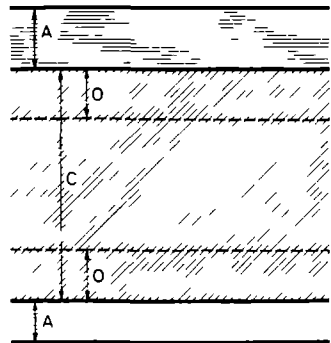Although this Koster-Slater problem still has the same dimension as the secular problem (11), this

FIG. 1. Schematic drawing of the crystal with adsorbed layers. Layers $\Re$ are not shown because they are nonphysical, they were only added to make the unperturbed crystal periodic.

can be easily reduced if we introduce the following properties:

(i) After removal of the layers $\mathfrak{R}$, some solutions of the perturbed equations are localized on $\mathfrak{R}$, others on $\mathfrak{C}$. We are interested in the latter, which satisfy the relations

$$\underline{P}^R\underline{c} \approx \underline{0}, \qquad \underline{P}^C\underline{c} = \underline{c} \tag{20}$$

(ii) The matrix $\underline{V}(E)$ contains many blocks which are zero, as expressed by (15) and shown in Fig. 2.

Usually,[13,14] Eqs. (19) are projected by $\underline{P}^O$ and then solved in the subspace $\mathfrak{O}$. In view of our algorithm for numerical solution of these equations, which applies to Hermitian matrices, we multiply the equations (19) by $\underline{P}^O\underline{V}(E)$, substitute (15) and (20), and use the properties of the projection matrices (13), to obtain

$$\underline{P}^O\underline{W}(E)\underline{P}^O\underline{c} \quad \{\underline{P}^O[\underline{V}^S(E)\underline{P}^R + \underline{V}^T\underline{P}^O]\underline{G}(E)$$
$$\times[\underline{P}^O\underline{V}^T + \underline{P}^R\underline{V}^S(E)]\underline{P}^O - \underline{P}^O\underline{V}^T\underline{P}^O\}\underline{c} = \underline{0} . \tag{21}$$

The matrix $\underline{P}^O\underline{W}(E)\underline{P}^O$ contains zeroes except for the submatrix corresponding to the outer crystal layers $\mathfrak{O}$. Therefore we can reduce Eqs. (21) to a smaller set, only over the space $\mathfrak{O}$.

$$\underline{W}^O(E)\underline{c}^O = \underline{0} , \tag{22}$$

where $\underline{W}^O(E)$ is the (Hermitian) nonzero submatrix of $\underline{P}^O\underline{W}(E)\underline{P}^O$ over the layers $\mathfrak{O}$. The equations for the perturbed problem have now been simplified as much as possible and prepared into such a form that a slightly generalized version of Williams's algorithm can be applied to solve for the energies E. These can be substituted into (21) or (19) and the coefficients $\underline{c}$ can be calculated by standard methods (solving a set of homogeneous linear equations).

IV ADSORPTION

On the crystal of the previous section we adsorb N layers of atoms of a different type. These layers are assumed to have the same periodicity in the $\vec{a}_1$ and $\vec{a}_2$ directions as the crystal, so that we can construct layer orbitals

$$a_q(n)\rangle \quad |a_q^{k_1,k_2}(n)\rangle$$
$$- \sum_{m_1=1}^{\nu_1}\sum_{m_2=1}^{\nu_2}|\chi_q(m_1, m_2, n)\rangle e^{i(k_1m_1+k_2m_2)} , \tag{23}$$

which obey the same periodic boundary conditions (1). Atomic orbitals are labelled by $q = 1, \ldots, \mu$; adsorbed layers by $n = 1, \ldots, N$. The space spanned by the adsorbed-layer orbitals is denoted by $\mathfrak{a}$, the corresponding projection matrix by

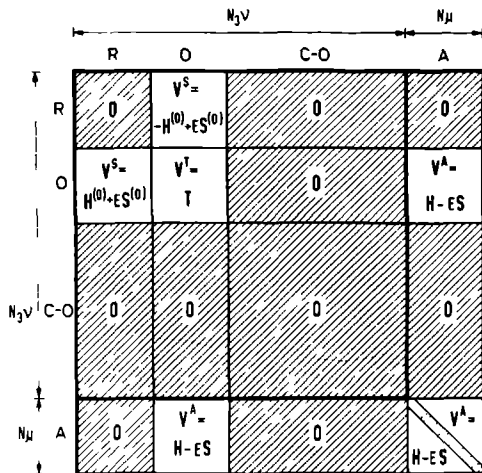$$\underline{P}^A \quad \sum_{n=1}^{\nu}\underline{P}^n . \tag{24}$$

FIG 2. Block structure of the perturbation matrix $\underline{V}$

Using a matrix notation, we now imply the indices to run over N_3 crystal layers with ν layer orbitals each and over N adsorbed layers with μ layer orbitals. Consequently, the resolution of the identity matrix becomes

$$\underline{I} = \underline{P}^R + \underline{P}^C + \underline{P}^A ,$$
$$= \underline{P}^R + \underline{P}^O + \underline{P}^{C-O} + \sum_{n=1}^{N}\underline{P}^n . \tag{25}$$

Adsorption effects can also be treated by the resolvent method. Unless N is very large, it is most convenient to define an unperturbed problem of isolated adsorbate layers,[56] in addition to the unperturbed crystal problem described by (6) and (7). For an adsorbate layer n we write

$$\sum_{q'=1}^{\mu}(\langle a_q(n)|H|a_{q'}(n)\rangle$$
$$- E_i^{(0)}(n)\langle a_q(n)|a_{q'}(n)\rangle)c_i^{(0)}(n) = 0 , \tag{26}$$

where the solutions are numbered by $l = 1, \ldots, \mu$. For the total unperturbed system, the secular problem reads

$$(\underline{P}^R + \underline{P}^C)[\underline{H}^{(0)} - E_i^{(0)}\underline{S}^{(0)}](\underline{P}^R + \underline{P}^C)\underline{c}_i^{(0)}$$
$$+ \sum_{n=1}^{N}\underline{P}^n[\underline{H}^{(0)} - E_i^{(0)}(n)\underline{S}^{(0)}]\underline{P}^n\underline{c}_i^{(0)}(n) = \underline{0} . \tag{27}$$

The perturbation V^A which adds the interactions between the crystal and the adsorbate layers and between adsorbate layers among each other, corresponds to the following matrix:

$$\underline{V}^A(E) = \underline{\Delta H}^A - E\underline{\Delta S}^A,$$

$$= \underline{P}^A(\underline{H} - E\underline{S})\underline{P}^O + \underline{P}^O(\underline{H} - E\underline{S})\underline{P}^A + \underline{P}^A(\underline{H} - E\underline{S})\underline{P}^A$$

$$- \sum_{n=1}^{N} \underline{P}^n(\underline{H}^{(0)} - E\underline{S}^{(0)})\underline{P}^n . \tag{28}$$

We have assumed that the direct interactions with the adsorbed atoms are restricted to the outer crystal layers ϴ. If necessary, the set ϴ is extended with respect to the previous section. The resolvent matrix derived from the unperturbed problem (27) reads

$$\underline{G}(E) = (\underline{P}^R + \underline{P}^C)\left(\sum_{i=1}^{N3\nu} \underline{c}_i^{(0)}(E - E_i^{(0)})^{-1}\underline{c}_i^{(0)\dagger}\right)(\underline{P}^R + \underline{P}^C) + \sum_{n=1}^{N} \underline{P}^n\left(\sum_{i=1}^{\mu} \underline{c}_i^{(0)}(n)[E - E_i^{(0)}(n)]^{-1}\underline{c}_i^{(0)}(n)^\dagger\right)\underline{P}^n ,$$

$$= \underline{G}(E)^{R+C} + \underline{G}(E)^A . \tag{29}$$

This resolvent must be substituted into the Koster-Slater equations (19), together with the perturbation matrix

$$\underline{V}(E) = \underline{V}^S(E) + \underline{V}^T + \underline{V}^A(E) \tag{30}$$

given by (15) and (28). Again taking into account the zeroes in this perturbation matrix (see Fig. 2) and the fact that the solutions $\underline{c}$ are now localized on ϴ+ɑ, we obtain, after multiplication by $(\underline{P}^A + \underline{P}^O)\underline{V}(E)$:

$$(\underline{P}^O + \underline{P}^A)\underline{W}(E)(\underline{P}^A + \underline{P}^O)\underline{c} = \{[\underline{P}^O\underline{V}^S(E)\underline{P}^R + \underline{P}^O\underline{V}^T\underline{P}^O + \underline{P}^A\underline{V}^A(E)\underline{P}^O]\underline{G}(E)^{R+O}[\underline{P}^O\underline{V}^A(E)\underline{P}^A + \underline{P}^O\underline{V}^T\underline{P}^O + \underline{P}^R\underline{V}^S(E)\underline{P}^O]$$

$$+ [\underline{P}^O\underline{V}^A(E)\underline{P}^A + \underline{P}^A\underline{V}^A(E)\underline{P}^A]\underline{G}(E)^A[\underline{P}^A\underline{V}^A(E)\underline{P}^A + \underline{P}^A\underline{V}^A(E)\underline{P}^O]$$

$$- [\underline{P}^O\underline{V}^T\underline{P}^O + \underline{P}^A\underline{V}^A(E)\underline{P}^O + \underline{P}^O\underline{V}^A(E)\underline{P}^A + \underline{P}^A\underline{V}^A(E)\underline{P}^A]\}\underline{c} = \underline{0} . \tag{31}$$

Defining $\underline{W}(E)^{O+A}$ as the nonzero submatrix of $(\underline{P}^O + \underline{P}^A)\underline{W}(E)(\underline{P}^A + \underline{P}^O)$ over the layers ϴ+ɑ, we can solve a smaller problem—namely the one over those layers only:

$$\underline{W}(E)^{O+A}\underline{c}^{O+A} = \underline{0} . \tag{32}$$

Since the matrix $\underline{W}(E)^{O+A}$ is Hermitian, these equations are of the type that can be solved by the algorithm described in the next section.

V NUMERICAL SOLUTION OF THE KOSTER-SLATER EQUATIONS

The Koster-Slater equations for a crystal with two surfaces and adsorption have been brought into a standard form which can be generalized as

$$\underline{W}(E)\underline{c} = [\underline{V}(E)\underline{G}(E)\underline{V}(E) - \underline{V}(E)]\underline{c} = \underline{0} . \tag{33}$$

In the earlier applications of the resolvent method to this problem,[16-22] one solved Eq. (19) for the energy by searching for the roots of the equation

$$\det[\underline{G}(E)\underline{V}(E) - \underline{I}] = 0 . \tag{34}$$

Instead, we will search for the zeroes in the (real) eigenvalues of the Hermitian matrix $\underline{W}(E)$, which, of course, are also the zeroes of $\det[\underline{W}(E)]$ and the solutions of Eq. (34) if $\underline{V}(E)$ is nonsingular in the subspace considered. These zeroes can be calculated by an elegant algorithm because the matrix $\underline{W}(E)$ and its eigenvalues $\lambda_j(E)$ have some special properties (the same kind of properties were proved for the expectation value of a general resolvent by Löwdin[19]):

(1) When an eigenvalue $\lambda_j(E)$ passes through zero as a function of E, it always goes from positive to negative value with increasing E. In other words, if $\lambda_j(E_0) = 0$, it follows that

$$\left(\frac{d\lambda_j(E)}{dE}\right)_{E=E_0} < 0 . \tag{35}$$

This is proved in the Appendix.

(11) The eigenvalues of $\underline{W}(E)$ have poles, as do the matrix elements of $\underline{W}(E)$ and those of $\underline{G}(E)$, at $E = E_i^{(0)}$, the eigenvalues of the unperturbed problem. One can prove (see the Appendix) that the number of eigenvalues $\lambda_j(E)$ which have a pole at a certain $E_i^{(0)}$ equals the degeneracy $d_i^{(0)}$ of this unperturbed energy. Moreover, it can be shown that at the poles the eigenvalues $\lambda_j(E)$ always pass from $-\infty$ to $+\infty$ with increasing E.

These properties easily lead to the following theorem: The number of zeroes E_0 of all eigenvalues $\lambda_j(E)$ of $\underline{W}(E)$ in a given energy interval $E_1 < E_2$ is equal to

$$n_0(E_1, E_2) = n_+(E_1) - n_+(E_2) + \sum_{\substack{i \\ E_1 < E_i^{(0)} < E_2}} d_i^{(0)} , \tag{36}$$

when $n_+(E_1)$ and $n_+(E_2)$ are the number of positive eigenvalues of $\underline{W}(E_1)$ and $\underline{W}(E_2)$, respectively.

Using this theorem, the values of the energy roots E_0 can be determined by repeated bisection of the interval, until the required accuracy is reached. As the positions of the poles $E_i^{(0)}$, and their degeneracies $d_i^{(0)}$ are known from the unperturbed equations, the only problem that remains is to calculate the number of positive eigenvalues $n_+(E)$ of the matrix $\underline{W}(E)$ at given points E. Sever-

al procedures are possible: (i) complete diagonalization of the matrix $\underline{W}$ and counting the number of positive eigenvalues; (ii) tri-diagonalization of $\underline{W}$ and using the Sturm sequence property[57] for the parameter $\mu - 0$; and (iii) bringing $\underline{W}$ into upper-triangular form by the Gauss elimination process[58] and counting the number of positive diagonal elements. This number can be proved to equal the number of positive eigenvalues of $\underline{W}$ (see the Appendix).

Applying standard techniques to perform these manipulations on the complex Hermitian matrix $\underline{W}$, it appears that the third procedure is about three times faster than the second and about twenty times as rapid as the first. (They all increase in time with the third power of the dimension of $\underline{W}$.)

An advantage of the algorithm based on formula (36) for calculating the energy solutions of (33) is that it also calculates those energies of the perturbed system which coincide with an unperturbed energy and, thus, with a pole in the resolvent. In this case, one or more eigenvalues $\lambda_j(E)$ of $\underline{W}(E)$ go to zero, which corresponds to a solution of Eq. (33), whereas some other eigenvalues go to infinity. Such solutions cannot be found by the usual methods, which look for the zeroes of the determinant in (34). As pointed out in the Introduction, this advantage is of practical importance, since we wish to calculate also those one-electron energies lying within the crystal-bulk bands.

VI DISCUSSION

In the previous sections we worked out a method for the quantitative calculation of one-electron states in finite crystals, with or without adsorption. We can now compare this method in more detail with the more traditional methods mentioned in the Introduction.

In comparison with the resolvent method for semi-infinite crystals, this method is more suitable for quantitative calculations on real crystals, such as semiconductors or transition metals. It does not neglect overlap effects between atomic orbitals and calculates all interaction matrix elements explicitly, up to a given distance. Moreover, it calculates, not merely the strictly localized surface or adsorption states lying outside the crystal-energy bands, but *all* one-electron states.

One can object to the finite-crystal model on the grounds that it does not take into account really long-range effects. We do not think that this omission is very serious, however, because: (i) one can treat crystals up to about $10 \times 10 \times 10$ atoms; (ii) one can test the model by comparing crystals of different sizes; and (iii) the effects of the surface and, particularly, of chemisorption seem to be rather localized. Moreover, it could well be argued that crystals of this size are already of physical interest themselves.

Compared with quantitative MO calculations on finite clusters, we have a great reduction in computation time, which enables us to treat much larger clusters and to take into account interactions over a more extended range. This is illustrated by the following arguments for crystals without adsorption: If we have a cluster of $N_1 \times N_2 \times N_3 = N$ atoms and perform a traditional MO calculation, the number of matrix elements over atomic orbitals that must be evaluated is proportional to $N^2 = N_1^2 N_2^2 N_3^2$; the time for solving the secular problem is proportional to $N^3 = N_1^3 N_2^3 N_3^3$. If we impose periodic boundary conditions in two directions and use two-dimensional Bloch orbitals, as we do in our method, we have to calculate a number of matrix elements over atomic orbitals which is proportional to $N_1 N_2 N_3^2$. Transformation to Bloch orbitals takes only a negligible time. The time for solution of the secular problem then becomes proportional to $N_1 N_2 N_3^3$. By using the resolvent method, as described in this paper, the latter time can be even further reduced. The time for solution of the unperturbed periodic-crystal problem is proportional to $N_1 N_2 N_3$. The dimension of the Koster-Slater equations is smaller than the dimension of the secular problem by a factor N_o/N_3, where N_o is the number of outer crystal layers directly interacting with the surface. The time for solving the Koster-Slater equations is hard to estimate, as the algorithm contains some steps which are proportional to N_o^3 and other steps proportional to N_3^x, with x approximately equal to 1.5. At any rate, it follows that the Koster-Slater problem increases less rapidly with the crystal size than the secular problem, but since the Koster-Slater equations are more complex, the proportionality constant is larger. Therefore we conclude that the application of the resolvent method becomes advantageous when the ratio N_3/N_o surpasses a certain limit. If this is not the case, we rather solve the secular problem over layer orbitals, which is still much better than the traditional cluster calculations both in time saved and in the avoidance of undesirable boundary effects.

Besides the general resolvent method for surface states and adsorption, we have developed efficient special methods for the case where the effects of the surface potential (the Tamm perturbation) on the one-electron states become negligible. The perturbed wave functions themselves may give rise to a surface potential, however. These methods will be described in a future paper.

The complete procedure for calculating the one-electron states of a crystal with two surfaces and, possibly, some adsorbed layers, as derived in this paper, has been programmed in FORTRAN for an IBM 370 computer. The structure of the program

is shown schematically in Fig. 3. Calculations for hydrogen adsorption on nickel and copper surfaces are underway.

APPENDIX

The applicability of the algorithm for numerical solution of the Koster-Slater equations rests on a number of properties of which the proof shall be outlined in this Appendix.

We wish to find the energies E_0 and the coefficients $\underline{c}_0$ for which the equation

$$\underline{G}(E)\underline{V}(E)\underline{c} = \underline{c} \qquad (A1)$$

becomes an identity:

$$\underline{G}(E_0)\underline{V}(E_0)\underline{c}_0 = \underline{c}_0 . \qquad (A2)$$

These solutions are obtained by looking at the eigenvalue problem

$$\underline{W}(E)\underline{c}(E) = \left[\underline{V}(E)\underline{G}(E)\underline{V}(E) - \underline{V}(E)\right]\underline{c}(E) = \lambda(E)\underline{c}(E) \qquad (A3)$$

and searching for those energies E_0 for which $\lambda(E_0) = 0$. The first property that we invoke reads

$$\left(\frac{d\lambda(E)}{dE}\right)_{E_0} < 0 . \qquad (A4)$$

Williams[52] has proved this as follows for orthonormal bases and $\underline{V}$ not depending on E:

$$\frac{d\lambda}{dE} = \frac{d}{dE}\underline{c}(E)^\dagger \underline{W}(E)\underline{c}(E) ,$$

$$= \frac{d\underline{c}^\dagger}{dE}\underline{W}\underline{c} + \underline{c}^\dagger \underline{W}\frac{d\underline{c}}{dE} + \underline{c}^\dagger \frac{d\underline{W}}{dE}\underline{c} \qquad (A5)$$

For $E = E_0$, we can substitute the identity (A2) to obtain

$$\left(\frac{d\lambda}{dE}\right)_{E_0} = \underline{c}_0^\dagger \left(\frac{d\underline{W}}{dE}\right)_{E_0}\underline{c}_0 = \underline{c}_0^\dagger \underline{V}\left(\frac{d\underline{G}}{dE}\right)_{E_0}\underline{V}\underline{c}_0 . \qquad (A6)$$

On the same orthonormal basis the resolvent matrix $\underline{G}(E)$ reads

$$\underline{G}(E) = \sum_i \underline{c}_i^{(0)}(E - E_i^{(0)})^{-1}\underline{c}_i^{(0)\dagger} \qquad (A7)$$

and its derivative becomes

$$\frac{d\underline{G}}{dE} = -\underline{G}\,\underline{G} . \qquad (A8)$$

Substituting this result into (A6) and using the identity (A2) again, we find that

$$\left(\frac{d\lambda}{dE}\right)_{E_0} = -\underline{c}_0^\dagger\underline{V}\underline{G}(E_0)\underline{G}(E_0)\underline{V}\underline{c}_0 = -\underline{c}_0^\dagger\underline{c}_0 = -1 . \qquad (A9)$$

In our problem, with a nonorthonormal basis and $\underline{V}(E)$ dependent on E, we obtain some extra terms in the derivative of Eq. (A6):

$$\left(\frac{d\lambda}{dE}\right)_{E_0} = \underline{c}_0^\dagger\left(\frac{d\underline{W}}{dE}\right)_{E_0}\underline{c}_0 ,$$

$$= \underline{c}_0^\dagger\left(\frac{d\underline{V}}{dE}\underline{G}\underline{V}\right)_{E_0}\underline{c}_0 + \underline{c}_0^\dagger\left(\underline{V}\underline{G}\frac{d\underline{V}}{dE}\right)_{E_0}\underline{c}_0$$

$$+ \underline{c}_0^\dagger\left(\underline{V}\frac{d\underline{G}}{dE}\underline{V}\right)_{E_0}\underline{c}_0 - \underline{c}_0^\dagger\left(\frac{d\underline{V}}{dE}\right)_{E_0}\underline{c}_0 \qquad (A10)$$

Two of these terms cancel after using (A2), so that

$$\left(\frac{d\lambda}{dE}\right)_{E_0} = \underline{c}_0^\dagger\left(\underline{V}\frac{d\underline{G}}{dE}\underline{V}\right)_{E_0}\underline{c}_0 + \underline{c}_0^\dagger\left(\frac{d\underline{V}}{dE}\right)_{E_0}\underline{c}_0 \qquad (A11)$$

Using the fact that $\underline{V}(E)$ is linear in E, and that [according to Eqs. (15) and (28)] $d\underline{V}/dE$ equals a submatrix of the overlap matrix, and substituting the expression (16) or (29) for $\underline{G}(E)$, we have proved, similarly to the proof just given, that

$$\left(\frac{d\lambda}{dE}\right)_{E_0} < 0 .$$

The second important property of the eigenvalues $\lambda(E)$ of $\underline{W}(E) = \underline{V}(E)\underline{G}(E)\underline{V}(E) - \underline{V}(E)$ is their behavior at the poles $E_i^{(0)}$ of $\underline{G}(E)$. In the neighborhood of a pole $E_i^{(0)}$, we write $E = E_i^{(0)} + \epsilon$, with ϵ very small. For $\epsilon \to 0$ all matrix elements of $\underline{G}(E)$, and also those of $\underline{W}(E)$, go to infinity. In each matrix element of $\underline{G}(E)$, given by Eq. (A7), only $d_i^{(0)}$ terms in the sum behave as ϵ^{-1}, whereas the rest remains finite. (Remember that $d_i^{(0)}$ is the degeneracy of $E_i^{(0)}$.) In the limit of $\epsilon \to 0$ we can write $\underline{G}(E)$ effectively as

$$\underline{G}(E) = \epsilon^{-1}\sum_{i=1}^{d_i^{(0)}} \underline{c}_i^{(0)}\underline{c}_i^{(0)\dagger} . \qquad (A12)$$

This matrix projects the total space onto a subspace of dimension $d_i^{(0)}$; so it has the rank $d_i^{(0)}$. Also the matrix $\underline{W}(E)$ must have this rank, because the term linear in $\underline{V}(E)$ is small with respect to ϵ^{-1} and the transformation $\underline{V}(E)\underline{G}(E)\underline{V}(E)$ with nonsingular $\underline{V}(E)$ does not change the rank Consequently, only $d_i^{(0)}$ eigenvalues $\lambda(E)$ behave as ϵ^{-1}, while the other remain small Since the matrix $\underline{G}(E)$ given by Eq. (A12) is positive definite for $\epsilon \downarrow 0$ and negative definite for $\epsilon \uparrow 0$, we conclude that at each pole $E_i^{(0)}$ just $d_i^{(0)}$ eigenvalues $\lambda(E)$ pass from $-\infty$ to $+\infty$.

These two properties are sufficient to calculate the number of zeroes in the eigenvalues $\lambda(E)$ of $\underline{W}(E)$ in a given interval (E_1, E_2), when the number of positive $\lambda(E)$ is known in the end points E_1, E_2
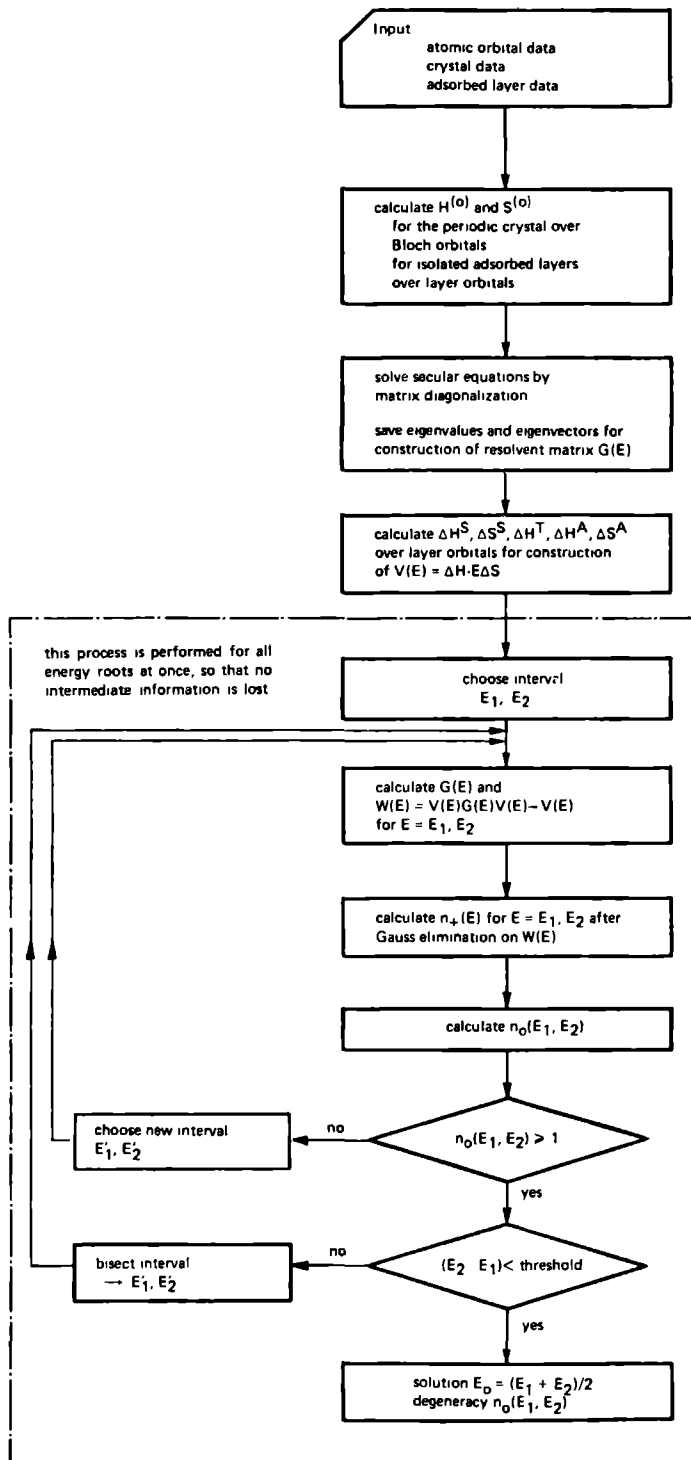
Input
  atomic orbital data
  crystal data
  adsorbed layer data

calculate $H^{(o)}$ and $S^{(o)}$
  for the periodic crystal over
  Bloch orbitals
  for isolated adsorbed layers
  over layer orbitals

solve secular equations by
matrix diagonalization

save eigenvalues and eigenvectors for
construction of resolvent matrix $G(E)$

calculate ΔH^S, ΔS^S, ΔH^T, ΔH^A, ΔS^A
over layer orbitals for construction
of $V(E) = \Delta H - E \Delta S$

this process is performed for all
energy roots at once, so that no
intermediate information is lost

choose interval
E_1, E_2

calculate $G(E)$ and
$W(E) = V(E)G(E)V(E) - V(E)$
for $E = E_1$, E_2

calculate $n_+(E)$ for $E = E_1$, E_2 after
Gauss elimination on $W(E)$

calculate $n_0(E_1, E_2)$

$n_0(E_1, E_2) \geqslant 1$

choose new interval
E'_1, E_2 no

$(E_2 - E_1) <$ threshold   yes

bisect interval
$\rightarrow E'_1$, E'_2 no

yes

solution $E_0 = (E_1 + E_2)/2$
degeneracy $n_0(E_1, E_2)$

FIG. 3. Flow chart of
the FORTRAN program for
computing the one-electron
energies in finite crystals,
with or without adsorption.

87

[Eq. (36)].

The fastest method to calculate the number of positive eigenvalues of a given complex Hermitian matrix W (dimension n) is by the Gauss elimination process,[58] which brings W into an upper-triangular form. The number of positive diagonal elements of the triangular matrix equals the number of positive eigenvalues of W. This is shown most easily for tri-diagonal Hermitian matrices W'. For such a matrix one can calculate the Sturm sequence for any parameter μ, which is the sequence of determinants $D_i(\mu)$ of the principal minors of $W' - \mu I$ with increasing size, $i = 0, 1, \ldots, n$; $D_0(\mu) = 1$. It has been proved[57] that the number of agreements in sign between the consecutive elements $D_i(\mu)$ equals the number of eigenvalues of W' which are strictly greater than μ. So the number of positive eigenvalues of W' is directly calculated by putting $\mu = 0$. Actually, this property can be used if we bring W into tri-diagonal form—for instance, by the Householder method.[59] This method is slower, however, than the Gauss elimination process.

Instead of using the Sturm sequence for $\mu = 0$ (i.e., the elements D_i), and counting the agreements in sign, one can count the number of positive

quotients D_i/D_{i-1}.[60] Now, these quotients are exactly the elements which we obtain on the diagonal after Gauss elimination on a general matrix.[58] Thus we have only to prove that the Sturm-sequence property also holds for the determinants D_i of the principal minors of a general Hermitian matrix W. The proof for tri-diagonal matrices[57] is based on the separation theorem[61] for the eigenvalues of a Hermitian matrix and those of its principal minors, which for such matrices is valid in the strict sense. For general Hermitian matrices it holds only in the non-strict sense,[61] i.e., with $\leq$ signs instead of $<$ signs. If none of the determinants D_i of the principal minors would be equal to zero, however, none of the principal minors can have a zero eigenvalue either, and we effectively have strict separation around zero. On that condition, the Gauss elimination method can be used to calculate the number of positive eigenvalues of W. If any of the elements D_i does equal zero, the elimination process would fail anyway. In this situation, we can invoke the technique of pivoting,[58] which for our purpose is only permitted if we interchange rows and columns simultaneously, i.e., keep the same elements on the diagonal.

*Present address: Dept. of Molecular Sciences, University of Warwick, England.

[1] D. L. Smith and R. P. Merrill, J. Chem. Phys. 52, 5861 (1970).

[2] G. Maire, J. R. Anderson, and B. B. Johnson, Proc. R. Soc. Lond. A 320, 227 (1970).

[3] H. D. Hagstrum and G. E. Becker, J. Chem. Phys. 54, 1015 (1971).

[4] G. E. Becker and H. D. Hagstrum, Surface Sci. 30, 505 (1972).

[5] D. E. Eastman, Phys. Rev. B 3, 1769 (1971).

[6] D. E. Eastman and J. K. Cashion, Phys. Rev. Lett. 27, 1520 (1971).

[7] P. W. Tamm and L. D. Schmidt, J. Chem. Phys. 54, 4775 (1971).

[8] C. Kohrt and R. Gomer, Surface Sci. 24, 77 (1971).

[9] J. Lapujoulade and K. S. Neil, J. Chem. Phys. 57, 3535 (1972).

[10] E. W. Plummer and A. E. Bell, J. Vac. Sci. Tech 9, 583 (1972).

[11] J. Küppers, Surface Sci. 36, 53 (1973).

[12] J. M. Ziman, *Principles of the Theory of Solids* (Cambridge U. P., London, 1964).

[13] J. Koutecký, Adv. Chem. Phys. 9, 85 (1965).

[14] S. G. Davison and J. D. Levine, in *Solid State Physics*, edited by H. Ehrenreich, F. Seitz and D. Turnbull (Academic, New York, 1970), Vol. 25, p. 1.

[15] G. F. Koster and J. C. Slater, Phys. Rev. 95, 1167 (1954).

[16] J. Koutecký and M. Tomášek, Phys. Rev. 120, 1212 (1960).

[17] J. Koutecký, Czech. J. Phys. B 12, 184 (1962).

[18] J. Koutecký, Surface Sci. 1, 280 (1964).

[19] M. Tomášek, Surface Sci. 2, 8 (1964).

[20] J. Koutecký and M. Tomášek, Surface Sci. 3, 333 (1965).

[21] J. D. Levine and S. Freeman, Phys. Rev. B 2, 3255 (1970).

[22] S. Freeman, Phys. Rev. B 2, 3272 (1970).

[23] T. L. Einstein and J. R. Schrieffer, Phys. Rev. B 7, 3629 (1973).

[24] T. B. Grimley, Proc. Phys Soc. 72, 103 (1958).

[25] J. Koutecký, Phys. Rev. 108, 13 (1957).

[26] M. Tomášek and J. Koutecký, Czech. J. Phys. B 10, 268 (1960).

[27] J. Koutecký and S. G. Davison, Intern. J. Quant. Chem. 2, 73 (1968).

[28] E. T. Goodwin, Proc. Cambridge Philos. Soc. 35, 232 (1939).

[29] K. Artmann, Z. Phys. 131, 244 (1952).

[30] G. R. Baldock, Proc. Cambridge Philos. Soc. 48, 457 (1952).

[31] T. B. Grimley, Adv. Catalysis 12, 1 (1960).

[32] A. T. Amos and S. G. Davison, Physica. (Utrecht) 30, 905 (1964).

[33] S. G. Davison and J. Koutecký, Proc. Phys. Soc. 89, 237 (1966).

[34] J. Koutecký, Trans. Faraday Soc. 54, 1038 (1958).

[35] D. M. Newns, Phys Rev. 178, 1123 (1969).

[36] T. B. Grimley and M. Torrini, J. Phys. C 6, 868 (1973).

[37] P. Markov and D. Lazarov, Compt. Rend. Acad. Bulgare Sci. 22, 455 (1969).

[38] A. J. Bennett, B. Mc Carroll, and R. P. Messmer, Surface Sci. 24, 191 (1971).

[39] A. J. Bennett, B. McCarroll, and R. P. Messmer, Phys. Rev B 3, 1397 (1971).

[40] D. J. M Fassaert, H. Verbeek, and A. van der Avoird, Surface Sci. 29, 501 (1972)

[41] R. C. Baetzold, J. Chem. Phys 55, 4363 (1971).

[42] R. C. Baetzold, Surface Sci. 36, 123 (1973).

[43]G. Blyholder, J. C. S. Chem. Comm. 17, 625 (1973).

[44]H. Deuss and A. van der Avoird, Phys. Rev. B 8, 2441 (1973).

[45]W. Shockley, Phys. Rev. 56, 317 (1939).

[46]I. E. Tamm, Z. Phys. 76, 849 (1932).

[47]I. M. Lifshitz, Zh. Eksp. Teor. Fiz. 17, 1017 (1947); 17, 1076 (1947).

[48]H. Margenau and G. M. Murphy, *The Mathematics of Physics and Chemistry* (Van Nostrand, Princeton, 1956).

[49]P. -O. Löwdin, Intern. J. Quant. Chem. 2, 867 (1968), and references therein.

[50]P. -O. Löwdin, J. Chem. Phys. 18, 365 (1950).

[51]G. H. Wannier, Phys. Rev. 52, 191 (1937).

[52]A. R. Williams (private communication).

[53]J. Korringa, Physica (Utrecht) 13, 392 (1947).

[54]W. Kohn and N. Rostoker, Phys. Rev. 94, 1111 (1954).

[55]We have chosen the matrix formulation of the theory because for nonorthogonal basis functions it takes a simpler appearance than the operator formalism. In operator form, the projection operators would read

$$P^{\mathfrak{X}} = \sum_{m \in \mathfrak{X}} \sum_{\rlap{$\scriptstyle\rho$}=1}^{\nu} \sum_{m'=1}^{N_3} \sum_{\rho'=1}^{\nu} |a_{\rho}(m)\rangle (\underline{S}^{-1})_{\rho m, \rho' m'} \langle a_{\rho'}(m')|,$$

and they satisfy the relations

$$P^{\mathfrak{X}} |a_{\rho}(m)\rangle = |a_{\rho}(m)\rangle \quad \text{if } m \in \mathfrak{X},$$
$$= 0 \qquad\qquad \text{if } m \not\in \mathfrak{X}.$$

[56]If we want to calculate adsorption energies, the reference system should contain noninteracting adsorbate atoms (or molecules) instead of layers. The energy correction corresponding to layer formation can be calculated immediately from the solutions of Eq. (26).

[57]J. H. Wilkinson, *The Algebraic Eigenvalue Problem* (Clarendon, Oxford, 1965), p. 300.

[58]Reference 57, p. 200.

[59]Reference 57, p. 290.

[60]W. Barth, R. S. Martin, and J. H. Wilkinson, in *Handbook for Automatic Computation II. Linear Algebra*, edited by J. H. Wilkinson and C. Reinsch (Springer-Verlag, New York, 1971), p. 249.

[61]Reference 57, p. 103.

Resolvent method for quantitative calculations on surface states and adsorption. II. Adsorption on Shockley surfaces

S. P. Liebmann,* A. van der Avoird, and D. J. M. Fassaert

Institute of Theoretical Chemistry, University of Nijmegen, Nijmegen, The Netherlands
(Received 4 September 1974)

Recently, a method has been developed for the quantitative calculation of surface and adsorption effects on one-electron states in finite crystals. This method, which is based on the linear-combination-of-atomic-orbitals or tight-binding model, uses the Koster-Slater resolvent method for computing the energies and orbital coefficients. Since the resolvent matrix is constructed numerically, an algorithm was described to solve the Koster-Slater equations numerically as well. The present paper shows a particularly efficient manner to prepare the Koster-Slater equations for this algorithm, which is applicable to crystals with Shockley surfaces and adsorption.

I. INTRODUCTION

The electronic properties of solid surfaces and the phenomena occurring on adsorption have been the subject of much research, both experimental and theoretical. Experimentally, more and more data are becoming available for adsorption on well-defined surfaces,[1-11] but the interpretation and correlation of these data, which should lead to a better understanding of adsorption interactions, leave many open questions. Theoretically, two types of methods have been applied to this problem, both using mainly the linear-combination-of-atomic-orbitals (LCAO) or tight-binding scheme. The first group of methods calculates the surface and adsorption states in a semi-infinite crystal model.[12-14] Although these methods are very useful for the interpretation of general phenomena, such as the occurrence of strictly localized surface states, they must introduce various simplifying approximations and, therefore, they remain rather qualitative and cannot do justice to the complexity of interesting crystals such as transition metals. Particularly, the interpretation of spectroscopic data for adsorbed atoms or molecules calls for a more quantitative treatment. Also, the calculation of total surface and adsorption energies is practically impossible by these methods.

A more quantitative approach is followed by the methods of the second kind, applying molecular-orbital (MO) techniques to finite clusters of atoms.[15-21] Results from such calculations are distorted by undesirable boundary effects, however, because the clusters have to stay rather limited in size.

In a previous paper[22] we proposed a LCAO method which works on finite crystals, just as the cluster methods, and calculates all interaction matrix elements between atomic orbitals explicitly within the (semiempirical) MO scheme that is used. By invoking different features from the semi-infinite crystal methods, such as periodic boundary conditions parallel to the surface and the application of the Koster-Slater resolvent technique, we have considerably reduced the time required for actual computations. Therefore, we can treat larger crystals than the usual cluster calculations and take into account interactions over a more extended range. Typical aspects of our procedure, described in Ref. 22, are the numerical calculation of the resolvent matrix and the algorithm for the numerical solution of the Koster-Slater equations. These are still the most time-consuming steps, though, and we must make them as efficient as possible. In the present paper, we describe simplified procedures for finite crystals having two surfaces without extra surface potentials and, also, for adsorption on these "Shockley" surfaces. First, we shall give a brief account of the general method and show in which parts improvements will be made.

II. GENERAL METHOD

The crystal and the adsorbed layers are assumed to be periodic in two directions, $\vec{a}_1$ and $\vec{a}_2$, with finite numbers of unit cells, N_1 and N_2, respectively. Besides eliminating boundary effects in these directions, this periodicity implies that, working in a LCAO model, we have a set of basis layer orbitals

$$|a_p(m)\rangle = \sum_{m_1=1}^{N_1} \sum_{m_2=1}^{N_2} |\chi_p(m_1, m_2, m)\rangle e^{i(k_1 m_1 + k_2 m_2)}, \quad (1)$$

which are noninteracting for different (k_1, k_2). The atomic orbitals $|\chi_p(m_1, m_2, m)\rangle$ are centered in the unit cell with the origin $m_1\vec{a}_1 + m_2\vec{a}_2 + m\vec{a}_3$, the index $p = 1, \ldots, \nu$ labels different atomic orbitals in the unit cell. On the basis of these layer orbitals we introduce a matrix representation, the matrix index running over all crystal layer orbitals (layers: $m = 1, \ldots, N_3$; atomic orbitals: $p = 1, \ldots, \nu$) and, in case of adsorption, also over the adsorbed layer orbitals (layers: $n = 1, \ldots, N$; atomic orbitals:

$q = 1, \ldots, \mu$). (Capitals denote matrices, small letters column vectors.)

Using the resolvent method in order to find the solutions, E and $\underline{c}$, of the secular equations for this system

$$(\underline{H} - E\underline{S})\underline{c} = \underline{0} \tag{2}$$

we need an "unperturbed" system, which is most conveniently defined as the crystal periodic in *three* directions together with some *isolated* adsorbate layers The reason for this choice is that the unperturbed equations

$$(\underline{H}^{(0)} - E_i^{(0)}\underline{S}^{(0)})\underline{c}_i^{(0)} = \underline{0} \tag{3}$$

are particularly simple for this special system, even if they must be solved numerically.[22] From the numerical solutions of the unperturbed problem we can construct the resolvent matrix by a finite summation over $i = 1, \ldots, N_3\nu$ or, in case of adsorption, over $i = 1, \ldots, N_3\nu + N\mu$

$$\underline{G}(E) = \sum_i \underline{c}_i^{(0)}(E - E_i^{(0)})^{-1}\underline{c}_i^{(0)\dagger}. \tag{4}$$

The perturbation which carries the unperturbed system into the real system of interest has the following effects.

(a) It removes so many layers R from the periodic crystal, that the remaining crystal C has two surfaces, which are only interacting with inside layers (just as the removal of a segment from a circle creates two ends) These surfaces are called "Shockley" surfaces. The perturbation V^S which annihilates the interactions between R and C actually has only matrix elements between layers R and some outer crystal layers O, the inner layers C-O are not directly affected This is so because we assume the interaction matrix elements between (localized) atomic orbitals to become negligible beyond a given distance.

(b) It adds a surface potential V^T which modifies the H-matrix elements of the outer layers O In the present paper we shall discuss the case that this "Tamm" perturbation V^T effectively equals zero.

(c) In case of adsorption, it adds the interactions between the adsorbed layers A and the crystal layers and between adsorbed layers among each other. This interaction V^A is localized within the adsorbed layers A and the outer crystal layers O.

The total perturbation $V^S + V^T + V^A$ modifies the unperturbed secular matrices $\underline{H}^{(0)}$ and $\underline{S}^{(0)}$ only in certain regions, by amounts $\underline{\Delta H}$ and $\underline{\Delta S}$ This is most easily expressed by projection matrices $\underline{P}^R$, $\underline{P}^O$, $\underline{P}^{C-O}$, and $\underline{P}^A = \sum_{n=1}^N \underline{P}^n$, which have unit matrices in the diagonal blocks corresponding to the regions indicated and zero otherwise. Multiplication by a projection matrix $\underline{P}^X$ means restriction of the indices to the layer orbitals contained in the region

X. Now, we can write the effects of the perturbation as

$$\underline{\Delta H}^S = -\underline{P}^R\underline{H}^{(0)}\underline{P}^O - \underline{P}^O\underline{H}^{(0)}\underline{P}^R,$$
$$\underline{\Delta S}^S = -\underline{P}^R\underline{S}^{(0)}\underline{P}^O - \underline{P}^O\underline{S}^{(0)}\underline{P}^R,$$
$$\underline{\Delta H}^T = \underline{P}^O\underline{T}\,\underline{P}^O, \tag{5}$$
$$\underline{\Delta H}^A = \underline{P}^A\underline{H}\,\underline{P}^O + \underline{P}^O\underline{H}\,\underline{P}^A + \underline{P}^A\underline{H}\,\underline{P}^A - \sum_{n=1}^N \underline{P}^n\underline{H}^{(0)}\underline{P}^n,$$
$$\underline{\Delta S}^A = \underline{P}^A\underline{S}\,\underline{P}^O + \underline{P}^O\underline{S}\,\underline{P}^A + \underline{P}^A\underline{S}\,\underline{P}^A - \sum_{n=1}^N \underline{P}^n\underline{S}^{(0)}\underline{P}^n.$$

The matrix $\underline{T}$ describes the effect of the surface potential on the outer layers O. If we define the matrix

$$\underline{V}(E) = \underline{\Delta H} - E\underline{\Delta S}, \tag{6}$$

which depends on the energy of the perturbed system, the perturbed secular equations (2) can be written

$$\underline{V}(E)\underline{c} = -(\underline{H}^{(0)} - E\underline{S}^{(0)})\underline{c}. \tag{7}$$

Multiplying these equations by the resolvent matrix (4) and using the properties of the latter,[22] we obtain the Koster-Slater equations

$$\underline{G}(E)\underline{V}(E)\underline{c} = \underline{c}. \tag{8}$$

The dimension of these equations is considerably reduced with respect to the original secular problem (2) if we substitute the matrix $\underline{V}(E)$ as given by (5) and (6) and realize that the solutions $\underline{c}$ which we are seeking are located in the crystal region C (in case of adsorption, in the region $C + A$). This is worked out in the following sections.

At this point we only recall that Eq. (8) can be solved numerically for E and $\underline{c}$ by the following procedure Equation (8) is multiplied by $\underline{V}(E)$ to obtain

$$\underline{W}(E)\underline{c} = [\underline{V}(E)\underline{G}(E)\underline{V}(E) - \underline{V}(E)]\underline{c} = \underline{0}. \tag{9}$$

Then we search for the zeroes in the (real) eigenvalues of the complex Hermitian matrix $\underline{W}(E)$, which are the energy solutions of (9). Substituting these into (8) or (9) we calculate the coefficients $\underline{c}$ by standard techniques (solving a set of homogeneous linear equations). The algorithm to calculate the energies E, which is based on the properties of the eigenvalues of $\underline{W}(E)$, is described in paper I.[22] This algorithm uses a bisection procedure select an interval (E_1, E_2); calculate the number of roots in this interval $n_0(E_1, E_2)$; if $n_0(E_1, E_2) > 0$ bisect the interval, etc., until the required accuracy is reached. In each cycle we have to construct the matrices $\underline{G}(E)$ and $\underline{V}(E)$ for a given energy E and to perform the operations required for the calculation of $\underline{W}(E) = \underline{V}(E)\underline{G}(E)\underline{V}(E) - \underline{V}(E)$. These operations are rather time consuming, the more since they

91

have to be performed in complex arithmetic, which is a serious limit on the practical applicability of this method. In the following sections we show for Shockley surfaces and adsorption how to avoid a considerable part of these operations and, thereby, to make the procedure much more efficient.

III. SHOCKLEY SURFACES

According to our procedure for general surfaces we would (more precisely) multiply Eq. (8) by $\underline{P}^O\underline{V}(E)$ with $\underline{V}(E) = \underline{V}^S(E) + \underline{V}^T$, substitute (5) and (6) and solve Eq. (9) in the subspace O.[22] If V^T equals zero, the matrix $\underline{P}^O\underline{V}(E)$ becomes equal to $\underline{P}^O\underline{V}^S(E)\underline{P}^R$ and its rank is determined by $\dim(R)$, the dimension of the space R, which is smaller than $\dim(O)$. Generally, $\dim(O) = 2 \times \dim(R)$ because the layers R in the unperturbed (periodic) crystal are connected with outer layers O at *two* surfaces. For this reason the matrix

$$\underline{W}^{OO}(E) = \underline{P}^O\underline{V}^S(E)\underline{P}^R\underline{G}(E)\underline{P}^R\underline{V}^S(E)\underline{P}^O \qquad (10)$$

becomes singular in the subspace O and we cannot apply the algorithm to find the solutions E by looking for the zeroes in the eigenvalues of $\underline{W}(E)$, since half of the eigenvalues are identically zero. This difficulty could easily be removed by choosing the Tamm perturbation nonzero but very small, so that it practically does not influence the solutions of Eq. (9). It is more efficient, though, to use a special equation for Shockley surfaces which is much faster to solve than the general one.

We start with Eq. (8), substitute $\underline{V}(E) = \underline{V}^S(E)$ given by (5) and (6) and use the fact that $\underline{P}^C\underline{c} = \underline{c}$, because the solutions $\underline{c}$ are located on the crystal C. Use of the relations between the projection matrices, $\underline{P}^R\underline{P}^C = \underline{0}$; $\underline{P}^O\underline{P}^C = \underline{P}^O$, yields

$$\underline{G}(E)\underline{P}^R\underline{V}^S(E)\underline{P}^O\underline{c} = \underline{P}^C\underline{c} . \qquad (11)$$

Multiplying this equation by $\underline{P}^R$, denoting the matrix $\underline{P}^R\underline{G}(E)\underline{P}^R$ by $\underline{G}^{RR}(E)$ and incorporating the Shockley perturbation into a new set of coefficients

$$\underline{d}^R(E) = \underline{P}^R\underline{V}^S(E)\underline{P}^O\underline{c} , \qquad (12)$$

we are left with the equation

$$\underline{G}^{RR}(E)\underline{d}^R(E) = \underline{0} . \qquad (13)$$

This equation can be solved in the subspace R. The matrix $\underline{G}^{RR}(E)$ is Hermitian and has the correct properties, so that the algorithm of Paper I can be applied to $\underline{G}^{RR}(E)$ instead of $\underline{W}^{OO}(E)$ for the calculation of the energy solutions E. This procedure is much faster for two reasons. In the first place, the dimension of $\underline{G}^{RR}(E)$ is twice as small as the dimension of $\underline{W}^{OO}(E)$ and, therefore, the Gauss elimination process which is part of the algorithm requires less time. Secondly, the matrix $\underline{G}^{RR}(E)$ is

just the restriction of $\underline{G}(E)$ to the layers R, so we can omit the matrix operations needed in each bisection cycle for the construction of $\underline{W}(E) = \underline{V}(E)\underline{G}(E)\underline{V}(E) - \underline{V}(E)$ from $\underline{G}(E)$ and $\overline{\underline{V}}(E)$.

According to a proof by Freeman,[23] Eq. (13) yields *all* energy roots E_0 for the crystal with Shockley surfaces. The coefficients $\underline{c}$ can be calculated by substituting these roots back into (13), solving the set of homogeneous linear equations for the coefficients $\underline{d}^R(E_0)$ and substituting these coefficients into (11), multiplied by $\underline{P}^C$:

$$\underline{c} = \underline{P}^C\underline{c} = \underline{P}^C\underline{G}(E_0)\underline{P}^R\underline{d}^R(E_0) . \qquad (14)$$

IV. ADSORPTION

We want to follow a similar procedure for adsorption on Shockley surfaces. In this case, the unperturbed system consists of the periodic crystal $R + C$ and some isolated adsorbate layers, $n = 1, \dots, N$, and the resolvent matrix can be written

$$\underline{G}(E) = (\underline{P}^R + \underline{P}^C)\underline{G}(E)(\underline{P}^C + \underline{P}^R) + \sum_{n=1}^{N}\underline{P}^n\underline{G}(E)\underline{P}^n . \qquad (15)$$

When the Tamm perturbation is zero, i.e., $\underline{H} = \underline{H}^{(0)}$ for the crystal layers O as well as for individual adsorbed layers $n \in A$, the perturbation matrix reads

$$\underline{V}(E) = \underline{P}^R\underline{V}^S(E)\underline{P}^O + \underline{P}^O\underline{V}^S(E)\underline{P}^R + \underline{P}^O\underline{V}^A(E)\underline{P}^A$$
$$+ \underline{P}^A\underline{V}^A(E)\underline{P}^O + \sum_{n=1}^{N}\sum_{n'=1}^{N}\underline{P}^n\underline{V}^A(E)\underline{P}^{n'} , \quad n' \neq n \qquad (16)$$

According to the general method, we would have to solve Eq. (9) in the subspace $O + A$, with the matrix $\underline{W}(E) = \underline{V}(E)\underline{G}(E)\underline{V}(E) - \underline{V}(E)$ constructed from (15) and (16). In most practical cases, where we do not have too many adsorbed layers, the dimension of this subspace is larger than $\dim(R) + 2 \times \dim(A)$, which appears to be the rank of the matrix $\underline{W}(E)$ in these systems. So we have tried to replace the matrix $\underline{W}(E)$ by a smaller matrix of the size $\dim(R) + 2 \times \dim(A)$ and to avoid, at the same time, many of the matrix operations required for the construction of $\underline{W}(E)$ from the expressions (15) and (16).

We start by substituting (15) and (16) into the Koster-Slater equations (8), using the property that $\underline{c}$ is now located in $C + A$: $(\underline{P}^C + \underline{P}^A)\underline{c} = \underline{c}$, and the relations between the projection matrices. If we multiply the resulting equations by $\underline{P}^R$, $\underline{P}^A$, and $\underline{P}^O$, respectively, we find the equations

$$\underline{P}^R\underline{G}(E)\underline{P}^R\underline{V}^S(E)\underline{P}^O\underline{c} + \underline{P}^R\underline{G}(E)\underline{P}^O\underline{V}^A(E)\underline{P}^A\underline{c} = \underline{0} , \qquad (17a)$$

$$\sum_{n=1}^{N}\underline{P}^n\underline{G}(E)\underline{P}^n\underline{V}^A(E)\underline{P}^O\underline{c}$$
$$+ \sum_{n=1}^{N}\sum_{n'=1}^{N}\underline{P}^n\underline{G}(E)\underline{P}^n\underline{V}^A(E)\underline{P}^{n'}\underline{c} = \underline{P}^A\underline{c} , \quad n' \neq n \qquad (17b)$$

$$\underline{P}^O\underline{G}(E)\underline{P}^R\underline{V}^S(E)\underline{P}^O\underline{c} + \underline{P}^O\underline{G}(E)\underline{P}^O\underline{V}^A(E)\underline{P}^A\underline{c} = \underline{P}^O\underline{c} . \tag{17c}$$

Before proceeding with the preparation of these equations to suit the algorithm for the calculation of E, we introduce some additional definitions. The matrices describing the interactions between the crystal and the adsorbed layers are denoted as

$$\underline{V}^{AO}(E) = \underline{P}^A\underline{V}^A(E)\underline{P}^O; \quad \underline{V}^{OA}(E) = \underline{V}^{AO}(E)^\dagger . \tag{18}$$

The interaction matrix between different adsorbed layers, which has zero diagonal blocks, is divided into two triangular matrices:

$$\underline{V}^{AA'}(E) = \sum_{n=1}^{N}\sum_{n'=1}^{n-1} \underline{P}^n\underline{V}^A(E)\underline{P}^{n'}; \quad \underline{V}^{A'A}(E) = \underline{V}^{AA'}(E)^\dagger . \tag{19}$$

These matrices obey the relations

$$\underline{V}^{AA'}(E) + \underline{V}^{A'A}(E) = \underline{P}^A\underline{V}^A(E)\underline{P}^A - \sum_{n=1}^{N} \underline{P}^n\underline{V}^A(E)\underline{P}^n ,$$

$$\underline{P}^n\underline{V}^{AA'}(E)\underline{P}^{n'} = \begin{cases} \underline{P}^n\underline{V}^A(E)\underline{P}^{n'}, & \text{if } n' < n \\ \underline{0} , & \text{if } n' \geq n . \end{cases} \tag{20}$$

Different parts of the resolvent matrix are denoted as

$$\underline{G}^{RR}(E) = \underline{P}^R\underline{G}(E)\underline{P}^R; \quad \underline{G}^{RO}(E) = \underline{P}^R\underline{G}(E)\underline{P}^O, \text{ etc.,}$$

and the diagonal block matrix over adsorbed layers as

$$\underline{G}^A(E) = \sum_{n=1}^{N} \underline{P}^n\underline{G}(E)\underline{P}^n . \tag{21}$$

Using these definitions, (17) reads

$$\underline{G}^{RR}(E)\underline{P}^R\underline{V}^S(E)\underline{P}^O\underline{c} + \underline{G}^{RO}(E)\underline{V}^{OA}(E)\underline{c} = \underline{0} , \tag{22a}$$

$$\underline{G}^A(E)\underline{V}^{AO}(E)\underline{c} + \underline{G}^A(E)\underline{V}^{AA'}(E)\underline{c}$$
$$+ \underline{G}^A(E)\underline{V}^{A'A}(E)\underline{c} = \underline{P}^A\underline{c} , \tag{22b}$$

$$\underline{G}^{OR}(E)\underline{P}^R\underline{V}^S(E)\underline{P}^O\underline{c} + \underline{G}^{OO}(E)\underline{V}^{OA}(E)\underline{c} = \underline{P}^O\underline{c}. \tag{22c}$$

Equation (22c) is replaced by the sum of multiplying (22c) by $\underline{V}^{AO}(E)$ and (22b) by $\underline{V}^{AA'}(E)$. Then we substitute the new variables:

$$\underline{d}^R(E) = \underline{P}^R\underline{V}^S(E)\underline{P}^O\underline{c} ,$$
$$\underline{d}^A(E) = [\, \underline{V}^{AO}(E) + \underline{V}^{AA'}(E)\,]\underline{c} , \tag{23}$$
$$\underline{c}^A = \underline{P}^A\underline{c} ,$$

which are linearly independent if $\dim(O) + \dim(A) \geq \dim(R) + 2\times\dim(A)$, obtaining:

$$\underline{G}^{RR}(E)\underline{d}^R(E) + \underline{G}^{RO}(E)\underline{V}^{OA}(E)\underline{c}^A = \underline{0} ,$$
$$\underline{G}^A(E)\underline{d}^A(E) + [\, \underline{G}^A(E)\underline{V}^{A'A}(E) - \underline{P}^A\,]\underline{c}^A = \underline{0}, \tag{24}$$
$$\underline{V}^{AO}(E)\underline{G}^{OR}(E)\underline{d}^R(E) + [\, \underline{V}^{AA'}(E)\underline{G}^A(E) - \underline{P}^A\,]\underline{d}^A(E)$$
$$+ [\, \underline{V}^{AO}(E)\underline{G}^{OO}(E)\underline{V}^{OA}(E)$$
$$+ \underline{V}^{AA'}(E)\underline{G}^A(E)\underline{V}^{A'A}(E)\,]\underline{c}^A = \underline{0} .$$

If these equations are written in matrix form (Fig. 1) it is easily verified that the matrix multiplying the new coefficients is Hermitian. The algorithm applied to $\underline{W}(E)$ in the general method in order to find the roots of Eq. (9) can now be applied to this matrix. Again, this is more efficient since the matrix of Fig. 1 usually has a smaller dimension and its construction requires much less operations. A large part is just the restriction of $\underline{G}(E)$ to the
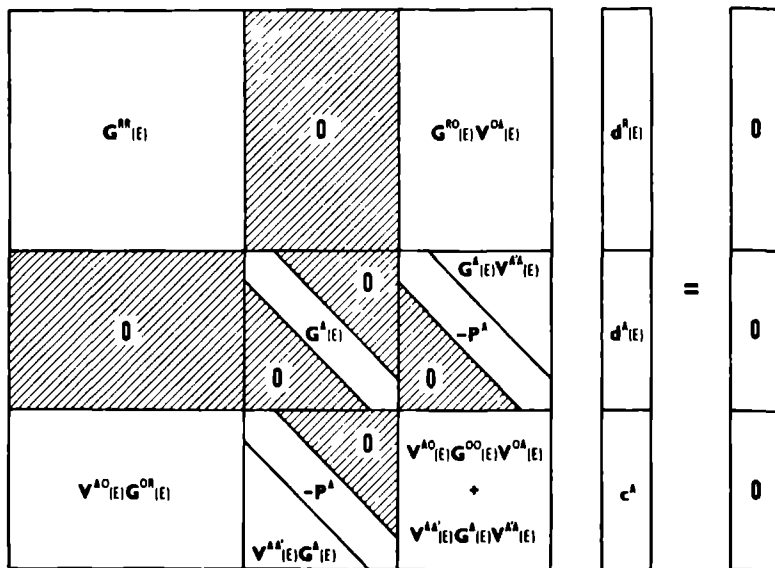

FIG. 1. Structure of the equations for adsorption on Shockley surfaces.

93

subspaces R and A, most of the remaining parts are simpler than $\underline{W}(E)$, which is readily seen by comparison with Eq (31) of Paper I Especially when we have just a single adsorbed layer, this simplification becomes obvious because the matrix $\underline{V}^{AA'}(E)$ does not exist.

V CONCLUSION

Summarizing the preceding sections, we conclude that for Shockley surfaces and adsorption the Koster-Slater equations (8) may be prepared in such a form that the numerical algorithm for the calculation of the perturbed energies can be applied The E-dependent matrix multiplying the coefficients of the perturbed wave function, or linear combinations of these [Eq (23)], is Hermitian This is not attained by multiplication with the perturbation matrix yielding the matrix $\underline{W}(E)$ of Eq (9), which is singular in this case, but by some specific manipulations and substitutions yielding Eqs. (13) and (24) The advantages of the latter procedure are that the matrices in (13) and (24) have smaller dimensions and are much easier to construct than the matrix $\underline{W}(E)$ of Eq. (9) This is

of crucial importance since the construction of these matrices and their triangularization must be carried out in each cycle of the bisection algorithm for determining the energy roots The procedures described in this paper were incorporated into the computer program of Paper I

When the Tamm perturbation, accounting for the effect of the surface potential on the one-electron states does not equal zero, the matrix $\underline{W}(E)$ is non-singular in the subspace O, or $O + A$ for adsorption, in which Eq (9) should be solved Still, by the same kind of substitutions described in this paper one can try to simplify the form of $\underline{W}(E)$ and, thus, save much time in calculating the energies.

*Present address Dept of Molecular Sciences, University of Warwick, England.

[1]D L Smith and R P Merrill, J Chem Phys 52, 5861 (1970)

[2]G Maire, J R Anderson, and B B Johnson, Proc R Soc Lond A 320, 227 (1970)

[3]H D Hagstrum and G E Becker, J Chem Phys 54, 1015 (1971)

[4]G E Becker and H D Hagstrum, Surf Sci 30, 505 (1972)

[5]D E Eastman, Phys Rev B 3, 1769 (1971)

[6]D E Eastman and J K Cashion, Phys Rev Lett 27, 1520 (1971)

[7]P W Tamm and L D Schmidt, J Chem Phys 54, 4775 (1971)

[8]C Kohrt and R Gomer, Surf Sci 24, 77 (1971)

[9]J Lapujoulade and K S Neil, J Chem Phys 57, 3535 (1972)

[10]E W Plummer and A E Bell, J Vac Sci Technol 9, 583 (1972)

[11]J Küppers, Surf Sci 36, 53 (1973)

[12]T B Grimley, Adv. Catal. Relat Subj 12, 1 (1960)

[13]J Koutecký, Adv Chem Phys 9, 85 (1965)

[14]S. G Davison and J. D Levine, Solid State Phys 25, 1 (1970).

[15]P Markov and D Lazarov, C R Acad Bulgare Sci 22, 455 (1969)

[16]A J Bennett, B McCarroll, and R P Messmer, Surf Sci 24, 191 (1971)

[17]A J Bennett, B Mc Carroll, and R P Messmer, Phys Rev B 3, 1397 (1971)

[18]D J M Fassaert, H Verbeek, and A van der Avoird, Surf Sci 29, 501 (1972)

[19]R C Baetzold, J Catal 29, 129 (1973)

[20]R C Baetzold, Surf Sci 36, 123 (1973)

[21]G Blyholder, Surf Sci 42 249 (1974)

[22]A van der Avoird S P Liebmann, and D J M Fassaert, Phys Rev B 10, 1230 (1974)

[23]S Freeman, Phys Rev B 2, 3272 (1970)

Chapter IV

LCAO STUDIES FOR HYDROGEN CHEMISORPTION
ON TRANSITION-METAL SURFACES

Remarks on the adsorption bonding with transition metals;
rôle of the d- and conduction electrons

In this chapter three articles have been reprinted which report
our Extended Hückel LCAO studies on the adsorption of (atomic)
hydrogen at various surface sites of nickel and, for a few examples,
also copper crystals. In the first and third paper single atom ad-
sorption on clusters is discussed, and in the second one monolayer
adsorption on finite periodic crystals is considered. In the following,
we shall give some additional comments on the results.

1. We have extensively discussed in section 2.9 of Chapter II the
changes which occur in model systems in the local density of states on
the adatom and at the surface as a consequence of the chemisorptive
interaction. Now, we want to look for these effects in our actual re-
sults. Although the situation is more complicated than for the models
discussed, because of full monolayer adsorption and the existence of
both a d-band and an sp-band, analogous effects may be identified. For
instance, split-off states appear above and below the d-band as well as
the conduction band, as may be observed from figures 6 and 7 of the
second paper. So, strong adsorption takes place and one may conclude,
at least for the adsorbate interaction with the substrate conduction
band, that correlation effects are perhaps not very important (see
Chapter II, section 2.7). Further, more than the maximum of two split-
off states found by Cyrot-Lackmann and Einstein, may occur, as well as
simultaneous virtual states inside the band, because the situation

is more complicated in our case (e.g., the number of orbitals involved in the surface molecule is larger).

2. In our paper of 1972 we have noted, for the first time, that the conduction (4s) electrons play an important rôle in the chemisorption bond. This result has been confirmed since by several other authors using quite different techniques such as CNDO [1] and Xα-DVM [2]. Also some ab initio calculations on NiH [3-6] and other transition-metal hydrides [7-11] indicate that a strong interaction exists between the metal 4s orbital and the hydrogen 1s orbital. Therefore, it is also necessary to take the conduction band into account in chemisorption studies on transition metals, which has up to now often been omitted.

3. In the first paper we have (also) found a strong interaction between a single hydrogen atom and a copper cluster. Although the 3d orbitals were not involved in the adsorption bond, their absence was compensated by an increased 4s contribution. These findings have been confirmed in a few calculations on hydrogen monolayer adsorption on finite periodic layer crystals, which are similar to the computations described in the second paper. Using copper parameters, we found only a very small overlap population between the hydrogen 1s and the 3d substrate orbitals and a considerable increase (about 50%) of the overlap population with the conduction band, as compared to nickel. The adsorption energies were rather similar to those for the nickel crystals.

4. From the above mentioned results it appears that the strength of the chemisorption bonding does not depend in a simple way on the occupation of the d-band. But, if we conclude on the contrary that the adsorption bonding with nickel and copper mainly takes place via the 4s orbitals and not via the 3d band, it is somewhat harder to explain the different catalytic behaviour of these metals than one has imagined for a long time. There is, for instance, the experimental observation that nickel <u>does</u> dissociate H_2 at low temperatures and copper does not,

although for both metals the adsorption energy of hydrogen atoms is sufficiently high to make the dissociation of H_2 energetically possible [12,13].

Deuss and Van der Avoird [14], realizing that the adsorption interaction mainly occurs via Ni(4s), proposed a certain rôle of the 3d orbitals in lowering the activation barrier for dissociative chemisorption of H_2 (see Chapter II, section 3). Melius et al. [4,5] also ascribed a similar rôle to the 3d electrons. In contrast to Deuss and Van der Avoird, however, they assumed that the 3d orbitals do not take part in the adsorption bonding at all, but simply provide those symmetry states which according to the Woodward-Hoffmann rules lower this activation barrier. If the 3d electrons are to influence the energy along the reaction path, however, they should have some coupling with the electrons directly involved in the bonding (i.e., metal 4s and hydrogen 1s). In any case, it can be concluded that the participation of partly filled d-electron shells in the chemisorptive interaction with molecular hydrogen may provide an unactivated reaction path, although their actual contribution to the adsorption bond can be relatively small.

References

[1] G. Blyholder, J. Chem. Phys. 62, 3193 (1975).

[2] T. Tanabe, H. Adachi and S. Imoto, to be published.

[3] A.B. Kunz, M.P. Guse and R.J. Blint, Chem. Phys. Lett. 37, 512 (1976).

[4] C.F. Melius, Chem. Phys. Lett., to be published.

[5] C.F. Melius, J.W. Moskowitz, A.P. Mortola, M.B. Baillie and M.A. Ratner, to be published.

[6] L.G.C. Houben and J.Th.A. Stuart, unpublished results.

[7] P.S. Bagus and H.F. Schaefer III, J. Chem. Phys. 58, 1844 (1973).

[8] P.R. Scott and W.G. Richards, J. Phys. B: Atom. Molec. Phys. 7, 500 (1974).

[9] P.R. Scott and W.G. Richards, J. Chem. Phys. 63, 1690 (1975).

[10] A.B. Kunz, M.P. Guse and R.J. Blint, J. Phys. B: Atom. Molec. Phys. 8, L358 (1975).

[11] R.J. Blint, A.B. Kunz and M.P. Guse, Chem. Phys. Lett. **36**, 191 (1975).

[12] C.S. Alexander and J. Pritchard, J. C. S. Faraday Trans. I **68**, 202 (1972).

[13] K. Christmann, O. Schober, G. Ertl and M. Neumann, J. Chem. Phys. **60**, 4528 (1974).

[14] H. Deuss and A. van der Avoird, Phys. Rev. B **8**, 2441 (1973).

MOLECULAR ORBITAL MODELS FOR HYDROGEN ADSORPTION ON DIFFERENT SITES OF A NICKEL CRYSTAL

D J M FASSAERT, H VERBEEK* and A VAN DER AVOIRD

*Institute of Theoretical Chemistry, University of Nijmegen,
Nijmegen, The Netherlands*

Model calculations for the chemisorption of hydrogen atoms on nickel (111), (100) and (110) surfaces are carried out by means of the Extended Huckel MO method After comparison of the results obtained on a cluster of 13 nickel atoms with the properties of the metal, adsorption at different surfaces was studied by truncating this cluster and adsorbing a hydrogen atom on it, so that the environment of the adsorption site has the correct symmetry

It can be concluded that the adsorption of a hydrogen atom over a surface nickel atom is energetically more favourable than adsorption in some surface holes Also the surface potential is more negative in the first case The adsorption energy decreases with an increasing number of neighbours to the surface atom

It appeared further that the structure of the "surface molecule" is more important for determining which d-orbitals play a rôle in chemisorption than is the interaction with the "bulk" metal atoms Moreover, we found that the 4s orbitals are very important for covalent adsorption Although the chemisorption of hydrogen atoms on copper is of a different type (the 3d orbitals not being involved), the greater binding to the 4s orbitals causes the adsorption energy to be comparable with the nickel case

1. Introduction

The concept of a "surface molecule", which describes the localized bonding between a chemisorbed species and a small number of substrate atoms[1]), has been used by theorists[2-13]) and experimentalists[14]) to calculate and interpret the phenomena occurring on adsorption Several theoretical treatments have checked the validity of this concept for certain systems or, more generally, as a function of some typical system parameters[15-22])

The purpose of the present investigation is to obtain some quantitative information about atomic hydrogen adsorbed on a transition-metal such as nickel, a system which is interesting and relatively well studied experimentally As we intend to obtain these quantitative results by means of a standard molecular orbital method, we can only study the interaction of a hydrogen

---

* Present address Koninklijke/Shell Laboratorium, Amsterdam, The Netherlands

atom with a limited number of metal atoms. Nevertheless, we hope that these model calculations will permit us to make some conclusions about the degree of localization of the adsorption bond. A further essential object of this work is to determine which transition-metal orbitals play a rôle in chemisorption and what is the effect of the partly filled d-band and of the conduction electrons. We think this knowledge to be useful in order to check assumptions on this matter made in previous theoretical treatments of the same system[2,12,13]. It can also help to improve the crude analysis of the rôle of multi-centre forces in the dissociation of H_2 on nickel[13].

The calculations have been carried out for hydrogen on different crystallographic surfaces of face-centered cubic nickel in order to examine the effect of a different environment of the adsorption site. We hope that the applied model represents the experimental situation sufficiently well to allow some theoretical predictions about the surface potential and the adsorption energy.

2. Description of the model

2.1 CLUSTERS

Since the adsorption models only consist of a limited number of metal atoms we want to consider first the effect of truncating the crystal. This investigation is carried out on a cluster of 13 nickel atoms, representing one atom with its complete nearest neighbour environment in the fcc crystal (fig. 1a). The symmetry group of this complex is O_h, the nearest neighbour distance is taken equal to the metallic value (2.49 Å = 4.70 atomic units).

The next calculations were performed on systems of 10, 9 or 8 nickel atoms obtained from the original cluster by removing some atoms such that the central metal atom has the nearest neighbour environment of an atom at the (111), (100) or (110) surface, respectively (figs. 1b, c and d). The symmetry groups of these clusters are C_{3v}, C_{4v} and C_{2v}.

Subsequently, we "adsorb" a hydrogen atom on these surface clusters, at a variable height above the central nickel atom (figs. 2a, b, c). The resulting complexes have C_{3v}, C_{4v} and C_{2v} symmetry, just as the original metal clusters. As this symmetry is exactly the same as the symmetry of an isolated hydrogen atom adsorbed on a semi-infinite metal crystal, we expect that these models can serve to investigate the effect of the (direct) environment on the properties of the adsorption site. Actually, the study of neighbour effects is made by comparison to an isolated NiH molecule, which is also calculated.

We have also examined what happens when a hydrogen atom is adsorbed on a cluster which is just like one of those in figs. 1b or 1c, but inverted. The hydrogen atom is now placed in the centre of a "hole" between 3 or 4 "surface" nickel atoms, respectively, at variable height (figs. 2d and 2e). It
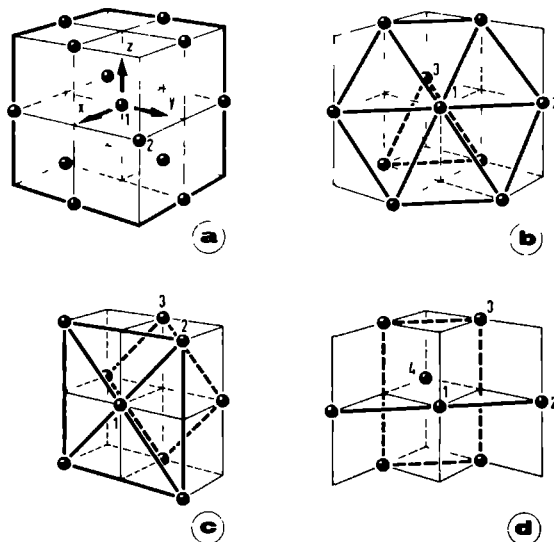
Fig. 1. (a) bulk cluster, (b) (111) surface cluster, (c) (100) surface cluster, (d) (110) surface cluster.
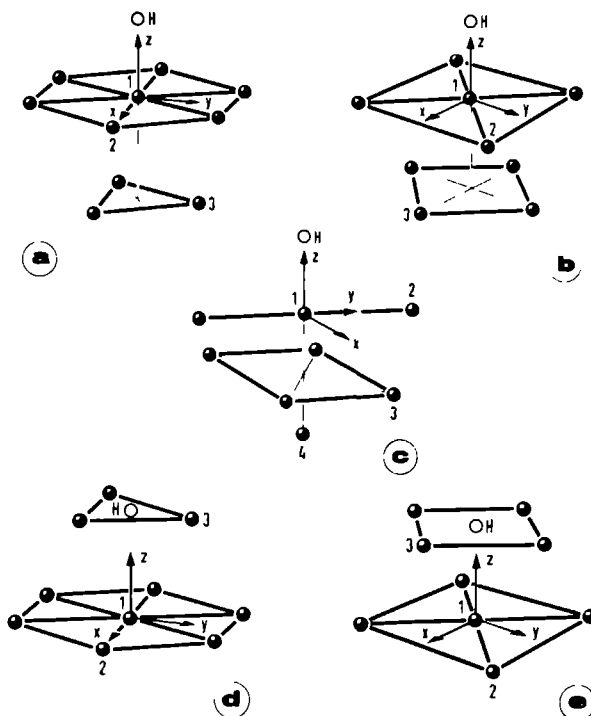

Fig 2. Models for hydrogen adsorption: (a) on the (111) surface, (b) on the (100) surface, (c) on the (110) surface, (d) in a (111) surface hole, (e) in a (100) surface hole.

must be noted, however, that these surface nickel atoms are not provided with their complete nearest neighbour environment, as the central surface atoms are in the clusters of figs. 2a, b and c.

2.2. ATOMIC ORBITALS AND VALENCE ELECTRONS

As we did not wish to make any a priori assumptions about the d-orbitals involved in adsorption bonding, we have taken all five 3d orbitals on each nickel atom. The 4s orbitals of nickel were included as well, in order to represent the conduction electrons. The atomic orbitals are expressed in the coordinate system shown in fig. 1 for the central metal atom and parallel coordinates on all other atoms. The radial parts of the orbitals, a single Slater type function for the 4s and a "double zeta" function for the 3d orbitals, are approximate atomic SCF orbitals[23]) (table 1). Each nickel

TABLE 1

Atomic orbitals and valence state ionization energies

	Exponents (a_0^{-1})	Contraction coefficients	α (eV)	β (eV)	γ (eV)
Ni 3d	5.75 $\}$ 2.00 $\}$	0.5683 $\}$ 0.6292 $\}$	8.38	12.97	1.76
4s	1.50	1.0	6.97	8.16	0.91
Cu 3d	5.95 $\}$ 2.30 $\}$	0.5933 $\}$ 0.5744 $\}$	10.60		
4s	1.55	1.0	7.75		
H 1s	1.0	1.0	13.60	27.18	13.62

atom has 10 valence electrons and an effective core charge of +10 units. For reference purposes we have also made some calculations using only the nickel 3d orbitals and taking into account 9 valence electrons (core charge +9). A hydrogen atom contains a 1s-orbital (exponent 1.0) and 1 electron.

Since much evidence has been put forward to relate the adsorption behaviour of transition metals to the number of "holes" in the d-band, we thought that it would be worthwhile to use these models tentatively to consider this relation. For this reason we have applied some of our original calculations to the adsorption of hydrogen on copper. In this qualitative study only one calculation was made with the copper atomic orbitals[23]); in most cases we used the nickel orbitals, taking 11 valence electrons.

2.3. THE MOLECULAR ORBITAL METHOD

For a study of the surface molecule concept it would be most appropriate

to consider the influence of the surrounding crystal as a perturbation. Hydrogen adsorption on different nickel surfaces could, for instance, be treated as a NiH molecule in different crystal fields. Since, however, the influence of the crystal in this system is mainly a covalency or delocalization effect, the most convenient way to obtain quantitative information is by a Molecular Orbital method. The most serious drawback of this method is the difficulty in defining the boundary conditions of relatively small clusters such that they represent a semi-infinite, or at least large, crystal. Bennett et al.[21] found a solution to this problem for layer structures, such as graphite, but for a "really three-dimensional" crystal this is still an object for further study. In the interpretation of the results presented here we have tried to correct for the smallness of the clusters by considering relative effects.

The simplest MO–LCAO method applicable to these models is the Extended Hückel method[24]. The overlap matrix elements S_{pq} of the secular equations

$$(H - \varepsilon S)\, c = 0 \tag{1}$$

are calculated with the atomic orbitals χ_p specified above. The diagonal matrix elements H_{pp} are set equal to the empirical atomic Valence State Ionization Energies (VSIE)[25, 26]; the non-diagonal elements are approximated by the Wolfsberg-Helmholz formula[27]:

$$H_{pq} = K S_{pq} (H_{pp} + H_{qq})/2. \tag{2}$$

Since metallic nickel has 0.6 holes in the d-band, the atomic Valence State for nickel was taken as $3d^{9.4}\, 4s^{0.6}$, for which the Ionization Energies were obtained by linear interpolation (table 1). The Wolfsberg–Helmholz constant was usually chosen as $K = 1.75$; the effect of variations in K has been examined. Transformation of the secular equations with the matrix $S^{-1/2}$ and application of an algorithm for the calculation of matrix eigenvalues and eigenvectors, yield the orbital energies ε_i and the molecular orbitals

$$\varphi_i = \sum_p \chi_p c_{pi}. \tag{3}$$

Before relating the results of an Extended Hückel calculation to experimental quantities as binding energies and dipole moments we have to make some comments. The Extended Hückel method does not explicitly calculate the electron–electron or the electron–core interactions. Therefore it is impossible to compute exactly the LCAO total energy of a molecule. The same restriction holds for molecular binding or dissociation energies, which are defined as the energy differences between the molecule and its separate parts. It has been shown[28], however, that a reasonably good approximation to the binding energy can be given in terms of the orbital

energies:

$$\Delta E = \sum_{\substack{\text{molecule} \\ \text{AB}}} n_i^{AB} \varepsilon_i^{AB} - \sum_{\substack{\text{part} \\ \text{A}}} n_i^A \varepsilon_i^A - \sum_{\substack{\text{part} \\ \text{B}}} n_i^B \varepsilon_i^B, \qquad (4)$$

where the summations extend over all orbitals of the indicated species, multiplied by their occupation numbers, n_i. This expression is based on the assumption that the extra electronic repulsion in the molecule, compared with the separate parts, equals the extra internuclear repulsion. Using it we must remember two limitations:

(1) for small distances it underestimates the repulsion because of this assumption.

(2) for large distances it converges, in case of heteronuclear molecules, to the binding energy between ions, just as the exact SCF binding energy often does.

There is enough practical experience, however, to apply this formula with some confidence in the region around the chemical bonding distance, especially for our aim, which is the calculation of the relative stability of bonding between a hydrogen atom and some clusters of metal atoms.

Another shortcoming of the Extended Hückel method hinders us if we want to calculate the work function change or surface dipole moment. A method of doing this approximately would be to compute the Mulliken atomic charges[29] on the hydrogen and the metal atoms. It is known, however, that the atomic charges calculated from Extended Hückel MO's are too large. The usual way to correct this is the introduction of a charge-dependent H matrix by writing, for instance[25]:

$$H_{pp} = -\alpha_p - \beta_p q_A - \gamma_p q_A^2, \qquad (5)$$

where α_p is the VSIE of the atomic orbital χ_p, β_p and γ_p describing its charge dependence, and q_A is the Mulliken charge of the atom to which χ_p belongs. The molecular orbitals and the atomic charges are then determined by an iterative procedure. This process yields more realistic charges indeed, but, as we have observed, it also introduces into our models an unrealistic effect in the binding energies given by eq. (4). This can be understood as follows: if there is a shift of electron charge from nickel to hydrogen, the orbital energies change according to (5). The single hydrogen orbital is raised in energy, but all nickel orbitals, including those which are not bonding to hydrogen, are lowered by approximately the same amount. This leads to a large drop in the average orbital energy and, therefore, to an enormous increase in the binding energy calculated by formula (4) with the lowered MO's and the original atomic orbital energies. Within the framework of the Extended Hückel method this problem can only be solved by assuming that the nickel orbital energies depend considerably

less on the atomic charge than the hydrogen orbital energy does, an assumption for which we could not find any evidence in the literature, however.

For the interpretation of our results we have chosen the following solution. By performing some iterative calculations we have confirmed that the relative charges do not change by iteration. Therefore we have mostly applied the original non-iterative Extended Hückel method, using the VSIE's of the neutral atoms. The effect of the exaggerated ionicity on the binding energies is checked. The surface dipole moments can only be interpreted relative to each other, as their absolute values are too high.

3. Results and discussion

3.1. THE BULK NICKEL CLUSTER

As we wish, at first, to compare the results of our calculations on relatively small clusters to experimental data on large crystals or to band calculations on infinite crystals, we would like to use concepts as: band width, occupation of bands, Fermi level, etc. These concepts must be defined in terms of our discrete set of orbital energy levels and MO coefficients. We shall use the following definitions:

The width of the d-band is the energy difference between the highest and the lowest orbital with a strong d-character. The Fermi level is the energy of the highest occupied MO. The amount of d-character of the electrons in a definite cluster is:

$$N^d = \sum_{\substack{\text{all atoms} \\ k}} N_k^d , \qquad (6)$$

where N_k^d is the total gross population[29] of the d-orbitals on atom k. An analogous formula defines the amount of s-character. If n^d is the average 3d-character per atom, then $(10 - n^d)$ is the number of holes in the d-band. The charge of an atom[29], q_k, is the core charge minus the gross atomic population, $N_k = N_k^d + N_k^s$.

For comparison of the binding energy calculated for small nickel clusters by formula (4) with the experimental cohesion energy of the metal, we must note that in the bulk cluster only the central nickel atom has its complete nearest neighbour environment, whereas the 12 surrounding atoms only have 5 nearest neighbours each. In the surface clusters even part of these environments are removed. Considering the nearest neighbour interactions as the most important we can "renormalize" the binding energy calculated for the cluster by multiplying it by the ratio of the coordination number in the metal (12) to the average coordination number in the cluster. If this quantity is divided by the number of cluster atoms it can be related to the metallic cohesion energy.

Some results of non-iterative calculations on the four nickel clusters shown in fig. 1 are listed in table 2. The "d-band width" of the bulk cluster (1.81 eV) is smaller than the values calculated by Fletcher[30] (2.7 eV), Hanus[31] (≈ 5 eV) and Yamashita et al.[32] (≈ 4 eV). To explain this effect we have also performed some tight-binding calculations on an infinite nickel crystal (space symmetry group Fm3m = O_h^5) using the Extended

<center>TABLE 2</center>

<center>Results for the nickel clusters (the numbering of the atoms is indicated in fig. 1)</center>

	Bulk cluster	(111) surface cluster	(100) surface cluster	(110) surface cluster
d-band width (eV)	1.81	1.67	1.63	1.59
Fermi level (eV)	-7.64	-7.72	-7.66	-7.69
Holes in d-band	0.68	0.67	0.59	0.54
Total binding energy (eV)	22.7	17.1	15.0	13.3
"Renormalized" cohesion energy (eV)	3.8	4.3	4.5	4.7
Atomic charge $q(1)$	2.54	1.37	0.12	0.02
$q(1)_{surface} - q(1)_{bulk} = \Delta q(1)$	–	-1.17	-2.42	-2.52
$\Delta q(2)$	–	-0.01	-0.05	-0.04
$\Delta q(3)$	–	$+0.19$	$+0.44$	$+0.30$
$\Delta q(4)$	–	–	–	$+0.35$

Hückel formalism and the method of Slater and Koster[33]. Taking the parameter choice indicated for the clusters we found a d-band width of 2.8 eV; with a Wolfsberg–Helmholz constant $K = 2.0$ this value becomes 3.8 eV (compared to 2.44 eV for the bulk cluster). From this result, together with evidence in the literature[34, 35] that the Extended Hückel method yields reasonable valency band widths, we conclude that the narrow "d-band" is a consequence of the limited size of the cluster. The 4s "band width" of 18.4 eV computed for the bulk cluster is close to the width of the conduction band calculated by Hanus[31] (16.4 eV). This agreement must be fortuitous, however, since, in accordance with previous experience[34], a tight-binding calculation of the infinite crystal yields a conduction band which is too broad (≈ 90 eV).

The Fermi level is calculated to be lower (-7.64 eV) than the experimental value of ≈ -5 eV [Farnsworth and Madden[36] -5.22 eV, Gerlach and Rhodin[37] -4.75 eV]. The position of the Fermi level varies little with a different Wolfsberg–Helmholz constant, but is, of course, strongly dependent on the VSIE's substituted in the diagonal elements H_{pp}. In the bulk cluster the "number of holes in the d-band" is 0.68 which agrees well with the experimental values lying around 0.6.

For the cohesion energy, "renormalized" for the correct number of nearest neighbours, we found a value of 3.8 eV per atom, the experimental cohesion energy being 4.40 eV[38]).

Calculations with only 3d orbitals on the nickel atoms and 9 valence electrons yielded a slightly smaller band width (1.75 eV). The Fermi level was found to be -7.79 eV. If 4 or 5 extra electrons are added, making 9.3 to 9.4 d-electrons per atom, then the Fermi level is the same height as that from the calculations including the 4s-orbitals (-7.64 eV). Apparently, in this model there is not much interaction between the 3d and the 4s band.

From these comparisons we can conclude that the atomic orbitals and the parameters used in the Extended Hückel method are reasonably good. The VSIE's are probably somewhat too large, but the relative position of the 3d and 4s orbitals is well represented. Conclusions about adsorption which are made hereafter, should be checked for their sensitivity with respect to changes in the absolute values of the VSIE's and in the Wolfsberg–Helmholz constant K.

As mentioned already in the description of the model, the atomic charges calculated with the Extended Hückel method for this relatively small nickel cluster are rather high, $+2.54$ units on the central atom, -0.21 on each of its neighbours. Therefore all surface and adsorption effects on the charge distribution should be considered relative to this bulk cluster.

3.2. SURFACE CLUSTERS

If some atoms are removed from the bulk cluster in order to obtain models for the environment of a nickel atom at a (111), (100) or (110) surface (figs. 1b, 1c, 1d), the symmetry of the original system is lowered. The orbitals which form a basis for two or three-dimensional representations of the group O_h split into doubly or non-degenerate orbitals. No specific difference can be observed between the "bulk" t_{2g} and e_g orbitals, which are bonding and non-bonding, respectively, according to a hypothesis of Goodenough[39]) [used in adsorption models of Bond[40]) and Shopov et al.[12])]. Both symmetry orbitals are present in the top of the "d-band" of the bulk cluster and they are affected by the same amount at the occurrence of the "surface".

A distinct effect, however, is found on the charge distribution. Negative charge is shifted to the surface atoms, especially to the central nickel atom, which is transferred from its bulk surroundings to a surface environment. This shift of electrons to the surface increases in the order (111) < (100) < (110), with a decreasing number of neighbours to the surface atoms (table 2). Some iterative Extended Hückel calculations using formula (5), show lower absolute values of the atomic charges, but the same relative effects.

The occurrence of the surface also caused an increase in the amount of d-character of the electrons and a larger cohesion energy per nearest neighbour bonding. Both effects increased in the order (111)<(100)<(110).

3.3. HYDROGEN ADSORBED ON THE CENTRAL NICKEL ATOM

The binding energy of a hydrogen atom adsorbed on the central nickel atom of the surface clusters (figs. 2a, 2b, 2c) is calculated according to formula (4) by subtracting the energy of the hydrogen atom and the metal cluster separately from the energy of the combined system. The results, together with the binding energy of a NiH molecule, are shown in fig. 3a as a function of the distance between the hydrogen atom and the central nickel atom.
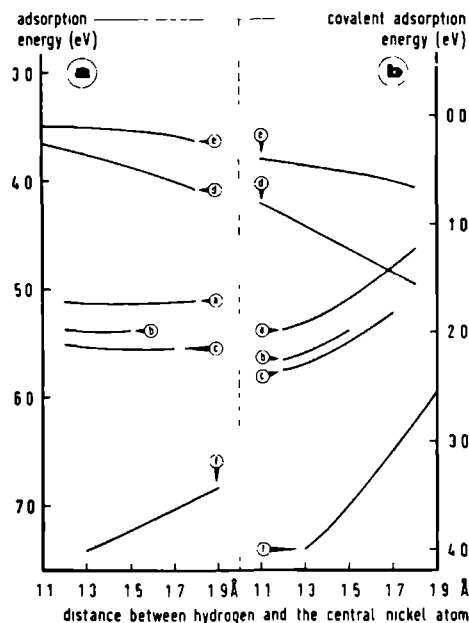
Fig. 3. Binding energy for a hydrogen atom adsorbed: on the (111) surface (curve a), on the (100) surface (curve b), on the (110) surface (curve c), in a (111) surface hole (curve d), in a (100) surface hole (curve e), of nickel (3d and 4s electrons), compared with NiH (curve f)

The binding energy at the equilibrium distance, 1.4 to 1.5 Å (the experimental distance in nickelhydride is 1.47 Å [41]), the sum of the covalent radii of Ni and H is 1.6 Å), is higher than the experimental adsorption energy of hydrogen atoms on nickel [42] (2.91 eV). It clearly shows a decrease when the nickel atom bound to hydrogen is surrounded by an increasing number of neighbours or, in other words, when the surface is more closely packed.

In order to analyze this result it is convenient to transform the orbitals in all clusters to a set of coordinate systems with the z-axes perpendicular to the surface (figs. 2a, 2b, 2c; the hydrogen atom lies on the z-axis of the central nickel atom). The most important gross atomic orbital populations, atomic charges and overlap populations are given in table 3. From the overlap populations it becomes evident that the hydrogen atom is most strongly bonded to the central nickel atom, especially to the $3d_{z^2}$ and $4s$ orbital. The effect of the other nickel atoms on this bond is smaller and apparently decreases the bond strength. The overlap population between the hydrogen orbital and the central nickel $4s$ orbital is relatively large and rises with increasing binding energy, whereas the overlap population with $3d_{z^2}$ is smaller and shows the opposite effect; therefore, it is probable that the $4s$ orbital plays an important rôle in the covalent bonding between nickel and hydrogen.

Examining the orbital populations we find a large charge transfer from the central nickel $3d_{z^2}$ orbital to the hydrogen. Compared to this electron transfer the other effects of adsorption on the charge distribution are small. In describing the model we have noticed already that this accumulation of charge on the hydrogen atom is probably enhanced by the Extended Hückel method. Consequently, also the Extended Hückel binding energies are too large, due to an exaggerated shift of electrons from the higher nickel orbitals to the lower hydrogen orbital. Therefore we have corrected the calculated binding energies by subtracting the atomic orbital energy differences multiplied by the charge shifts occurring on hydrogen adsorption. The result, which could be called the "covalent binding energy" is plotted in fig. 3b. This binding energy does not show a minimum as a function of distance and is lower than the experimental adsorption energy. This could be caused by the fact that the real situation does not correspond to zero ionicity, but lies somewhere in between the results of figs. 3a and 3b. It is striking, however, that the order of adsorption strengths on different surfaces is unchanged.

From the negative charge on the hydrogen atom it may be concluded that hydrogen adsorption gives rise to a more negative surface potential, although the effect is probably smaller than calculated by the non-iterative Extended Hückel method. The variations in this hydrogen charge for different clusters are so small that it is not justified to make any conclusions about relative effects on various surfaces.

Calculations with 3d orbitals only and 9 valence electrons per nickel atom yield larger binding energies (fig. 4a) and an opposite, although smaller, dependence on the number of neighbours of the central nickel atom (compared to the calculations including 4s orbitals shown in fig. 3a). This is not in contradiction to our earlier conclusion that the central nickel 4s orbital

TABLE 3a

Most important orbital populations and atomic charges for hydrogen on nickel; the Ni(1)–H distance is 1.5 A; the numbering of the atoms is indicated in fig. 2

	(111) surface cluster	(111) surface cluster + H	(100) surface cluster	(100) surface cluster + H	(110) surface cluster	(110) surface cluster + H
$3d_{z^2}(1)$	1.904	0.972	1.979	0.928	1.962	0.931
$3d_{xz}(1)$	1.960	1.967	1.759	1.759	1.860	1.860
$3d_{yz}(1)$	1.960	1.967	1.759	1.759	1.971	1.971
$3d_{x^2-y^2}(1)$	1.167	1.364	1.992	1.992	1.956	1.961
$3d_{xy}(1)$	1.167	1.364	1.913	1.913	1.744	1.861
total 3d(1)	8.158	7.635	9.401	8.351	9.493	8.583
4s(1)	0.468	0.368	0.477	0.391	0.485	0.415
total 3d(2)	9 465	9.457	9.635	9.585	9.635	9.626
4s(2)	0.753	0.724	0.625	0.595	0.618	0.577
total 3d(3)	9.457	9.419	9.186	9.314	9.378	9.420
4s(3)	0.565	0.663	0.584	0.654	0.535	0.562
total 3d(4)	–	–	–	–	9.419	9.397
4s(4)	–	–	–	–	0.446	0.582
$q_{Ni(1)}$	+ 1.37	+ 2.00	+ 0.12	+ 1.26	+ 0.02	+ 1.00
$q_{Ni(2)}$	− 0.22	− 0.18	− 0.26	− 0.18	− 0.25	− 0.20
$q_{Ni(3)}$	− 0.02	− 0.08	+ 0.23	+ 0.03	+ 0.09	+ 0.02
$q_{Ni(4)}$	–	–	–	–	+ 0.13	+ 0.02
q_H	–	− 0.66	–	− 0.67	–	− 0.69

	(111) surface cluster	(111) surface cluster + H in hole	(100) surface cluster	(100) surface cluster + H in hole		NiH
$3d_{z^2}(1)$	1.904	1.570	1.979	1.748	$3d_{z^2}$	0.971
$3d_{xz}(1)$	1.960	1.967	1.759	1.759	total 3d	8.971
$3d_{yz}(1)$	1.960	1.967	1.759	1.759	4s	0.390
$3d_{x^2-y^2}(1)$	1.167	1.364	1.992	1.992	q_{Ni}	+0.64
$3d_{xy}(1)$	1.167	1.364	1.913	1.913	q_H	−0.64
total 3d(1)	8.158	8.234	9.401	9.171		
4s(1)	0.468	0.357	0.477	0.331		
total 3d(2)	9.465	9.522	9.635	9.695		
4s(2)	0.753	0.762	0.625	0.603		
$3d_{z^2}(3)$	1.959	1.921	1.985	1.960		
$3d_{xz}(3)$	1.807	1.824	1.918	1.916		
$3d_{yz}(3)$	1.947	1.928	1.633	1.710		
$3d_{x^2-y^2}(3)$	1.983	1.910	1.912	1.836		
$3d_{xy}(3)$	1.761	1.762	1.738	1.840		
total 3d(3)	9.457	9.344	9.186	9.262		
4s(3)	0.565	0.431	0.584	0.468		
$q_{Ni(1)}$	+ 1.37	+ 1.41	+ 0.12	+ 0.50		
$q_{Ni(2)}$	− 0.22	− 0.28	− 0.26	− 0.30		
$q_{Ni(3)}$	− 0.02	− 0.22	+ 0.23	+ 0.27		
q_H	–	− 0.38	–	− 0.39		

Overlap populations with the hydrogen 1s orbital; the Ni(1)–H distance is 1.5 Å; the numbering of the atoms is indicated in fig. 2

	(111) surface cluster + H	(100) surface cluster + H	(110) surface cluster + H
$3d_{z^2}(1)$	0.0600	0.0526	0.0452
4s(1)	0.1399	0.1479	0.1589
total (1)	0.1999	0.2005	0.2041
4s(2)	− 0.0029	0.0004	0.0005
total (2)	− 0.0021	0.0016	0.0014
4s(3)	− 0.0087	− 0.0089	− 0.0087
total (3)	- 0.0093	− 0.0094	− 0.0086
4s(4)	–	–	− 0.0080
total (4)	–	–	− 0.0091

TABLE 3b (continued)

	(111) surface cluster + H in hole	(100) surface cluster + H in hole	NiH	
$3d_{z^2}(1)$	0.0394	0.0432	$3d_{z^2}$	0.0241
4s(1)	0.0477	0.0527	4s	0.2080
total (1)	0.0871	0.0958	total	0.2321
4s(2)	− 0.0071	− 0.0066		
total (2)	− 0.0058	− 0.0052		
$3d_{z^2}(3)$	0.0038	0.0045		
$3d_{zz}(3)$	0.0	0.0005		
$3d_{yz}(3)$	0.0079	0.0		
$3d_{z^2-y^2}(3)$	0.0158	0.0162		
$3d_{xy}(3)$	0.0	0.0		
4s(3)	0.0705	0.0441		
total (3)	0.0980	0.0653		

is largely responsible for the covalent bonding of a hydrogen atom; it is the consequence of a higher ionicity. If the ionic contribution to the binding energy is subtracted, as described previously, the covalent binding energy is lower than in the model with 4s orbitals (fig. 4b). That the effect of the surrounding nickel atoms is reversed and is smaller can be explained by assuming that the main part of this effect is repulsive (in agreement with the conclusion from fig. 3) and is caused by the 4s orbitals of these nickel atoms.

3.4. HYDROGEN ADSORBED IN A NICKEL SURFACE "HOLE"

If a hydrogen atom is adsorbed in a "hole" between 3 or 4 surface atoms of a (111) or (100) nickel face, it is placed perpendicularly over the central

nickel atom lying in the second layer, which is 2.03 Å or 1.76 Å, respectively, below the surface. The other nickel atoms can now, however, certainly not be considered as a perturbation, since some of them are at approximately the same distance to the hydrogen atom. The models used for hydrogen adsorption in these positions are shown in figs. 2d and 2e. In fig. 3a the
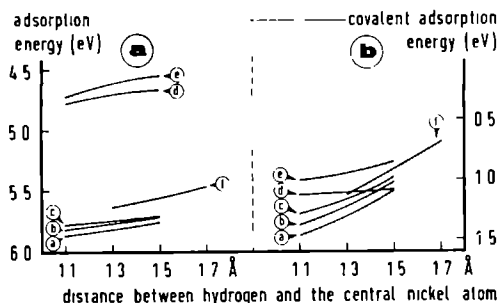

Fig. 4. Binding energy for a hydrogen atom adsorbed on nickel (3d electrons only), compared with NiH. The labeling of the curves is indicated in fig. 3.

calculated binding energies are plotted as a function of the distance between the hydrogen atom and the central nickel atom directly under it. These binding energies are lower than the values calculated for hydrogen adsorbed over a surface nickel atom. Besides the overlap populations of the hydrogen atom with the central nickel atom, also the overlap populations with the 3 or 4 neighbouring surface atoms are important now. These overlap populations are smaller than the one between hydrogen and the central nickel atom in the clusters of figs. 2a, b and c, although their sum is larger. Also the charge transfer effect from nickel to hydrogen is smaller, which might provoke the question whether the lower binding energies are not caused by a lower ionicity. Fig. 3b, however, where the "covalent binding energies" are compared, shows that this is not the case.

The lowering of the charge transfer (the charge on hydrogen is now more equally supplied by the bonding 3d and 4s orbitals) is such a distinct effect that we can conclude that hydrogen adsorption in a surface hole causes a less negative surface potential than adsorption on the surface atoms.

Calculations with just the nickel 3d electrons only confirm the previous conclusions.

Several of the calculations for hydrogen adsorption on nickel were repeated with different parameters or employing the iterative Extended Hückel method. The Wolfsberg-Helmholz constant was taken as $K=2.0$ or $K=2-|S_{pq}|$[43]) instead of the usual value $K=1.75$. The VSIE's of the

TABLE 4a

Most important orbital populations and atomic charges for hydrogen on copper; the Cu(1)–H distance is 1 5 A, the numbering of the atoms is indicated in fig 2

	(111) surface cluster	(111) surface cluster + H	(100) surface cluster	(100) surface cluster + H	(110) surface cluster	(110) surface cluster + H
$3d_{z^2}(1)$	1 996	1 979	1 996	1 846	1 994	1 887
$3d_{xz}(1)$	1 991	1 991	1 989	1 989	2 000	2 000
$3d_{yz}(1)$	1 991	1 991	1 989	1 989	1 995	1 995
$3d_{x^2-y^2}(1)$	1 978	1 967	1 992	1 992	1 989	1 978
$3d_{xy}(1)$	1 978	1 967	1 957	2 000	1 977	1 977
total 3d(1)	9 933	9 894	9 922	9 816	9 955	9 837
4s(1)	0 519	0 347	0 706	0 390	0 633	0 414
total 3d(2)	9 975	9 978	9 980	9 982	9 976	9 980
4s(2)	1 134	1 054	1 206	1 232	1 291	1 153
total 3d(3)	9 971	9 967	9 967	9 972	9 978	9 976
4s(3)	0 994	0 948	0 940	0 833	0 967	0 990
total 3d(4)	–	–	–	–	9 964	9 963
4s(4)	–	–	–	–	1 133	0 898
$q_{Cu(1)}$	+ 0 55	+ 0 76	+ 0 37	+ 0 79	+ 0 41	+ 0 75
$q_{Cu(2)}$	– 0 11	– 0 03	– 0 19	– 0 21	– 0 27	– 0 13
$q_{Cu(3)}$	+ 0 03	+ 0 08	+ 0 09	+ 0 20	+ 0 05	+ 0 03
$q_{Cu(4)}$	–	–	–	–	– 0 10	+ 0 14
q_H	–	– 0 82	–	– 0 72	–	– 0 76

	(111) surface cluster	(111) surface cluster + H in hole	(100) surface cluster	(100) surface cluster + H in hole		CuH
$3d_{z^2}(1)$	1.996	1.933	1.996	1.922	$3d_{z^2}$	1.877
$3d_{xz}(1)$	1.991	1.992	1.989	1.989	total 3d	9.877
$3d_{yz}(1)$	1.991	1.992	1.989	1.989	4s	0.480
$3d_{x^2-y^2}(1)$	1.978	1.988	1.992	1.992	q_{Cu}	+ 0.64
$3d_{xy}(1)$	1.978	1.988	1.957	2.000	q_H	− 0.64
total 3d(1)	9.933	9.893	9.922	9.891		
4s(1)	0.519	0.439	0.706	0.567		
total 3d(2)	9.975	9.976	9.980	9.977		
4s(2)	1.134	1.290	1.206	1.494		
$3d_{z^2}(3)$	1.998	1.995	1.998	1.993		
$3d_{xz}(3)$	1.994	1.996	1.996	1.990		
$3d_{yz}(3)$	1.992	1.965	1.988	1.994		
$3d_{x^2-y^3}(3)$	1.998	1.961	1.996	1.961		
$3d_{xy}(3)$	1.989	1.990	1.989	1.989		
total 3d(3)	9.971	9.907	9.967	9.928		
4s(3)	0.994	0.646	0.940	0.621		
$q_{Cu(1)}$	+ 0.55	− 0.67	+ 0.37	+ 0.54		
$q_{Cu(2)}$	− 0.11	− 0.27	− 0.19	− 0.47		
$q_{Cu(3)}$	+ 0.03	+ 0.45	+ 0.09	+ 0.45		
q_H	−	− 0.41	−	− 0.46		

Overlap populations with the hydrogen 1s orbital; the Cu(1)–H distance is 1.5 Å, the numbering of the atoms is indicated in fig. 2

	(111) surface cluster + H	(100) surface cluster + H	(110) surface cluster + H
$3d_{z^2}(1)$	−0.0510	−0.0024	−0.0202
$4s(1)$	0.2215	0.1740	0.1945
total (1)	0.1705	0.1717	0.1743
$4s(2)$	−0.0416	0.0031	−0.0277
total (2)	−0.0444	0.0006	−0.0302
$4s(3)$	0.0004	−0.0129	−0.0109
total (3)	0.0000	−0.0135	−0.0118
$4s(4)$	–	–	−0.0041
total (4)	–	–	− 0.0045

TABLE 4b (continued)

	(111) surface cluster + H in hole	(100) surface cluster + H in hole	CuH	
$3d_{z^2}(1)$	0.0104	0.0075	$3d_{z^2}$	0.0123
$4s(1)$	0.0179	−0.0442	$4s$	0.2185
total (1)	0.0282	−0.0367	total	0.2309
$4s(2)$	−0.0188	−0.0418		
total (2)	−0.0192	−0.0422		
$3d_{z^2}(3)$	−0.0001	−0.0010		
$3d_{xz}(3)$	0.0	0.0011		
$3d_{yz}(3)$	0.0066	0.0		
$3d_{x^2-y^2}(3)$	0.0086	0.0046		
$3d_{xy}(3)$	0.0	0.0		
$4s(3)$	0.1194	0.1039		
total (3)	0.1345	0.1086		

nickel 3d and 4s orbitals were shifted by an equal amount such that the experimental Fermi level in the bulk cluster was reproduced. Although these modifications changed the quantitative results somewhat, the effects discussed above are unaltered.

3.5. HYDROGEN ADSORBED ON COPPER

The greater activity of nickel in many reactions, as compared to copper, is usually ascribed to the partly filled d-band. There is, for instance, the effect that dissociative chemisorption of H_2 on nickel requires a much smaller activation energy tha⁻ on copper, whereas the adsorption energy of atomic hydrogen is not much larger [2.91 eV for nickel[42], 2.43 eV for copper[44, 45]]. We have tried by our model calculations to obtain some information which might help to explain the observed effects.

The most important change in going from nickel to copper is the extra valence electron, filling the d-band· and part of the conduction band. In addition there is a change in parameters such as the lattice constant, the energies and exponents of atomic orbitals. In most cases we have compared the results for hydrogen on nickel to the results obtained when one extra electron per metal atom is added. In one calculation (hydrogen adsorbed on the (100) surface) we have introduced all the copper parameters (table 1). The last calculation showed that for the qualitative comparison of the adsorption on nickel and copper it is sufficient to go from 10 to 11 valence electrons, keeping the other parameters constant.

The binding energies for hydrogen on "copper" are drawn in fig. 5a. The binding energy for hydrogen adsorbed over a surface atom is even somewhat larger than for nickel. However, the charge on hydrogen is also slightly higher and the covalent binding energies (fig. 5b) are comparable to nickel. The binding energy for adsorption in a surface "hole" is considerably lower than for nickel. Analyzing the results in terms of orbital and overlap populations (table 4) we observe that the metal 3d orbitals do not participate in the hydrogen bonding. All the binding that takes place, both covalent and ionic, is due to the metal 4s orbitals. This 4s bonding is stronger for
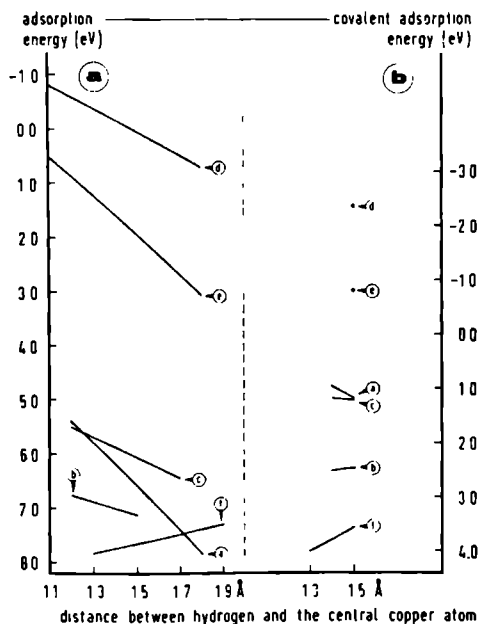
Fig. 5. Binding energy for a hydrogen atom adsorbed on copper (nickel 3d and 4s orbitals, 1 extra valence electron), compared with CuH. The labeling of the curves is indicated in fig. 3.

copper than for nickel, which could be explained by the fact that the metal 4s band is now exactly half filled. The order of the binding energies on different surfaces also deviates from the nickel case.

Although we find a very different bonding behaviour of the 3d electrons in copper as compared to nickel, this model gives no direct evidence for the greater activity of the latter metal. For the study of this subject we should extend it, for instance, to a model for dissociative chemisorption of H_2, such as described in ref. 13.

4. Conclusions

Bearing in mind the approximate nature of the model we think that some interesting conclusions can still be drawn. The binding between a nickel crystal and a hydrogen atom adsorbed on top of a surface atom is similar to a simple NiH molecular bond. The main interaction takes place between the nickel $3d_{z^2}$ orbital, pointing towards the H atom, the 4s orbital and the hydrogen 1s orbital. The adsorption energy decreases slightly with an increasing number of nickel atoms surrounding the "surface molecule". Whether this result means that the effect of the neighbouring nickel atoms is always repulsive or if it is only true for the specific environments in the (111), (100) and (110) surfaces is yet to be studied. In any case, the contrary result would be obtained if the interaction between a hydrogen atom and the nickel atoms were represented by a pairwise interaction potential of the Lennard-Jones type [46]).

The models for adsorption in a surface "hole" show that this position is energetically less favourable. The negative charge on the adsorbed atom is smaller than for hydrogen adsorbed over a surface atom, thus causing a less negative surface potential.

Our calculations including all 3d orbitals do not support the models discussed by Bond [40]) and calculated by Shopov, Andreev and Petkov [12]), based on the idea that the d-orbitals which afford the e_g representation ($d_{x^2-y^2}$ and d_{z^2} in the coordinate system of fig. 1) are non-bonding in the metal and are therefore particularly suitable for adsorption bonding. We have found no indication for a particulary important rôle of these e_g orbitals, neither in the models for hydrogen adsorption on the surface, nor in those for "hole" adsorption. On the contrary, we conclude that among the 3d orbitals the transformed d_{z^2} orbital pointing perpendicularly out of the surface is most important for chemisorption on the surface atoms. This is completely at variance with Bond's model because at the (111) surface, for instance, this orbital is written in the original coordinate system as $(d_{xy}+d_{xz}+d_{yz})/\sqrt{3}$ and thus belongs to the t_{2g} representation of the crystal point group.

Generally, we find that the structure of the surface molecule is more significant for determining which d-orbitals are primarily involved in chemisorption than is the interaction with the "bulk" metal atoms.

Another interesting effect emerging from our model calculations is the important rôle of the 4s orbitals in covalent adsorption bonding. For copper, where the 3d orbitals are not involved in the adsorption bond, the increased 4s contribution even compensates the decrease in adsorption energy.

Finally we want to point out two possible improvements of this model which can be made in order to consolidate its conclusions. Firstly, the effect of truncating the nickel crystal must be taken into account more elegantly. Secondly, the Extended Hückel method insufficiently prevents charge accumulations on certain atoms, whereas the iterative procedure with charge dependent orbital energies is unsatisfactory as these modified orbital energies enter directly into the binding energy. It would be preferable to replace the Extended Hückel formalism by a MO method which takes the electron repulsion explicitly into account.

References

1) T. B. Grimley, in: *Molecular Processes on Solid Surfaces,* Eds. E. Drauglis, R. D. Gretz and R. J. Jaffee (McGraw-Hill, New York, 1969) p. 299.
2) A. Sherman, C. E. Sun and H. Eyring, J. Chem. Phys. **3** (1934) 49.
3) D. D. Eley, Discussions Faraday Soc. **8** (1950) 34.
4) J. C. P. Mignolet, J. Chem. Phys. **21** (1953) 1298.
5) F. A. Matsen, A. C. Makrides and N. Hackerman, J. Chem. Phys. **22** (1954) 1800.
6) D. P. Stevenson, J. Chem. Phys. **23** (1955) 303.
7) I. Higuchi, T. Ree and H. Eyring, J. Am. Chem. Soc. **79** (1957) 1330.
8) G. Blyholder, J. Phys. Chem. **68** (1964) 2772.
9) A. Laforgue, J. Rousseau and B. Imelik, Advan. Chem. Phys. **8** (1965) 141.
10) N. N. Bulgakov and Y. A. Borisov, Kinetika i Kataliz **7** (1966) 608.
11) H. H. Dunken and C. Opitz, 4th Congr. Catalysis, Moscow (1968).
12) D. Shopov, A. Andreev and D. Petkov, J. Catalysis **13** (1969) 123.
13) A. van der Avoird, Surface Sci. **18** (1969) 159.
14) H. D. Hagstrum and G. E. Becker, J. Chem. Phys. **54** (1971) 1015.
15) W. G. Pollard, Phys. Rev. **56** (1939) 324.
16) T. B. Grimley, in: *Chemisorption,* Ed. W. E. Garner (Butterworths, London, 1957) p.17.
17) J. Koutecký, Trans. Faraday Soc. **54** (1958) 1038.
18) T. Toya, J. Res. Inst. Catalysis, Hokkaido Univ. **6** (1958) 308; **8** (1961) 209.
19) G. Blyholder and C. A. Coulson, Trans. Faraday Soc. **63** (1967) 1782.

20) D. M. Newns, Phys. Rev. **178** (1969) 1123.
21) A. J. Bennett, B. McCarroll and R. P. Messmer, Surface Sci. **24** (1971) 191; Phys. Rev. B3 (1971) 1397.
22) J. R. Schrieffer and R. Gomer, Surface Sci. **25** (1971) 315.
23) J. W. Richardson, W. C. Nieuwpoort, R. R. Powell and W. F. Edgell, J. Chem. Phys. **36** (1962) 1057.
24) R. Hoffman, J. Chem. Phys. **39** (1963) 1397.
25) H. Basch, A. Viste and H. B. Gray, Theoret. Chim. Acta **3** (1965) 458.
26) M. Zerner and M. Gouterman, Theoret. Chim. Acta **4** (1966) 44.
27) M. Wolfsberg and L. Helmholz, J. Chem. Phys. **20** (1952) 837.
28) J. Goodisman, J. Am. Chem. Soc. **91** (1969) 6552.
29) R. S. Mulliken, J. Chem. Phys. **23** (1955) 1833.
30) G. C. Fletcher, Proc. Phys. Soc. (London) **65** A (1952) 192.
31) J. G. Hanus, M.I.T. Solid State and Molecular Theory group, Quart. Progr. Rept. **44** (1962) 29.
32) J. Yamashita, M. Fukuchi and S. Wakoh, J. Phys. Soc. Japan **18** (1963) 999.
33) J. C. Slater and G. F. Koster, Phys. Rev. **94** (1954) 1498.
34) J.-M. André, G. S. Kapsomenos and G. Leroy, Chem. Phys. Letters **8** (1971) 195.
35) W. L. McCubbin, Chem. Phys. Letters **8** (1971) 507.
36) H. E. Farnsworth and H. H. Madden, J. Appl. Phys. **32** (1961) 1933.
37) R. Gerlach and T. N. Rhodin, in: *The Structure and Chemistry of Solid Surfaces*, Ed. G. A. Somorjai (Wiley, New York, 1969) p. 55-17.
38) J. S. Griffith, J. Inorg. Nucl. Chem. **3** (1956) 15.
39) J. B. Goodenough, Phys. Rev. **120** (1960) 67.
40) G. C. Bond, Platinum Metals Rev. **10** (1966) 87.
41) A. Heimer, Z. Physik **105** (1937) 56.
42) G. C. Bond, *Catalysis by Metals* (Academic Press, London, 1962).
43) L. C. Cusachs, J. Chem. Phys. **43** (1965) S 157.
44) J. Pritchard and F. C. Tompkins, Trans. Faraday Soc. **56** (1960) 540.
45) S. J. Holden and D. R. Rossington, J. Catalysis **4** (1965) 403.
46) R. J. Bacigalupi and H. E. Neustadter, Surface Sci. **19** (1970) 396.

LCAO STUDIES OF HYDROGEN CHEMISORPTION ON NICKEL

I. Tight-binding calculations for adsorption on periodic surfaces

D J M FASSAERT and A. VAN DER AVOIRD

Institute of Theoretical Chemistry, University of Nijmegen, Nijmegen, The Netherlands

The model we have used to study hydrogen chemisorption on nickel surfaces is a tight-binding Extended Huckel method applied to finite (periodic) crystals up to about 250 atoms, the non-orthogonal basis set comprising five 3d orbitals, one 4s orbital and three 4p orbitals per atom After calculating the band structure of fcc nickel, we have examined, by this model, the effect of the (100), (110) and (111) surfaces on the local density of states and the charge distribution The results agree closely with moment calculations of the density of states in semi-infinite crystals and with experimental (XPS, UPS and INS) spectra Extensive studies have been made of the influence of adsorption on the (partial) densities of states in order to illuminate the nature of the chemisorption bond Particularly, we have concluded that both the 3d electrons and the conduction electrons take part in this bond Equilibrium positions for adsorption on various sites have been determined and the adsorption energy has been computed and compared with experimental data We find that the stability of adsorption decreases in the order (110) > (100) > (111) and Atop > Bridge > Centred

1. Introduction

The last few years have shown a rapid increase in the number of quantum theoretical calculations on surfaces and adsorption stimulated mainly by the following two causes From the experimental side an increasing amount of data become available from many different techniques, mostly spectroscopical. on single surfaces which are structurally well-defined, for instance, by simultaneous LEED studies On the other hand, the computational methods for solids and molecules have advanced so far, that one is ready to attack the surface problem Especially the surfaces of semiconductors and transition metals, in view of their practical interest, are studied quite intensively

The quantum theoretical approaches to surfaces and adsorption can be divided into two categories The first group of methods is based on a semi-infinite crystal model, the second group on model clusters of limited size

The first model has been developed by Grimley [1], Koutecký [2] and others [3], and can now be applied to calculate adsorption energies, explicitly taking into account

the effect of electron repulsion on the adsorbed atom and some nearby surface atoms [4–6] This has been performed by Grimley and Pisani [4] in the Hartree Fock scheme and by Paulson and Schrieffer [6] in a Valence-Bond formalism Although one has found an elegant way to deal with the band structure of the under-lying solid in the form of a Green function or resolvent, this treatment is still so complicated that it has only been applied to hypothetical "cubium" crystals (Cubic crystals with one s-type orbital per atom, described by a tight binding scheme with only nearest neighbour interactions) In applications to real d-electron systems (transition metals) the form of the d-band was greatly oversimplified For instance, the density of d-states is replaced by a simple δ-function [7], a semi elliptical distri-bution [8] or other approximations [9,10]

The only semi-infinite crystal studies which incorporate the real structure of the d-band in fcc, bcc or hcp transition metals are those of Cyrot-Lackmann et al [11–15] and Heine [16], Haydock et al [17–19] They calculate the d-band density of states by a moment expansion technique or by a continued-fraction expansion of the (local) Green function The d band is described by a tight-binding scheme, and the effect of the conduction electrons and d-band/conduction band hybridization are neglected When discussing our results, we refer in more detail to these calculations, which also include some treatments of adsorption

The second type of methods use a cluster model for the surface or adsorption site These methods which are now applied to clusters up to 30 light atoms such as carbon or 15 transition-metal atoms, are the same as those used for large organic molecules or transition-metal complexes the Extended Huckel method [20], the CNDO method [21] and the SCF Xα Scattered Wave method [22–24] Although the semi-empirical methods are always hampered by some arbitrariness in the choice of parameters, one has collected so much material from molecular calculations by now, that a realistic interpretation of the results is nevertheless possible The main difficulty with these limited-size clusters is that they should be embedded in a larger crystal with covalent bonding occurring between the atoms This embedding is usually omitted or simulated by some artificial boundary conditions, the effects of which are not known

The calculations presented in this paper provide a link between the two different approaches of the surface problem We have calculated finite crystals by the LCAO or tight-binding method, approximating matrix elements over atomic orbitals by the Extended Huckel scheme This enables a direct comparison with cluster model re-sults On the other hand, by imposing Born–Von Kármán periodic boundary condi-tions on the crystal in directions parallel to the surface and transforming the secular matrix to Bloch type "layer orbitals", we have simplified the calculations to a large extent Thus, we have treated transition-metal crystals up to about 250 atoms, with 9 orbitals per atom The periodicity imposed on the crystals prevents the occurrence of undesired boundary effects and the crystal size permitted by this method is already sufficient to calculate the band structure, the density of states, etc , which can be compared with (semi-)infinite crystal results

As a typical example of practical importance we have studied the adsorption of

hydrogen atoms on different low index surfaces of fcc nickel as a function of the adatom position. Besides the 3d orbitals, 4s and 4p orbitals have been included since we know that, via hybridization, they have an effect on the band structure [25] and, particularly, we have found also [26] that they can strongly take part in adsorption bonding. Therefore, it seems better to include these orbitals than to omit them completely [4—19], although we realize that a tight-binding description of the conduction bands does probably not optimally represent all physical properties of the metal. We have given particular attention to the adsorption energies on different sites and to the effect of surface formation and hydrogen adsorption on the (local) charge distribution and density of states. Besides the possibility of comparing our results with either of the two traditional approaches, we also gain some insight into the localized character of the adsorption bond.

2. Description of the method

2.1. The model

In order to test the tight-binding Extended Hückel method and its parametrization, we have first performed some calculations of the bulk band structure of fcc nickel. The non-orthogonal atomic orbital basis set $\{_i\chi_p(r - R_m)\}; p = 1, ..., 9\}$, five 3d, one 4s and three 4p orbitals localized on the centres R_m, has been transformed into Bloch orbitals, after imposing Born—Von Kármán cyclic boundary conditions over N_1, N_2, N_3 unit cells. In order to obtain the one-electron states of the crystal a 9-dimensional (complex arithmetic) secular problem can be solved for each wave vector k independently. Usually in solid state theory one takes N_i ($i = 1$, 2, 3) infinitely large and calculates, in principle, all k points in the first Brillouin zone [27]. In practice, the calculation of any physical quantity has to be performed by summation over a certain number of representative points. In our model, since we intend to calculate surface and adsorption effects on finite crystals, we have studied both infinite and finite N_i. The latter choice corresponds to collecting a finite selection from the infinite crystal solutions, namely those Bloch waves of which the wave length is a divisor of the crystal dimensions. The effects of this selection are discussed.

For studying a specific surface plane, for instance (100), (110) or (111), we have chosen two of the lattice vectors, a_1 and a_2, parallel to this plane and simply omitted the cyclic boundary condition in the third, a_3, direction. Thus we have produced a crystal with two parallel surfaces which consists of N layers. If N is sufficiently large, which has been verified in our calculations, it can be assumed that these surfaces do not influence each other. In our crystal the bulk structure is continued up to the surfaces, but it is very simple to include the effect of surface dilation as long as the two-dimensional unit cell (a_1, a_2) is not perturbed. Also perturbations which double the unit cell dimensions, such as may occur by surface reconstruction or by half-monolayer adsorption, can be treated without too much difficulty.

We can benefit by the periodicity parallel to the surface if we introduce a basis of two-dimensional Bloch orbitals characterized by $k_\| = (k_1, k_2)$ and the layer number m and solve the following $9N$-dimensional secular problems over these "layer orbitals":

$$\sum_{m=1}^{N} \sum_{q=1}^{9} [H_{m'p;mq}(k_\|) - \epsilon(k_\|) S_{m'p;mq}(k_\|)] c_{mq}(k_\|) = 0 , \qquad (1a)$$

with

$$H_{m'p;mq}(k_\|) = \sum_{m_1=1}^{N_1} \sum_{m_2=1}^{N_2} \exp[i(k_1 m_1 + k_2 m_2)]$$

$$\times \langle \chi_p(r - m'a_3)|H|\chi_q(r - m_1 a_1 - m_2 a_2 - m a_3) \rangle , \qquad (1b)$$

and a corresponding expression for the overlap matrix elements.

For studying hydrogen adsorption on the different nickel surfaces we have proceeded as follows. An adsorption site is characterized by an (arbitrary) position vector a with respect to some surface atom. By means of the vectors a_1 and a_2 one generates a complete monolayer of hydrogen atoms on equivalent adsorption sites with the same periodicity as the surface. By adding one extra layer orbital characterized by the same $k_\|$, which is composed of hydrogen 1s orbitals, to the secular problem (1a), we describe the finite crystal with an adsorbed monolayer of hydrogen. This can easily be generalized to several monolayers and the resulting secular problems, with or without adsorption, can be solved by direct diagonalization or by invoking the resolvent methods of refs. [28, 29]. In practice, we have used the direct diagonalization method, except in some test cases, since these calculations involve a relatively small number of layers whereas the range of direct interactions between conduction band orbitals is rather large (see section 2.2). The resolvent method becomes advantageous when the number of layers is increased or nearest neighbour interactions are considered only.

2.2. Calculation of integrals

The overlap and H-matrix elements between atomic orbitals, which occur for instance in (1b), have been approximated by the Extended Hückel scheme, as we did in earlier cluster calculations [26]. The nickel nearest neighbour distance has been taken equal to 2.49 Å. The overlap elements $S_{pq}(R) = \langle \chi_p(r)|\chi_q(r - R) \rangle$ have been computed on the basis of Slater type orbitals, with double exponent for the 3d orbitals, single exponent for 4s and 4p, the exponents and contraction coefficients being given in table 1. We have assumed that the 4s and 4p orbitals in the nickel metal are somewhat less diffuse than in the free atom. For the hydrogen 1s orbital an exponent of 1.0 has been chosen, though we have performed some test calculations with a value of 1.2 which yielded quite similar results.

	Exponents (a_0^{-1})	Contraction coefficients	VSIE (eV)
Ni 3d	$\begin{cases}5\ 75 \\ 2\ 00\end{cases}$	$\begin{cases}0\ 5683 \\ 0\ 6292\end{cases}$	$-8\ 38$
4s	2 1	1 0	$-6\ 97$
4p	2 0	1 0	$-3\ 34$
H 1s	1 0	1 0	$-10\ 0$

The diagonal H-matrix elements $H_{pp}(R = 0) = \langle\chi_p(r)|H|\chi_p(r)\rangle$ have been approximated for the nickel orbitals by Valence State Ionization Energies [30], assuming a valence state configuration in the metal of $3d^{9\ 4}\ 4s^{0\ 6}$ (see table 1) For hydrogen the neutral atom value is $-13\ 6$ eV, but this value would result in a considerable, nonphysical electron transfer from nickel to hydrogen This effect can be avoided by adjusting the orbital energies to the atomic charges in an iterative Extended Huckel calculation This iterative method is more time consuming, however, and yields unsatisfactory results for the adsorption energy [26] Therefore, we have chosen the simpler solution to use a modified VSIE of $-10\ 0$ eV for hydrogen only, since we expect that the single hydrogen orbital is more affected by charge transfer than the large bulk of nickel orbitals In an iterative method this would correspond to a hydrogen charge of about $-0\ 3$ units, which is also the charge that we have actually found in our calculations The experience of Anders et al [31], who have also used this value and compared their results with iterative Extended Huckel calculations justifies our assumption The non-diagonal elements

$$H_{pq}(R) = \langle\chi_p(r)|H|\chi_q(r - R)\rangle, \qquad \text{with } p \neq q \text{ or } R \neq 0,$$

have been approximated by the Wolfsberg–Helmholz formula

$$H_{pq}(R) = KS_{pq}(R)[H_{pp}(R = 0) + H_{qq}(R = 0)]/2, \tag{2}$$

with the usual value of $K = 1\ 75$

Since the magnitude of these matrix elements $S_{pq}(R)$ and $H_{pq}(R)$ decreases with increasing interatomic distance R it is not necessary to consider all atom pairs in the entire crystal On the other hand, the inclusion of only nearest neighbour interactions appeared definitely insufficient for those elements involving 4s and 4p orbitals We have found that a range of 2 nickel nearest neighbour distances (5 0 Å) which allows every nickel atom in the bulk to interact directly with 4 shells of neighbours (54 atoms), is satisfactory The same range has been used for the nickel–nickel, the nickel–hydrogen and the hydrogen–hydrogen interactions Increase of this range to 3 nickel nearest neighbour distances (176 bulk atoms) yielded no visible improvement of the results Once the matrix elements over atomic orbitals have been calculated, they are easily transformed into integrals over Bloch or layer orbitals [formula (1b)]

2.3. Adsorption energy

One of the quantities we have calculated is the adsorption energy per hydrogen atom. According to the usual Extended Hückel scheme this energy can be defined as:

$$\Delta E_{ads} = \left(\sum_i N_i^A \epsilon_i^A - \sum_i N_i^C \epsilon_i^C \right) \Big/ N^H - \epsilon^H , \tag{3}$$

where ϵ_i^A, N_i^A and ϵ_i^C, N_i^C are the orbital energies and occupation numbers for the finite crystal, with and without hydrogen adsorption, respectively, N^H is the total number of hydrogen atoms and ϵ^H the energy of an isolated hydrogen atom. If the adsorption energy were thus calculated we would obtain a reasonable estimate in the neighbourhood of the chemisorption equilibrium positions. These positions are not known, however, particularly for adsorption over surface holes where the equilibrium heights cannot even be guessed reliably. Neither can they be calculated, because the Extended Hückel method often fails to predict an energy minimum as a function of the bond length. Therefore, the results would strongly depend upon rather arbitrary assumptions about the equilibrium positions unless we can improve our method to predict these positions correctly.
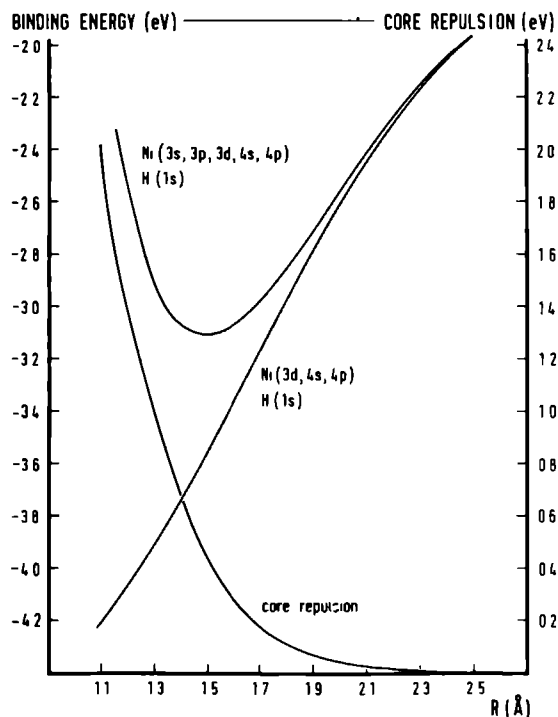
Fig. 1. Effect of nickel core repulsion on the Extended Huckel binding energy of NiH.

One reason for this defect of the Extended Hückel method is that it only accounts for the valence electrons. As we can observe from fig. 1 an Extended Hückel calculation of NiH including 3d, 4s, 4p on Ni and 1s on H predicts an ever increasing attraction in the range where the energy minimum should be. Including the fully occupied core orbitals 3s and 3p on Ni such a minimum is obtained. According to Anders et al. [31] we have fitted the (short range) core repulsion thus calculated by an exponential function, $a \exp(-bR)$ with R being the Ni–H distance, and added this pairwise potential between the nickel and the hydrogen atoms to the adsorption energy calculated by (3).

2.4. Density of states, population analysis

In solid state physics the *total* density of states is usually calculated by summation over a large number of specific [32] or random [33] points in the Brillouin zone. For finite crystals we can also calculate this quantity directly from its definition by simply counting the number of levels per energy interval.

The *local* density of states is commonly defined by:

$$n_p(\epsilon) = \sum_i |c_{pi}|^2 \, \delta(\epsilon - \epsilon_i) , \tag{4}$$

where c_{pi} is the coefficient of a given localized basis orbital (an atomic or layer orbital) $|\chi_p\rangle$ in the crystal orbital $|\psi_i\rangle$. In case we have more than one orbital $|\chi_p\rangle$ per atom, (4) defines the *partial* (local) density of states of type χ_p; the total density of states is obtained by summation over p. Although these definitions apply for an orthogonal basis set $|\chi_p\rangle$ they can be transferred to a non-orthogonal basis as well [34]. Because of overlap contributions, we obtain then a quantity which does not add up to the total density of states when summed over the complete basis $|\chi_p\rangle$. For this reason, we define instead for a *non-orthogonal* basis:

$$n_p(\epsilon) = \sum_i \left[|c_{pi}|^2 + \sum_{q \neq p} \mathrm{Re}(c_{pi}^* c_{qi} S_{pq}) \right] \delta(\epsilon - \epsilon_i) , \tag{5}$$

where S_{pq} is the overlap integral between the basis orbitals $|\chi_p\rangle$ and $|\chi_q\rangle$. When integrated up to the Fermi level this definition of $n_p(\epsilon)$ yields the Mulliken "gross orbital population", whereas definition (4) would yield the "net orbital population" [35].

3. Results and discussion

3.1. The periodic nickel crystal

The results of our band structure calculations with interactions included up to fourth order neighbours (54 atoms) in the fcc lattice are plotted in figs. 2, 3 and 4. We have also allowed for interactions up to ninth order neighbours (176 atoms) but
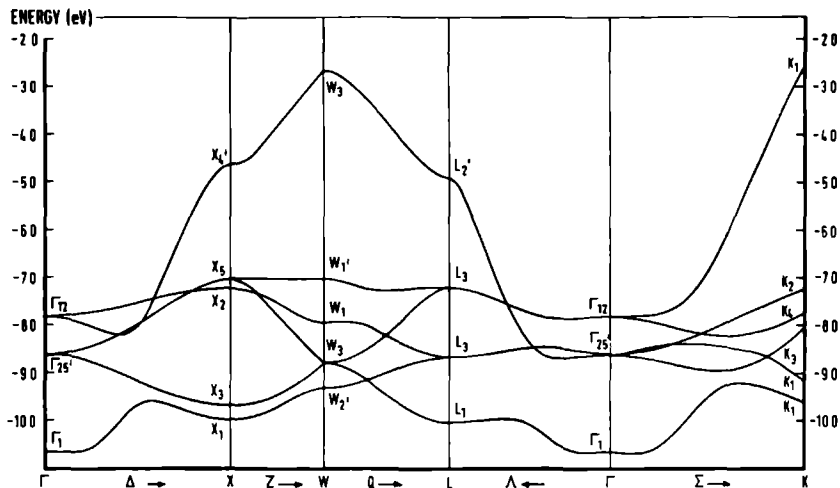
Fig. 2. Band structure of fcc nickel calculated by the Extended Hückel method. Only the first conduction band is shown. Group theoretical symbols for the points and axes in the Brillouin zone are taken from ref. [36].

this did not change the figures visibly. We have made the density of states curves somewhat less dependent on the finite number of levels, the specific choice of N_1, N_2, N_3 and the positions of the energy intervals in the histogram by applying the following smoothing procedure: for any interval of 0.1 eV we count the number of levels in the interval plus the number of levels in some neighbouring intervals multiplied by decreasing weight factors (0.09 : 0.24 : 0.34 : 0.24 : 0.09 according to a gaussian distribution).

We have found that the band structure is in fair agreement with the results of more elaborate band calculations on nickel, applying the tight-binding d-band plus nearly free electron conduction band model [25], the APW scheme [37] or the ab initio LCAO–SCF method [38,39]. The d-band is somewhat too narrow, although we have included 3d–4s–4p hybridization, and its position is somewhat too low relative to the conduction band. Also the Fermi level is found too low (−7.13 eV) in comparison with experimental values [40,41]. At first, we have tried to correct for these differences by adjusting the nickel VSIE's in the Extended Hückel method, but it appeared that the relative populations of the 3d and conduction band became somewhat less realistic, $3d^{8.6}$ $(4s\,4p)^{1.4}$, than the original populations, $3d^{9.2}$ $(4s\,4p)^{0.8}$, and that the charge transfer effects when forming a surface became improbably large. Therefore, we have maintained the usual Extended Hückel parametrization. Anyway, we may notice that in the other band structure calculations of nickel the absolute position of the bands is not computed at all [25,37,39] or is too low as well [38], the Fermi level being at −6.69 eV in the latter case.

The partial density of states distributions in fig. 4 demonstrate that all d-orbitals
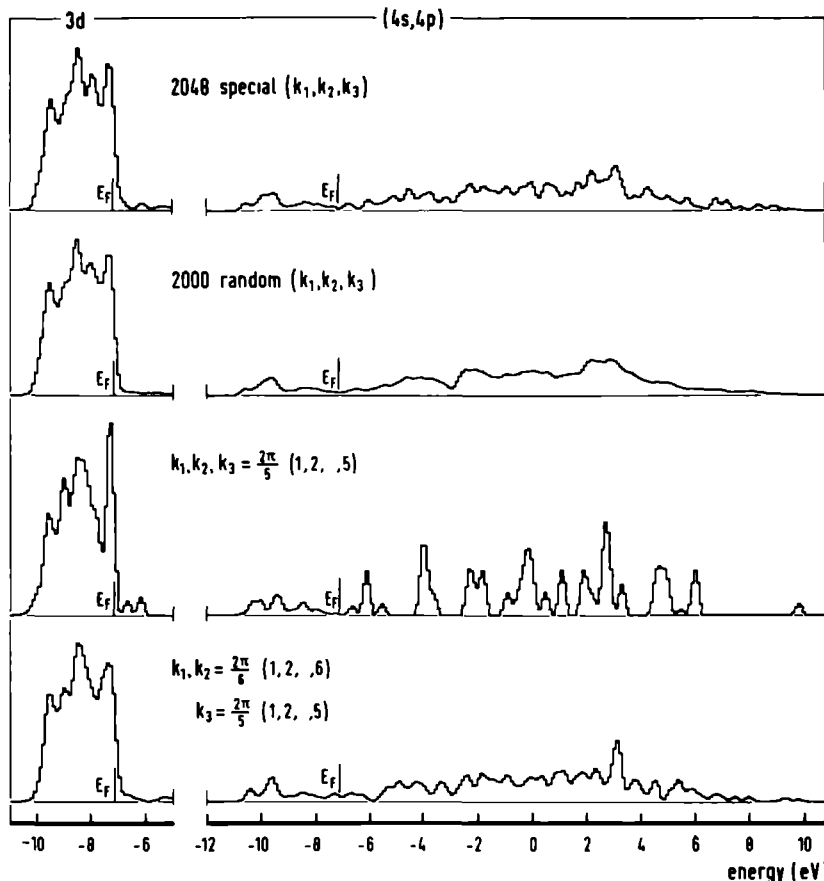
Fig. 3. Effect of *k*-point selection (periodic crystal dimensions) on the density of states of the 3d and conduction bands in fcc nickel. The Fermi-level is indicated by E_F.

yield important contributions to the entire d-band, but that specifically the t_{2g} type d-orbitals show extra peaks at the bottom and the top of the band, the top peak being more pronounced. This is in accordance with the conclusion from other band calculations [25,42] about a prominent peak of t_{2g} character at the top of the band, which causes the t_{2g} preference of the magnetic form factor in nickel [43]. There is also very close agreement between our results and the moment expansion calculations of Ducastelle and Cyrot-Lackmann [12], which lead, for instance, to the conclusion that the "t_{2g} band" has a larger second moment than the "e_g band" in fcc crystals. These conclusions support the general notions about the non-bonding nature of the e_g orbitals and the bonding/anti-bonding character of the t_{2g} orbitals (although this difference should not be understood too strictly), but they do not justify the simplified band picture by Goodenough [44].
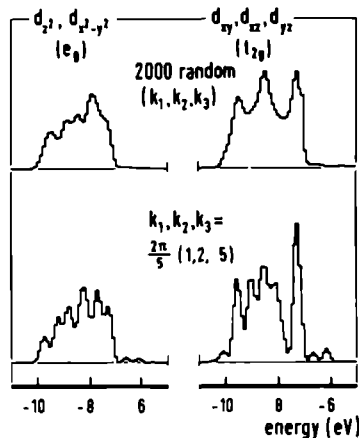
Fig 4 Partial density of states for the e_g and t_{2g} orbitals in the d-band of fcc nickel (point group O_h)

Table 2
Gross orbital populations for the bulk crystal ($N_1 = N_2 = N_3 = 5$) and for the surface layer of different 5-layer crystals ($N_1 = N_2 = 5$), local coordinate systems have been used at the different surfaces, the z-axes perpendicular to the surface, the x- and y-axes as in fig 8

	bulk	(100)	(110)	(111)
3 d_{z^2}	1 913	1 928	1 925	1 907
3 $d_{x^2-y^2}$	1 913	1 946	1 884	1 827
3 d_{xy}	1 794	1 693	1 841	1 827
3 d_{xz}	1 794	1 914	1 912	1 935
3 d_{yz}	1 794	1 914	1 948	1 935
4 s	0 668	0 694	0 680	0 733
4 p_x	0 042	0 048	0 040	0 048
4 p_y	0 042	0 048	0 048	0 048
4 p_z	0 042	0 026	0 020	0 038

From the orbital populations in table 2 it is easily calculated that the d-electrons in the metal have a slightly preferential e_g character (41 6% compared with 40% in the free atom) Also this value agrees very well with the 42% calculated by Desjonquères and Cyrot-Lackmann [15] The absolute orbital populations cannot be compared because these authors assume a total d-electron number of 9

The density of states distributions which have been produced for finite, rather small numbers of unit cells, $N_1, N_2, N_3 = 5$ or 6, are not very different from the results obtained with the usual solid state techniques, where these numbers are infinitely large, in principle It is interesting to note that the curves are relatively better when the N_i-values are different, because this leads to a larger number of indepen-

dent k-points in the Brillouin zone, independent in the sense that they are not connected by point group symmetry operations. Since the results even for values as small as $N_i = 5$ give a good impression of the band structure (if one does not wish to interpret every individual small peak), we can confidently use these finite values for studying surface and adsorption effects. All further conclusions have been tested with respect to their N_i-dependence, moreover. The same smoothing procedure for the density of states curves has been used throughout this paper.

3.2. The surfaces (100), (110) and (111)

The nickel lattices we have calculated to study these surfaces are periodic in the directions parallel to the surface over 5 X 5, 6 X 6 or 7 X 7 unit cells and consist of 5 or 6 layers. In fig. 5 the *local* densities of states in the *surface* layers are compared to the bulk densities from the periodic crystal and in figs. 6 and 7 the specific partial contributions to the d-band are analyzed. Table 2 shows the orbital populations at the surface and in the bulk.
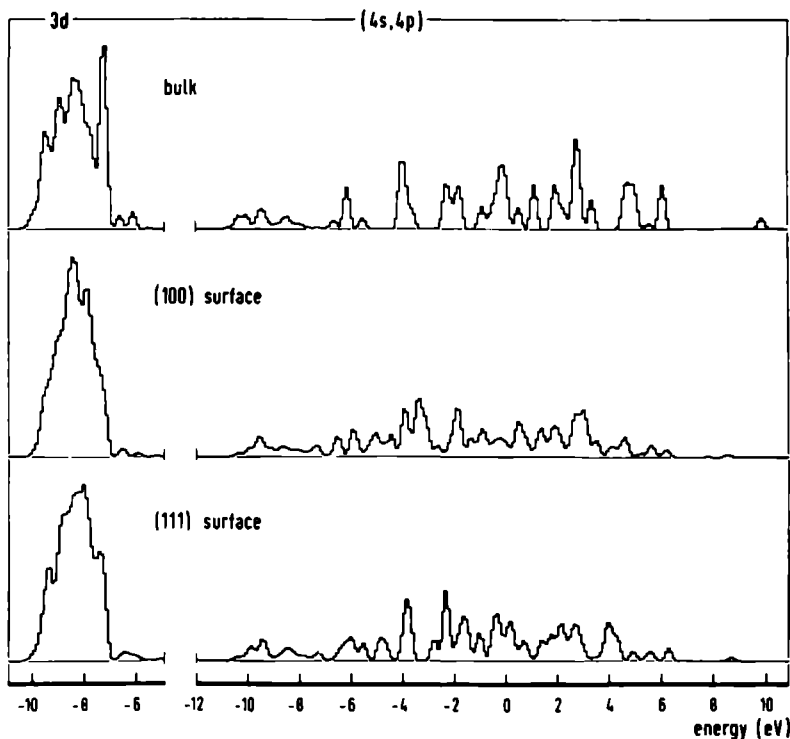
Fig. 5. Local densities of states in the (100) and (111) surface layers, compared with the bulk density of states in fcc nickel.

The results from fig. 5 are in excellent agreement with the conclusions from moment calculations [11−19] and from experimental UPS [45], XPS [46] and INS [47,48] data: the total d-band width is unaltered by the presence of the surface, but the second moment of the density of states distribution is reduced by a smaller slope at the edges. The d-band adopts more the shape of one central peak. The moment calculations, which include only d-orbitals with nearest neighbour interactions, predict that the second moment of the surface density of states is proportional to Z, the number of nearest neighbours of a surface atom. Indeed, we have found a larger band width reduction for the (100) surface ($Z = 8$) that for the (111) surface ($Z = 9$).

The effects of the surface on specific d-orbital densities, which can be observed

(a)
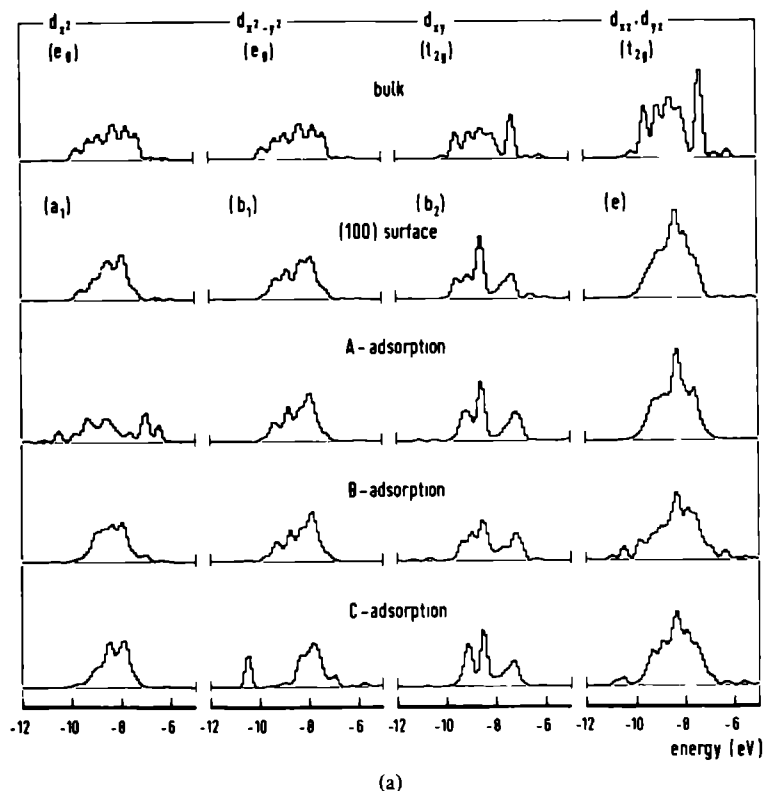
Fig. 6. Surface and adsorption effects on the partial local densities of states at the (100) surface. (a) Surface layer density of states of different 3d orbitals, denoted by the representation symbols of the point group C_{4v}; for comparison the bulk density of states is given. (b) Surface layer density of states of the 4s and 4p orbitals. (c) Local density of states in the adsorbed hydrogen layer, as compared to the density of states of an isolated H layer with the same periodicity.
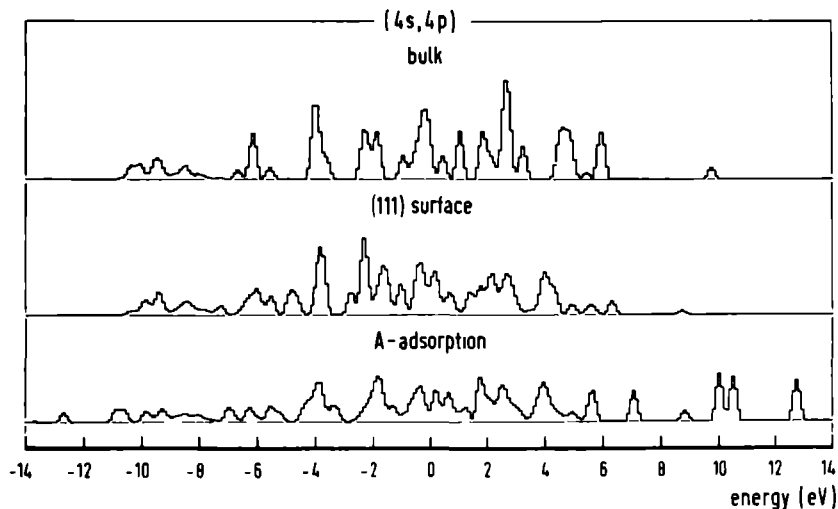
(b)

(c)

133
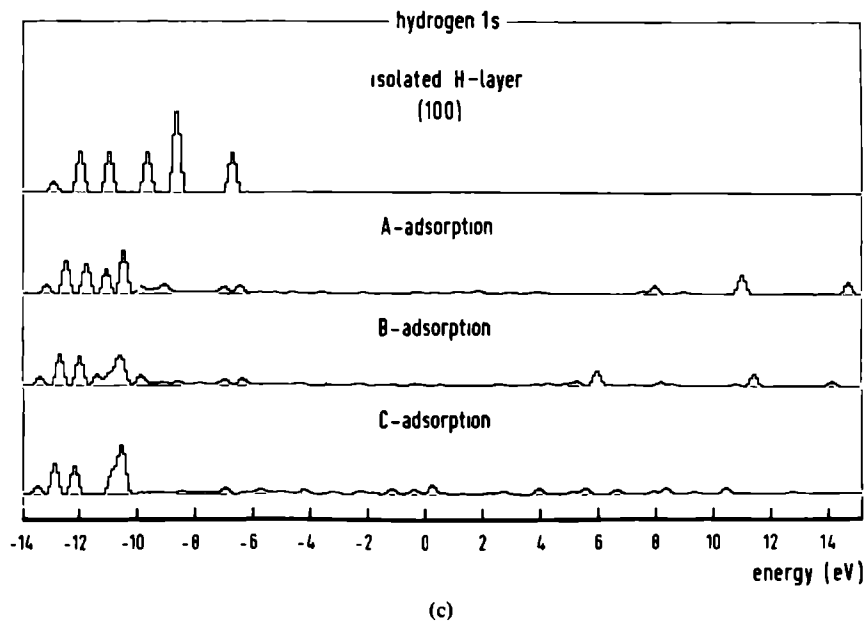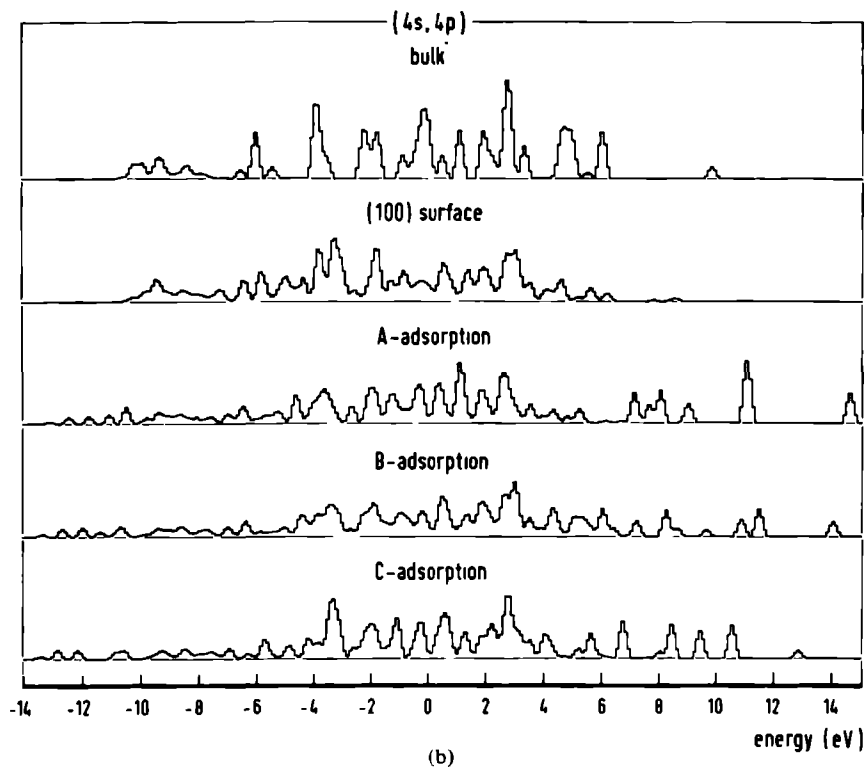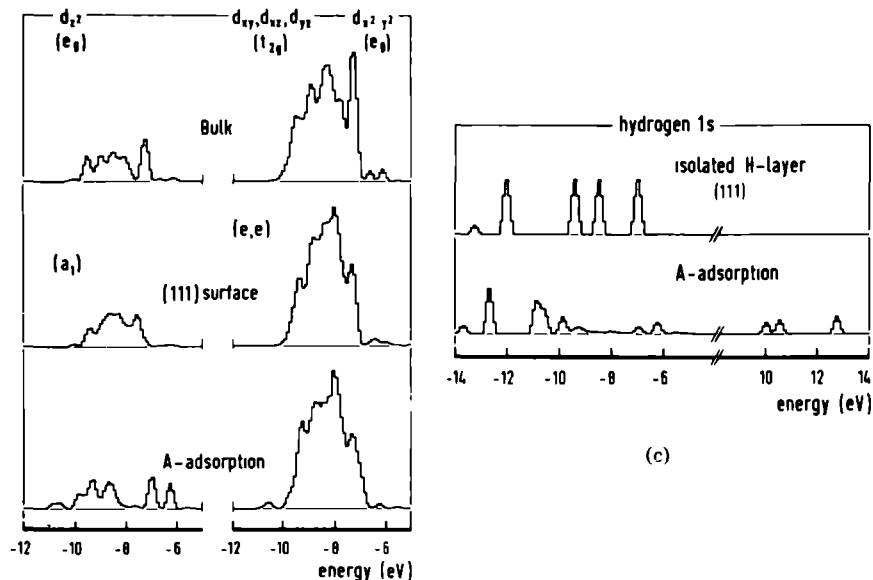
Fig. 7 Surface and adsorption effects on the partial local densities of states at the (111) surface (a) Surface layer density of states of different 3d orbitals denoted by the representation symbols of the point group C_{3v} For comparison the bulk density of states is given (b) Surface layer density of states of the 4s and 4p orbitals (c) Local density of states in the adsorbed hydrogen layer, as compared to the density of states of an isolated H layer with the same periodicity

in figs. 6 and 7, are quite well understandable if one remembers the former bonding character of these d-orbitals in the bulk (e_g or t_{2g}) and visualizes their orientation with respect to the surface. So, the orbitals protruding from the (100) surface, d_{z^2}, d_{xz}, d_{yz}, are more strongly influenced than the orbitals lying in the surface plane, $d_{x^2-y^2}$, d_{xy}; the t_{2g} orbitals d_{xz}, d_{yz} and d_{xy} are more affected than the e_g orbitals, d_{z^2} and $d_{x^2-y^2}$. In case of the (111) surface, the local d_{z^2} orbital pointing perpendicularly out of the surface, which is written as $(d_{xy} + d_{xz} + d_{yz})/\sqrt{3}$ in the bulk coordinate system (and thus belongs to the t_{2g} representation), is more influenced than the rest of the d-orbitals.

By integrating the partial density of states up to the Fermi level we have calculated the orbital occupation numbers in table 2. The latter give a direct measure of the aspherity of the d-electron charge distribution at the surface, which was recently calculated also by Desjonquères and Cyrot-Lackmann [15] using their moment ex-pansion method. For the (100) surface where the results can be directly compared, they are in good agreement: the order of the occupation numbers is the same except for the very small difference between d_{z^2} and d_{xz}, d_{yz}; the significantly lower occupation of d_{xy}, is obtained from both calculations. Note again that the absolute values differ because of Desjonquères and Cyrot-Lackmann's assumption of 9 d-electrons. For the (110) and (111) surfaces the relative occupation numbers cannot be compared directly, since Desjonquères et al. have expressed the d-orbitals always in the bulk coordinate system, whereas we have used d-orbitals adapted to the local symmetry at the surface.

3.3. Adsorption

The different sites on which hydrogen atoms have been adsorbed at the (100), (110) and (111) surfaces are shown in fig. 8. They can be denoted as A (atop), B (bridge) and C (centred). At the (110) surface two bridge positions are possible, B-long and B-short; at the (111) surface we have adsorption over an octahedral hole, C-oct., or over a tetrahedral hole, C-tet., with a nickel atom lying directly below the surface. The two-dimensional periodicity involved 5×5, 6×6 or 7×7 unit cells, the number of nickel layers has been taken as 5 or 6. At each site the adsorption energy per hydrogen atom has been calculated according to the method of section 2.3 as a function of the height over the surface and plotted in figs. 9a, b, c. The binding energies, hydrogen atomic charges and overlap populations at the equilibrium positions are collected in tables 3, 4 and 5. In order to get a more detailed insight into the nature of the chemisorption bond, the effect of adsorption on the local densities of states at the surface and in the hydrogen layer have been included in figs. 6 and 7.

The adsorption energy for various sites agrees fairly well with experimental values: an adsorption energy of 23 kcal/mole for molecular hydrogen [49–52] corresponds to a binding energy of 2.75 eV for hydrogen atoms. This value changes little over a rather large range of surface coverages; for a discussion of the heat of adsorption at monolayer coverage as compared with the initial heat of adsorption we refer to
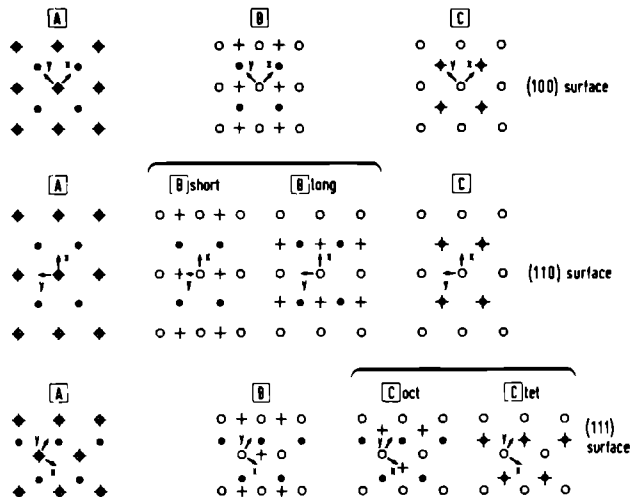
Fig 8 Schematic representation of different adsorption sites at the three low index surfaces (o) metal atoms in the first (surface) layer, (•) metal atoms in the second layer, (+) adsorbed hydrogen atoms

paper II. For comparable sites A, B or C, those surfaces are most favourable, (110) > (100) > (111), where the surface atoms have the smallest number of nearest neighbours This seems to be at variance with the experimental results [49–52], which are nearly equal for the three low index faces However, the differences in our calculated values are not very pronounced Moreover, we find an opposite effect from the 3d and the conduction electrons, as can be observed from the overlap populations in table 5, so that, for instance, a slight overestimate of the conduction band contribution could explain this difference For adsorption on different sites, we find that the stability decreases in the order A > B > C The maximum stability of the A-position is confirmed by some experimental data for hydrogen on Raney nickel [53]

The same qualitative conclusions have already been drawn from our earlier cluster calculations [26], but the differences between A, B and C sites are less pronounced now we have calculated equilibrium positions (which are quite different from the ones we had assumed for C-sites) The comparison with more recent cluster calculations is given in paper II Comparison with semi-infinite crystal calculations is difficult since those treatments which include real d-band systems [11–19] do not compute the adsorption energy, whereas other calculations are concerned with the hypothetical solid "cubium" [4,6,54,55] or other approximate models [7–10, 56] The results of the latter calculations depend strongly on the parametrization and it is hard to say which parametrization corresponds with the actual system of hydrogen adsorbed on nickel

The atomic charge on the hydrogen atoms according to Mulliken's definition is
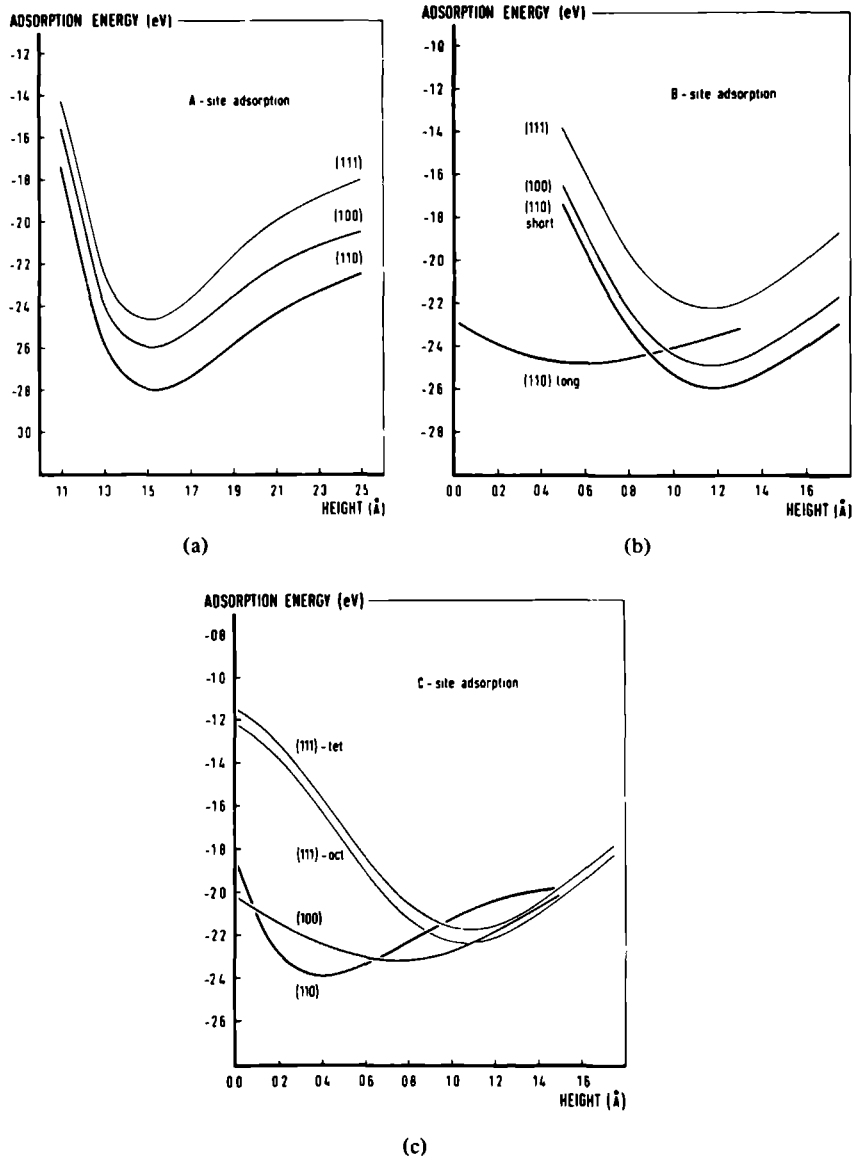
Fig. 9. Adsorption energy at different surfaces as a function of the height of the hydrogen atoms over the surface (including the repulsion with the nickel cores): (a) atop adsorption; (b) bridge adsorption; (c) centred adsorption.

found to have a maximum value for A-sites (about −0.35 unit charges) and to be somewhat smaller for B- and C-sites (−0.30 to −0.25 unit charges). The same effect

Table 3

Adsorption energies at equilibrium positions of the hydrogen atoms; distances are given with respect to the nearest surface Ni atom; periodicity $N_1 = N_2 = 5$

		Ni–H distance (A)	ΔE_{ads} (eV)	
			5 layers	6 layers
(100)	A	1.50	−2.60	−2.49
	B	1.70	−2.50	−2.39
	C	1.91	−2.32	−2.24
(110)	A	1.50	−2.80	−2.81
	B-short	1.70	−2.60	−2.59
	B-long	1.86	−2.48	−2.44
	C	2.19 [a]	−2.38	−2.30
(111)	A	1.50	−2.46	−2.38
	B	1.70	−2.23	−2.13
	C-tet.	1.81	−2.18	−2.08
	C-oct.	1.81	−2.24	−2.14

[a] The Ni–H distance for the Ni atom directly below the hole is 1.60 A.

Table 4

H-atom charges at equilibrium positions; 5-layer crystals, $N_1 = N_2 = 5$

	(100)	(110)	(111)
A-ads.	−0.36	−0.41	−0.33
B-ads.	−0.30	{−0.33 [a] −0.33	−0.25
C-ads.	−0.25	−0.27	{−0.23 [b] −0.24

[a] B-short and B-long, respectively.

[b] C-tet. and C-oct., respectively.

was qualitatively found from cluster calculations [26]. The average magnitude of this hydrogen charge justifies the assumption of a hydrogen VSIE of −10.0 eV (section 2.2) which corresponds rather well with a self-consistent result, although self-consistency has not been imposed.

From the partial density of states curves in figs. 6 and 7 we can clearly observe the interactions between the hydrogen orbitals and the nickel 3d, 4s and 4p orbitals. Some shifting and broadening of the hydrogen layer levels occurs and the positions of these peaks in the hydrogen density of states correspond with new peaks in the 3d, 4s and 4p densities of the metal caused by adsorption. Since the shifts of these peaks are relatively large compared with their broadening, one can hardly speak about "virtual" hydrogen levels [9]. This phenomenon points to a strong covalent bonding [57] of the hydrogen orbitals both to the conduction band orbitals 4s and 4p and to some of the 3d orbitals. Which specific d-orbitals take part in adsorption

Table 5
Overlap populations between an H atom (at equilibrium position) and the nearest surface Ni atom; 5-layer crystals, $N_1 = N_2 = 5$

		(100)	(110)	(111)
A	3d	0.066	0.052	0.074
	4s + 4p	0.214	0.236	0.211
B	3d	0.039	$\begin{cases}0.035\,[a]\\0.029\end{cases}$	0.043
	4s + 4p	0.108	$\begin{cases}0.113\,[a]\\0.092\end{cases}$	0.097
C	3d	0.023	$\begin{cases}0.009\,[b]\\0.050\end{cases}$	$\begin{cases}0.032\,[c]\\0.032\end{cases}$
	4s + 4p	0.049	$\begin{cases}0.025\,[b]\\0.127\end{cases}$	$\begin{cases}0.065\,[c]\\0.066\end{cases}$

[a] B-short and B-long, respectively.

[b] Overlap population with the nearest surface atom and the atom directly below the hole, respectively.

[c] C-tet. and C-oct., respectively.

bonding is determined by the environment of the adsorption site, rather than by the properties of the isolated surface. For instance, one observes very clearly from fig. 6 that on the (100) surface the d_{z^2} orbital mainly contributes to A-type adsorption, the d_{xz}, d_{yz} combination to B-type and $d_{x^2-y^2}$ to C-type. (Note again that these d-orbitals are expressed in a local coordinate system with the z-axis perpendicular to the surface plane, as shown in fig. 8.) From fig. 7 it follows that for the A-site at the (111) surface it is also the local d_{z^2}, which is written in bulk coordinates as $(d_{xy} + d_{xz} + d_{yz})/\sqrt{3}$, that yields the main contribution.

In relation to those models [58–60,15] which predict specific adsorption sites by considering the properties of the bulk metal or the isolated surface, we can make the following remarks. No specifically stable adsorption shows up on those sites, A and C at (100), where the interaction occurs with the former non-bonding (e_g) orbitals from the bulk. Neither those t_{2g} orbitals which are protruding from the surface ("dangling bonds"), at the B-site on (100) or the A-site on (111), show any particular activity. Also the occupation numbers of specific d-orbitals at the free surface [15] do not represent a good measure for the adsorption stability (which is not surprising since hydrogen chemisorption is primarily covalent, even though some charge transfer takes place). On the contrary, it is the structure (symmetry) of the "surface molecule" Ni_nH with $n = 1, 2, 3$ or 4 and its (direct) environment which determines the nature and relative stability of the chemisorption bond. More concrete information on the localized character of this bond is discussed in paper II.

Most calculations have been performed for a 5-layer nickel lattice with a 5 × 5 unit cell periodicity parallel to the surface. We have checked the conclusions from this model by repeating some of the calculations with 6 layers and 6 × 6 or 7 × 7

periodicity. The results of these tests demonstrate that the absolute adsorption energies vary a little, with the largest differences being found between odd and even numbers of layers. For A-site adsorption on the (100) surface we find, for instance, -2.56 eV for a 6 × 6 crystal, -2.64 eV for a 7 × 7 crystal as compared to -2.60 eV for a 5 × 5 crystal with 5 layers; a 5 × 5 crystal with 6 layers yields the value of -2.49 eV. The results of table 3 indicate, though, that all relative effects discussed in this section are invariant to the size of the crystal. Also the adsorption of two hydrogen layers on the opposite surfaces of a 5-layer crystal has not shown any mutual effects, so that we may safely assume that the finite, rather small, dimensions of our model systems do not significantly influence our conclusions for surface and adsorption effects.

4. Conclusions

Summarizing the main conclusions from the preceding sections we can make the following observations. Both the 3d electrons and the conduction electrons in the 4s—4p band of nickel take part in the chemisorption bond with hydrogen. Although the effect of the 4s and 4p orbitals may be somewhat overemphasized by the Extended Hückel method, since this method is strongly based on overlap criteria, our calculations do not justify the complete omission of the conduction electrons which is a starting point in many calculations for adsorption on transition metals [4—19].

Still, in those calculations which include all five 3d orbitals on the nickel atoms [11—19] the conclusions about surface effects on the d-band structure and on the aspherity of the d-electron charge distribution agree very closely with our results. Apparently, the neglect of d-band/conduction band hybridization does not affect these (relative) conclusions. The agreement between these results is the more interesting since our method (working in finite *k*-space with finite crystals) is quite different from the approach of Cyrot-Lackmann et al. [11—15] and Haydock et al. [17—19] (who use a semi-infinite crystal model and calculate the density of states by a continued-fraction expansion of the Green function). Unfortunately, not many results for adsorption on transition metals are available yet from these authors.

The stability of adsorption on different low index planes, (100), (110) and (111), increases with a decreasing number of nearest neighbours to the surface atoms. These differences are not very pronounced, however. Different sites on the same surface, show the following decrease in adsorption stability: A (atop) > B (bridge) > C (centred).

Finally it can be concluded that the stability and the nature of the chemisorption bond on nickel is not so much determined by the properties of the bulk metal or by the characteristics of the clean surface, but rather by the structure of the "surface molecule". This conclusion has been further elaborated by a comparison with cluster calculations in paper II, where also the localization of the chemisorption bond and the effect of the boundary conditions on the "surface molecule" are discussed.

Acknowledgement

References

[1] T.B. Grimley, Advan. Catalysis 12 (1960) 1.
[2] J. Koutecký, Advan. Chem. Phys. 9 (1965) 85.
[3] For references see the review article:
S.G. Davison and J.D. Levine, in: Solid State Physics, Vol. 25, Eds. H. Ehrenreich, F. Seitz and D. Turnbull (Academic Press, New York, 1970) p. 1;
and the recent paper:
W. Ho, S.L. Cunningham, W.H. Weinberg and L. Dobrzynski, Phys. Rev. B12 (1975) 3027.
[4] T.B. Grimley and C. Pisani, J. Phys. C (Solid State Phys.) 7 (1974) 2831.
[5] E.A. Hyman, Phys. Rev. B11 (1975) 3739.
[6] R.H. Paulson and J.R. Schrieffer, Surface Sci. 48 (1975) 329.
[7] G. Doyen and G. Ertl, Surface Sci. 43 (1974) 197.
[8] D.M. Newns, Phys. Rev. 178 (1969) 1123.
[9] T.B. Grimley, J. Vacuum Sci. Technol. 8 (1971) 31.
[10] B.J. Thorpe, Surface Sci. 33 (1972) 306.
[11] F. Cyrot-Lackmann, J. Phys. (Paris) Suppl. 31, C1 (1970) 67.
[12] F. Ducastelle and F. Cyrot-Lackmann, J. Phys. Chem. Solids 31 (1970) 1295.
[13] F. Cyrot-Lackmann and F. Ducastelle, Phys. Rev. B4 (1971) 2406.
[14] M.C. Desjonquères and F. Cyrot-Lackmann, J. Phys. (Paris) 36 (1975) L45.
[15] M.C. Desjonquères and F. Cyrot-Lackmann, to be published.
[16] V. Heine, Proc. Roy. Soc. (London) A331 (1972) 307.
[17] R. Haydock, V. Heine and M.J. Kelly, J. Phys. C (Solid State Phys.) 5 (1972) 2845.
[18] R. Haydock, V. Heine, M.J. Kelly and J.B. Pendry, Phys. Rev. Letters 29 (1972) 868.
[19] R. Haydock and M.J. Kelly, Surface Sci. 38 (1973) 139.
[20] R. Hoffmann, J. Chem. Phys. 39 (1963) 1397.
[21] J.A. Pople and D.L. Beveridge, Approximate Molecular Orbital Theory (McGraw-Hill, New York, 1970).
[22] J.C. Slater and K.H. Johnson, Phys. Rev. B5 (1972) 844.
[23] K.H. Johnson, and F.C. Smith, Phys. Rev. B5 (1972) 831.
[24] R.P. Messmer, C.W. Tucker and K.H. Johnson, Surface Sci. 42 (1974) 341.
[25] L. Hodges, H. Ehrenreich and N.D. Lang, Phys. Rev. 152 (1966) 505.
[26] D.J.M. Fassaert, H. Verbeek and A. van der Avoird, Surface Sci. 29 (1972) 501.
[27] C. Kittel, Introduction to Solid State Physics (Wiley, New York, 1953).
[28] A. van der Avoird, S.P. Liebmann and D.J.M. Fassaert, Phys. Rev. B10 (1974) 1230.
[29] S.P. Liebmann, A. van der Avoird and D.J.M. Fassaert, Phys. Rev. B11 (1975) 1503.
[30] H. Basch, A. Viste and H.B. Gray, Theoret. Chim. Acta 3 (1965) 458.
[31] L.W. Anders, R.S. Hansen and L.S. Bartell, J. Chem. Phys. 59 (1973) 5277.
[32] G.A. Burdick, Phys. Rev. 129 (1963) 138.
[33] F.M. Mueller, J.W. Garland, M.H. Cohen and K.H. Bennemann, Ann. Phys. 67 (1971) 19.
[34] T.B. Grimley, J. Phys. C (Solid State Phys.) 3 (1970) 1934.

[35] R.S. Mulliken, J. Chem. Phys. 23 (1955) 1833.
[36] L.P. Bouckaert, R. Smoluchowski and E. Wigner, Phys. Rev. 50 (1936) 58.
[37] J.W.D. Connolly, Phys. Rev. 159 (1967) 415.
[38] J. Langlinais and J. Callaway, Phys. Rev. B5 (1972) 124.
[39] J. Callaway and C.S. Wang, Phys. Rev. B7 (1973) 1096.
[40] H.E. Farnsworth and H.H. Madden, J. Appl. Phys. 32 (1961) 1933.
[41] R. Gerlach and T.N. Rhodin, in: The Structure and Chemistry of Solid Surfaces, Ed. G.A. Somorjai (Wiley, New York, 1969) p. 55–17.
[42] L. Hodges and H. Ehrenreich, J. Appl. Phys. 39 (1968) 1280.
[43] H.A. Mook, Phys. Rev. 148 (1966) 495.
[44] J.B. Goodenough, Phys. Rev. 120 (1960) 67.
[45] D.E. Eastman, in: Electron Spectroscopy, Ed. D.A. Shirley (North-Holland, Amsterdam, 1972).
[46] S. Hufner, G.K. Wertheim and J.H. Wernick, Phys. Rev. B8 (1973) 4511.
[47] H.D. Hagstrum and G.E. Becker, Phys. Rev. 159 (1967) 572.
[48] H.D. Hagstrum and G.E. Becker, J. Chem. Phys. 54 (1971) 1015.
[49] J. Lapujoulade and K.S. Neil, J. Chem. Phys. 57 (1972) 3535.
[50] J. Lapujoulade and K.S. Neil, Surface Sci. 35 (1973) 288.
[51] J. Lapujoulade and K.S. Neil, J. Chim. Phys. 70 (1973) 798.
[52] K. Christmann, O. Schober, G. Ertl and M. Neumann, J. Chem. Phys. 60 (1974) 4528.
[53] R. Stockmeyer, H.M. Conrad, A. Renouprez and P. Fouilloux, Surface Sci. 49 (1975) 549.
[54] F. Cyrot-Lackmann, M.C. Desjonquères and J.P. Gaspard, J. Phys. C (Solid State Phys.) 7 (1974) 925.
[55] W. Ho, S.L. Cunningham and W.H. Weinberg, Surface Sci. 54 (1976) 139.
[56] R.A. van Santen, Surface Sci. 53 (1975) 35.
[57] T.L. Einstein, Surface Sci. 45 (1974) 713.
[58] G.C. Bond, Platinum Metals Rev. 10 (1966) 87.
[59] D. Shopov, A. Andreev and D. Petkov, J. Catalysis 13 (1969) 123.
[60] W.H. Weinberg and R.P. Merrill, Surface Sci. 33 (1972) 493.

LCAO STUDIES OF HYDROGEN CHEMISORPTION ON NICKEL

II Cluster models for adsorption sites

D J M FASSAERT and A VAN DER AVOIRD

Institute of Theoretical Chemistry, University of Nijmegen, Nijmegen, The Netherlands

The adsorption of single hydrogen atoms, investigated by means of cluster calculations, has been compared with the adsorption of hydrogen monolayers on periodic crystals (paper I) From the similarity of the adsorption energy curves we conclude that the (direct and indirect) interactions between adsorbed hydrogen atoms are relatively small up to monolayer coverage For adsorption on different sites of ideal low index surfaces the stability decreases in the order Atop > Bridge > Centred For Atop adsorption it increases with a decreasing number of nearest neighbours to the nickel atom in the NiH "surface molecule", thus leading to especially strong adsorption sites at the edges of a stepped surface and to low stability in the notches In general, we find that the Ni_nH "surface molecule" with $n = 1, 2, 3$ or 4 determines the equilibrium positions for H adsorption, the inclusion of one shell of neighbours to the nickel atoms is sufficient to explain the differences in adsorption energy The Extended Huckel method is not well suited to study dissociative chemisorption of H_2, although some qualitative trends are correct

1. Introduction

In a previous paper [1] (henceforth called paper I) we have reported a number of calculations on the adsorption of hydrogen layers on ideal low index surfaces of nickel crystals with a finite periodicity in the two directions parallel to the surface and consisting of a limited number of layers We wished to compare these tight-binding Extended Huckel calculations on periodic crystals with cluster calculations in order to examine the degree of localization of the chemisorption bond, the concept of the "surface molecule" and the, possibly disturbing, effect of the boundaries of the clusters Thus we wanted to investigate which properties are correctly represented by cluster models and to what extent they can be used to gain insight in chemisorption phenomena and to make theoretical predictions Our earlier cluster calculations [2] are difficult to compare with the results of paper I, because we have somewhat improved the parameter choice in the latter paper and also included 4p-functions Moreover, we have now calculated equilibrium positions for the adsorbed atoms after taking into account the repulsions between the H atom and the Ni atom cores

Therefore, we have performed a new series of cluster calculations

Except for studying the adsorption of a H atom on models for ideal low index surfaces, we wanted to search especially for active adsorption sites, the structure and occurrence of which are of interest for heterogeneous catalysis, and to investigate the molecular adsorption of H_2 which has been studied formerly by another model [3]

2. Description of the model

2 1 The clusters

As before, we have started with an octahedral cluster of 13 nickel atoms, representing one atom with its complete nearest neighbour environment in the fcc crystal Next, we have truncated this parent cluster by removing some atoms, such that the central metal atom obtained the nearest neighbour environment of an atom at the ideal (100), (110) and (111) surfaces respectively The symmetry groups of these clusters, consisting of 9, 8 and 10 nickel atoms, are C_{4v}, C_{2v} and C_{3v} Subsequently, we have adsorbed a hydrogen atom on these surface clusters, at a variable height above the central nickel atom, A(atop)-adsorption Pictures of these clusters have been given in figs 1 and 2 of ref [2] In order to investigate the size effect we extended the (100) cluster with 4 extra surface atoms Further, we have calculated the case that the adsorbed H atom forms a bridge between two Ni atoms, B(bridge) adsorption, at the (100) surface, represented by a cluster of 14 atoms (see fig 1) As before, we have taken care that the two Ni atoms directly involved in the adsorption bonding, are provided with a complete nearest neighbour environment The adsorption of a H atom above a surface hole, C(centred)-adsorption, has been examined in a model obtained by inverting the 9-atomic (100) cluster In this case, however, the four surface Ni atoms which interact directly with the H atom, do not possess a complete nearest neighbour environment. For all the surface clusters the z-axis is chosen to be perpendicular to the surface
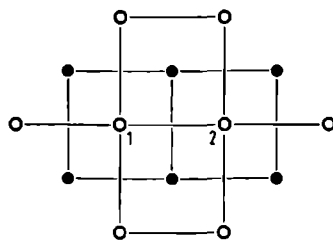

Fig 1 Schematic representation of the cluster used to study B-site adsorption of H atoms and dissociative chemisorption of H_2 on the (100) surface (o) metal atoms in the first (surface) layer (•) metal atoms in the second layer
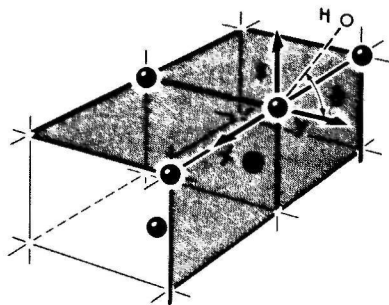
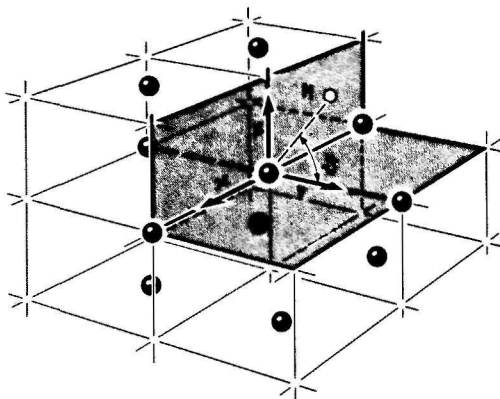Fig. 2. Model cluster (6 atoms) for H adsorption on the edge of a stepped (100) or (110) surface.

Fig. 3. Model cluster (11 atoms) for H adsorption in the notch of a stepped (100) or (110) surface.

The models discussed so far have been used to study the adsorption on ideal low index surfaces. Since we wanted to find out whether particularly active sites occur at stepped or indented surfaces, we have calculated some clusters representing the adsorption of a H atom at an edge or in a notch. A model for the edge is obtained by cleaving the (100) and (111) surface clusters along a second plane [truncating of the (110) cluster gives the same results as the (100) cluster], providing clusters of 6 and 7 Ni atoms, respectively. For the adsorption in an indentation we get a model system by removing 2 atoms from the 13-atomic parent cluster. Pictures for the 6- and 11-atomic clusters are given in figs. 2 and 3. In both cases the Ni atom which directly binds with the H atom is surrounded by the complete set of nearest neighbours which it possesses in the real physical situation. The most stable adsorption positions have been found by varying the angle θ and the distance between the H atom and the central Ni atom.

Finally, we wanted to examine to what extent it is possible to study the dissociative adsorption of molecular H_2 by the Extended Hückel method. To this end we have used the 14-atomic (100) surface cluster of fig. 1. Truncating of this cluster along a second plane supplied a model for the adsorption of H_2 at an edge.

2.2. The molecular orbital method; the parameters

For our calculations we have used the Extended Hückel method with a non-orthogonal basis set, consisting of 3d, 4s and 4p orbitals for nickel and a 1s orbital for hydrogen. The same parameters have been chosen as in paper I, as well as the same definition for the adsorption energy ΔE_{ads}, including the extra term which accounts for the repulsion between the H atom and the cores of the Ni atoms in order to calculate equilibrium positions. The nickel nearest neighbour distance has

been taken equal to 2.49 Å, as before. The Mulliken population analysis was used to calculate atomic charges and overlap populations.

3. Results and discussion

3.1. Adsorption on low index surface clusters

The energy curves obtained for A-site adsorption of a H atom on the ideal low index surface clusters have been plotted in fig. 4. It is striking that they agree very closely with the curves for a full H layer adsorbed on a periodic surface (fig. 9a of paper I), the equilibrium distances and adsorption energies being (nearly) the same (table 1). In principle, it cannot be excluded that this similarity between the periodic crystal results and the data from cluster calculations is caused by the cancellation of two different effects: the (direct and indirect) interaction between the hydrogen atoms in the periodic layer and the boundary effects in the clusters. This cancellation is quite improbable, however, since the similarity occurs in all examples calculated (also for B- and C-site adsorption, as will be discussed below), the clusters have
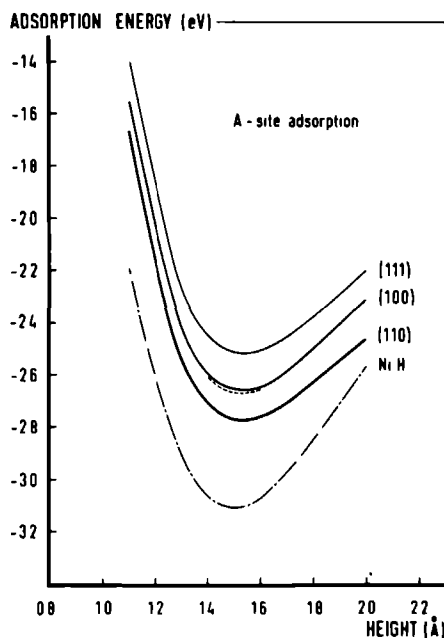

Fig. 4. Adsorption energy of a H atom on different surface clusters, as compared to the binding energy of NiH. The small dashed curve indicates the effect of extending the (100) surface cluster with 4 extra atoms.

146

Table 1
Comparison of the adsorption energies, the distances are given with respect to the surface, the clusters are described in the text and the periodic crystals are 5 × 5 periodic systems consisting of 5 layers (see paper I)

	Cluster		Periodic crystal	
	Equil dist (A)	ΔE_{ads} (eV)	Equil dist (A)	ΔE_{ads} (eV)
(100), A-site	1 54	−2 66	1 53	−2 60
(110), A-site	1 54	−2 77	1 54	−2 80
(111), A-site	1 54	−2 51	1.52	−2 46
(100), B-site	1 20	−2 59	1 19	−2 50
(100), C-site	0 70	−2 23	0 74	−2 32

different sizes and, particularly, the extension of a given cluster with 4 extra atoms did not yield a significant difference in the adsorption energy curve Therefore, we can practically rule out this possibility and conclude from our calculations that the adsorption energy for hydrogen atoms does not vary significantly up to full monolayer coverage. In other words, the direct and indirect interactions between adsorbed hydrogen atoms are relatively small. This result agrees with other model calculations [5,8] and also the recent experimental data from flash desorption and work function measurements on ideal single crystal surfaces [4–7] show that the adsorption energies are nearly constant This holds for coverages up to about half of the saturation coverage [7]. The only incertainty which is still present in the different measurements concerns the saturation coverage of chemisorbed hydrogen. From flash desorption experiments Lapujoulade and Neil [4–6] obtained a saturation coverage θ_{max} from 0 15 to 0.4 for the three surfaces, while Christmann et al. [7] observed a saturation population of about one H atom per Ni atom and May and Germer [9] estimated θ_{max} on the (110) plane to be in the range between 1 6 and 2 2 We would tentatively suggest that the strong decrease of the adsorption energy observed by Christmann et al starts after filling completely one of the possible adsorption sites (the β_2-state [7]) and that it is caused by the lower adsorption energy of the second adsorption site (the β_1-state [7]) and, possibly, by a repulsion between the adsorbed H atoms which are now at shorter distances from each other than the nickel nearest neighbour distance.

From the recent experimental results and our theoretical calculations it may be concluded that the older experimental results on metal powders, wires, films or supported catalysts [10] which show a stronger decrease of ΔE_{ads} with increasing coverage, must be caused by the inhomogeneity of the surface, which makes that sites with many different adsorption energies are available (see also section 3.2).

From table 2 it appears that the overlap populations for A-site adsorption on the clusters and the periodic crystals are essentially the same. The considerable differences in magnitude between the populations from the 3d electrons on the central Ni atom and those from the 4s electrons are due to corresponding differences in the overlap integrals. Therefore, we do not believe these overlap populations to form an absolute

Table 2

Companson of the overlap populations with the hydrogen 1s orbital for A-site adsorption, the Ni(1)−H distance is 1 5 Å Ni(1) is the central Ni atom and Ni(2), Ni(3), Ni(4) are nearest neigh-bours from the first (= surface), second and third layer, respectively The z-axis points perpen-dicularly to the surface

	(100)		(110)		(111)	
	Cluster	Periodic crystal	Cluster	Periodic crystal	Cluster	Periodic crystal
$3d_{z^2}(1)$	0 0756	0 0662	0 0688	0 0523	0 0798	0 0739
4s(1)	0 1649	0 1723	0 1719	0 1870	0 1593	0 1661
$4p_z(1)$	0 0393	0 0419	0 0449	0 0491	0 0403	0 0451
total (1)	0 2798	0 2804	0 2855	0 2884	0 2793	0 2851
3d(2)	0 0020	0 0017	0 0017	0 0015	0 0015	0 0012
4s + 4p(2)	0 0002	−0 0055	−0 0001	−0 0071	−0 0010	−0 0066
total (2)	0 0022	−0 0038	0 0016	−0 0056	0 0006	−0 0054
3d(3)	−0 0003	−0 0006	0 0002	−0 0003	−0 0005	−0 0007
4s + 4p(3)	−0 0020	−0 0018	−0 0023	−0 0018	−0 0018	−0 0016
total (3)	−0 0024	−0 0024	−0 0020	−0 0022	−0 0023	−0 0024
3d(4)	−	−	−0 0011	−0 0010	−	−
4s + 4p(4)	−	−	−0 0017	−0 0015	−	−
Total (4)	−	−	−0 0028	−0 0025	−	−

measure for the bond strength Nevertheless, we think that they indicate that the conduction electrons contribute strongly to the chemisorption bond As can be seen from fig 4, the A-site adsorption energy decreases in the order $(110) > (100) > (111)$, i.e. with an increasing number of nearest neighbours Apparently, these neighbours cause a repulsive effect as may be concluded from a comparison with the NiH binding energy, too. This seems to be at variance with the experimental results [4−7], which are nearly equal for the three low index faces As we remarked already in paper I, the differences in our calculated values are not very pronounced, however, and may be caused by a slight overestimate of the relative contribution of the conduction electrons, which are responsible for the repulsive effect of the neighbouring nickel atoms [2]

The effect of the cluster size has been examined by extending the original (100) cluster with four extra Ni atoms at the surface Although the charges on the metal atoms are very different (table 3), the adsorption energy (fig 4) and the overlap populations are the same So, we may conclude that our clusters are sufficiently large to study the chemisorption bonding of a H atom and that the boundary effects do not influence the adsorption energies

For cluster calculations on B-site and C-site adsorption at the (100) surface the adsorption energies at equilibrium distance are given in table 1, the adsorption energy curves have not been plotted since they are again very similar to the curves obtained for the periodic crystals It appears that for these clusters, the adsorption is favoured in the order $A > B > C$ just as for the periodic crystals

Table 3

Comparison of the charges on the 9- and 13-atomic (100) surface clusters with A-site adsorption; the Ni(1)−H distance is 1.5 Å. Ni(1) is the central Ni atom, Ni(2) and Ni(3) are nearest neighbours from the first (= surface) and second layer, respectively, Ni(4) is a next nearest neighbour from the first layer

	(100)-9Ni	(100)-9Ni + H	(100)-13Ni	(100)-13Ni + H
Ni(1)	−0.140	0.613	0.634	1.212
Ni(2)	−0.178	−0 131	−0.032	0 027
Ni(3)	0 213	0 076	0 207	0 128
Ni(4)	−	−	−0 334	−0.359
H	−	−0 392	−	−0.394

The maximum stability of A-adsorption has been confirmed by experimental data [11], but has not been found in recent cluster calculations by Blyholder [12], who concluded from CNDO results that the adsorption over a surface hole is more favourable. Since we have calculated equilibrium positions for adsorption now, we can assert that the discrepancy with the CNDO results is not due to our former assumptions [2] about these positions, as Blyholder suggested. Instead, we think that the explanation must be found in the size and shape of his clusters, several of which do not possess a complete nearest neighbour environment for the Ni atoms directly binding with the H atom. Actually, some of the adsorption site models do not even reflect the symmetry of the surface, which implies that these nickel atoms possess strongly different numbers of nearest neighbours.

Since the conclusions for adsorption on our periodic crystals and clusters are quite similar, we have searched for active sites for the adsorption of H atoms and investigated the dissociative adsorption of molecular H_2 by means of further cluster calculations.

3.2. Adsorption on non-ideal surface clusters

Adsorption at non-ideal surfaces has been studied on clusters which form a model for an edge or an indentation in the crystal. The H atom was directly bonded to the central Ni atom, because the largest adsorption energy has been found for A-site adsorption. Thus we wanted to investigate the occurrence of active sites, which may be of interest for heterogeneous catalysis.

Somorjai et al. [13,14] examined the adsorption of H_2, O_2 and some other molecules on stepped and high index surfaces of platinum. They found that the chemisorption characteristics are markedly different from those of low index platinum surfaces, the chemisorption taking place much more readily. In their opinion the reason for the increased chemical activity of the stepped surfaces lies in the differing atomic structures at the steps. A molecule adsorbed in the notch of a step has a larger number of nearest neighbour metal atoms than a molecule at a flat surface and therefore, there is an increased availability of metal atom orbitals at the stepped surface for adsorption and reaction.

Table 4
Adsorption energies for A-site adsorption on different clusters; the Ni—H distance is 1.5 Å; for the adsorption on non-ideal surfaces, the angle θ is optimized (see figs. 2 and 3)

	ΔE_{ads} (eV)
Notch-11Ni	−2.48
Ideal (111)-10Ni	−2.51
Ideal (100)-9Ni	−2.66
Ideal (110)-8Ni	−2.77
Edge-7Ni	−2.81
Edge-6Ni	−2.82
NiH	−3.08

From our calculations it may be concluded that the adsorption of a H atom at an edge is more favoured than in an indentation (the adsorption energies at the equilibrium positions are given in table 4). In other words, we find also in these cases that those sites are the most active ones for hydrogen adsorption, of which the Ni atom binding directly with the H atom, is surrounded by the least possible number of nearest neighbours (see table 4). These neighbours cause a repulsive effect. While we think our conclusions to originate mainly from covalent bonding. Anderson and Hoffmann [15] have reached similar conclusions from cluster calculations on the basis of charge-transfer considerations. Hydrogen chemisorption is primarily covalent, though.

Although we agree with Somorjai et al. [13] on the special activity of stepped and high index surfaces, our results do not confirm their hypothesis about the reason for the increased chemisorption activity. We find the most stable position for hydrogen adsorption to be on the edge. However, this conclusion may not hold for heavier atoms such as carbon, nitrogen and oxygen, which may prefer to form multi-center bonds. An indication for this can be found in the work of Anders et al. [16, 17], who concluded that a hydrogen atom adsorbs on top of a metal atom on the (100) surface of tungsten, whereas the nitrogen atom prefers the position above the surface hole.

3.3. The (dissociative) adsorption of H_2

The dissociative chemisorption of molecular hydrogen has been studied previously by Deuss and Van der Avoird [3] by means of a perturbation theory for exchange forces which is comparable with the valence-bond method. The activity of the 3d and 4s electrons was examined separately by a simple effective 4-electron model, representing two nickel and two hydrogen atoms. It appeared that the $3d_{z^2}$ orbitals protruding perpendicularly from the surface, could enable a H_2 molecule to become dissociatively chemisorbed without an activation energy, whereas the 4s electrons alone did not chemisorb a H_2 molecule unless a high activation-energy barrier was surmounted. By the Extended Hückel method it is possible to study much larger and more realistic systems. On the other hand, the Extended Hückel formalism may
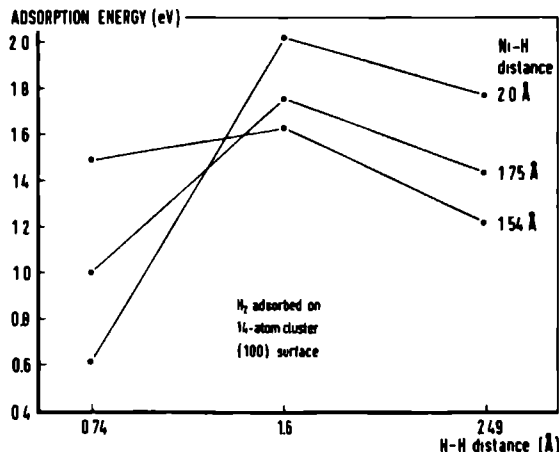
Fig. 5. Extended Huckel results for dissociative chemisorption of H_2.

be less suited to investigate the process of dissociative adsorption of H_2. Firstly, the distance between H_2 and the metal surface may not become too large, since the adsorbate—metal system then dissociates into ionic parts (as usually in the MO-formalism). Secondly, the H—H interaction in free H_2 is not well represented, the binding energy being 1.7—2.3 eV too large in the range from 0.74 to 2.0 Å, while the molecule collapses for shorter distances. Nevertheless, we have examined how far it is possible to study the dissociative chemisorption of molecular hydrogen by our cluster models.

The results for two H atoms symmetrically adsorbed parallel to the surface above the two central Ni atoms of the 14-atom (100) surface cluster (fig. 1) are given in fig. 5 for 3 H—H distances and 3 distances between the H atoms and the central metal atoms. The adsorption energy was computed with respect to the nickel cluster and a free H_2 molecule with the experimental equilibrium distance (0.74 Å). As can be seen from fig. 5, at larger distances from the surface a H_2 molecule is relatively more favourable and at shorter distances (the Ni—H equilibrium distance 1.54 Å) 2 separate Ni—H bonds are more stable; between these two states exists an activation barrier, however. From the overlap populations between the H atoms (see table 5)

Table 5
H—H overlap population for H_2 adsorbed on the 14-atomic (100) surface cluster

Ni—H distance	H—H distance		
	0.74 A	1.60 A	2.49 A
1.54 A	0.4030	0.0874	0.0067
1.75 A	0.4268	0.1175	0.0123
2.00 A	0.4370	0.1481	0.0109
Free H_2	0.4294	0.2559	0.1056

it appears that a considerable weakening of the H—H bond occurs, compared with a free H_2 molecule. It should be noted, though, that in all cases the adsorption energy is positive, i.e. the adsorbate-metal complex is always energetically unstable. The positive adsorption energy can be caused by the stability of H_2, which is too large, whereas the Ni—H bond energy is about correct. This may also explain the activation barrier which is predicted in contrast to our earlier calculations involving 3d electrons alone [3] and experimental experience. So, from the energy curves and the population analysis we find a distinct tendency to dissociative adsorption, the results being quantitatively wrong, however.

We have also calculated two cases of non-symmetrical H_2 adsorption, one atom adsorbing directly above a central Ni atom and the other one lying above a neighbouring surface hole or forming a bridge between the two central Ni atoms. In both cases the H atoms were placed in the equilibrium positions obtained for the single atom adsorption. Now, even less stability was found than for two H atoms adsorbed on top of the central Ni atoms at equilibrium distances. Finally, we have studied the molecular adsorption at an edge. A model system was obtained by truncating the cluster of fig. 1 along a second plane. The adsorption is somewhat more stable now, although the adsorption energy for molecular H_2 remains positive yet.

4. Conclusions

The results which we have obtained by cluster and periodic-crystal calculations agree very well, qualitatively as well as quantitatively. Going from the adsorption of a single H atom on a cluster to the adsorption of a full H monolayer on a finite crystal, the adsorption energies do not change significantly. So there exists now both theoretical and experimental [7] evidence that the adsorption energy varies only slightly over a considerable range of coverage θ. The rather fast decrease of the adsorption energy with increasing coverage which was observed in older experiments on catalyst samples, etc [10], must have been caused by the inhomogeneity of the surface.

Enlarging of the (100) cluster did not change the adsorption energy nor the overlap populations with the H atom. Therefore, we conclude that our clusters are sufficiently large to describe the chemisorption bonding, in spite of the charge effects occurring at the boundaries. Furthermore, the adsorption bond is rather localized as follows from the similar behaviour of the clusters and periodic crystals. The equilibrium positions of the adsorbate depend only upon the configuration of the directly bonding metal atoms. For instance, it appears from paper I that the equilibrium distances are equal for the three adsorption sites directly above a metal atom, for the three bridge positions between nearest neighbours and for the two surface holes at the (111) surface. This confirms the usefulness of the concept of the "surface molecule" to study chemisorption phenomena

In our model, the adsorption energy for the different low index surfaces decreases

in the order $(110) > (100) > (111)$, whereas the experimental values are about equal [4–7] However, the differences in our results are much smaller than those found by Blyholder [12] For the different sites the adsorption was found to become less favourable in the series A (atop) $>$ B (bridge) $>$ C (centred) This is at variance with Blyholder's order, but agrees with the results obtained by Anders et al [16] for the adsorption of a hydrogen atom on (100) surface clusters of tungsten Also the data obtained from recent inelastic neutron scattering experiments support the preference for A-sites [11]

With regard to the adsorption of molecular hydrogen, we found a qualitative tendency to dissociation from the adsorption energies and the H–H bond weakening The quantitative results are not very good, however This may probably be ascribed to the Extended Huckel method, which yields too much binding energy for the H_2 molecule and too large an ionic contribution when the Ni–H distance increases

In agreement with experimental evidence, we find a special activity on stepped surfaces and high index planes While Somorjai et al [13] supposed that the increased adsorption activity was caused by the enlarged number of metal atoms at a step available for interaction, from our calculations it is concluded that the most active sites for hydrogen adsorption are edges and protrusions, the least active ones being notches However, this conclusion may only hold for hydrogen atoms and not for heavier atoms, preferring the formation of multicentre bonds

References

[1] D J M Fassaert and A van der Avoird, Surface Sci 55 (1976) 291
[2] D J M Fassaert, H Verbeek and A van der Avoird, Surface Sci 29 (1972) 501
[3] H Deuss and A van der Avoird, Phys Rev B8 (1973) 2441
[4] J Lapujoulade and K S Neil J Chem Phys 57 (1972) 3535
[5] J Lapujoulade and K S Neil, Surface Sci 35 (1973) 288
[6] J Lapujoulade and K S Neil, J Chim Phys 70 (1973) 798
[7] K Christmann, O Schober, G Ertl and M Neumann, J Chem Phys 60 (1974) 4528
[8] T L Einstein and J R Schrieffer, Phys Rev B7 (1973) 3629
[9] J W May and L H Germer, in The Structure and Chemistry of Solid Surfaces, Ed G A Somorjai (Wiley, New York, 1969) p 51-2
[10] G C Bond, Catalysis by Metals (Academic Press, London, 1962)
[11] R Stockmeyer, H M Conrad, A Renouprez and P Fouilloux, Surface Sci 49 (1975) 549
[12] G Blyholder, J Chem Phys 62 (1975) 3193
[13] B Lang, R W Joyner and G A Somorjai, Surface Sci 30 (1972) 454
[14] K Baron, D W Blakely and G A Somorjai, Surface Sci 41 (1974) 45
[15] A B Anderson and R Hoffmann J Chem Phys 61 (1974) 4545
[16] L W Anders, R S Hansen and L S Bartell, J Chem Phys 59 (1973) 5277
[17] L W Anders, R S Hansen and L S Bartell, J Chem Phys 62 (1975) 1641

Appendix

MODEL HAMILTONIANS IN
CHEMISORPTION THEORY

The exact non-relativistic Hamiltonian describing a system of N electrons can be written as

$$H(1,\ldots,N) = \sum_{i=1}^{N} f(i) + \tfrac{1}{2} \sum_{i=1}^{N} \sum_{\substack{j=1 \\ j\neq i}}^{N} g(i,j) \tag{A 1}$$

with

$$f(i) = -\frac{\hbar^2}{2m} \nabla_i^2 - \sum_{\alpha} \frac{Z_\alpha e^2}{r_{\alpha i}} \quad,$$

$$g(i,j) = \frac{e^2}{r_{ij}} \quad.$$

In solid-state physics H is usually expressed in second-quantized form [1,2], which we can obtain as follows:

(i) Choose an orthonormal basis of spinorbitals in one-electron space: $\{|\psi_k\rangle, \quad k=1,\ldots,r\}$. The identity operator for electron i reads:

$$I(i) = \sum_{k=1}^{r} |\psi_k(i)\rangle\langle\psi_k(i)| \quad. \tag{A 2}$$

In the N-electron space, which is an N-fold (tensorial) product of one-electron spaces, the identity operator is given by:

$$I_N(1,\ldots,N) = \prod_{i=1}^{N} I(i) \quad. \tag{A 3}$$

(ii) In order to construct an N-electron function corresponding with a given occupation of spinorbitals (electron configuration), we define a creation operator $c_k^\dagger$ generating an electron in $|\psi_k\rangle$:

$$|\psi_k(1)> = c_k^\dagger |\Psi_{vac}>$$

$$|\Psi_{k_1,k_2}(1,2)> = c_{k_1}^\dagger c_{k_2}^\dagger |\Psi_{vac}>$$

$$\vdots$$

$$|\Psi_{k_1,\ldots,k_N}(1,\ldots,N)> = c_{k_1}^\dagger \ldots c_{k_N}^\dagger |\Psi_{vac}> \qquad \text{(A 4)}$$

with $|\Psi_{vac}>$ being the so-called vacuum state, a fictitious "zeroth-order determinant" in which no one-electron state is occupied. If we require the $c_k^\dagger$ to satisfy the anticommutation relations

$$\{c_k^\dagger, c_\ell^\dagger\} = c_k^\dagger c_\ell^\dagger + c_\ell^\dagger c_k^\dagger = 0 \quad , \qquad \text{(A 5a)}$$

we ensure that $|\Psi(1,\ldots,N)>$ is an antisymmetric (Slater determinant) function. We may also introduce the adjoint operator c_k which destroys an electron in $|\psi_k>$ or annihilates $|\Psi(1,\ldots,N)>$ altogether, if this state contains no electron in $|\psi_k>$. Now the following additional anticommutation relations hold:

$$\{c_k, c_\ell\} = 0 \qquad \text{(A 5b)}$$

$$\{c_k^\dagger, c_\ell\} = \delta_{k\ell} \qquad \text{(A 5c)}$$

and the number operator n_k is given by:

$$n_k = c_k^\dagger c_k \quad . \qquad \text{(A 6)}$$

For the one-electron part of the Hamiltonian we find, using the orthonormality of the basis:

$$\sum_{i=1}^{N} f(i) = I_N \left(\sum_{i=1}^{N} f(i) \right) I_N$$

(A 7)

$$= \sum_{k,\ell=1}^{r} \langle \psi_k(1) | f(1) | \psi_\ell(1) \rangle \sum_{i=1}^{N} | \psi_k(1) \rangle \langle \psi_\ell(1) | \quad .$$

Since the operator $\sum_{i=1}^{N} | \psi_k(1) \rangle \langle \psi_\ell(1) |$ acting on an arbitrary N-elec-

tron configuration wave function replaces a one-electron state $| \psi_\ell \rangle$ by $| \psi_k \rangle$, if $| \psi_\ell \rangle$ is occupied, and yields zero otherwise, it can be written in second-quantized form:

$$\sum_{i=1}^{N} | \psi_k(1) \rangle \langle \psi_\ell(1) | = c_k^\dagger c_\ell \quad .$$

(A 8)

Substituting this expression into (A 7) and following an analogous derivation for the two-electron operators, we obtain the N-electron Hamiltonian in second quantization:

$$H(1,\dots,N) = \sum_{k,\ell} \langle \psi_k(1) | f(1) | \psi_\ell(1) \rangle c_k^\dagger c_\ell +$$

(A 9)

$$\frac{1}{2} \sum_{k,\ell,m,n} \langle \psi_k(1) \psi_\ell(2) | g(1,2) | \psi_m(1) \psi_n(2) \rangle c_k^\dagger c_\ell^\dagger c_n c_m \quad .$$

Separating the spinorbitals $| \psi_k \rangle$ into a spatial part $| \phi_k \rangle$ and a spin-function $| \sigma \rangle$ ($= | \alpha \rangle$ or $| \beta \rangle$), we write:

$$H = \sum_{k,\ell} \sum_{\sigma} \langle \phi_k(1) | f(1) | \phi_\ell(1) \rangle c_{k\sigma}^\dagger c_{\ell\sigma} +$$

(A 10)

$$\frac{1}{2} \sum_{k,\ell,m,n} \sum_{\sigma,\sigma'} \langle \phi_k(1) \phi_\ell(2) | g(1,2) | \phi_m(1) \phi_n(2) \rangle c_{k\sigma}^\dagger c_{\ell\sigma'}^\dagger c_{n\sigma'} c_{m\sigma} \quad .$$

1. The Anderson Hamiltonian

In order to study the effects of magnetic impurities, Anderson [3] has introduced an approximate Hamiltonian, which is also used very often to investigate the interaction between an adsorbed atom and a metal substrate. The set $\{\phi_k, \phi_a\}$ is chosen as the orthonormal orbital basis for the total system. The functions ϕ_k are delocalized eigenstates of an effective one-electron Hamiltonian for the unperturbed semi-infinite metal with eigenvalues ε_k; ϕ_a is the localized adatom orbital with energy ε_a. Expressing the Hamiltonian (A 10) in this basis, we find the Anderson Hamiltonian, if the following assumptions are made:

$$<\phi_k(1)|f(1)|\phi_\ell(1)> = \varepsilon_k \, \delta_{k\ell} \quad , \tag{A 11a}$$

$$<\phi_a(1)|f(1)|\phi_a(1)> = \varepsilon_a \quad , \tag{A 11b}$$

with f being the one-electron Hamiltonian after chemisorption. This implies that the effects of chemisorption on ε_k and ε_a are neglected. Furthermore, no electron repulsions are considered, except between two electrons in ϕ_a. So, the Anderson Hamiltonian reads:

$$\begin{aligned}
H^A = & \sum_{k,\sigma} \varepsilon_k \, n_{k\sigma} + \sum_\sigma \varepsilon_a \, n_{a\sigma} + U \, n_{a\sigma} \, n_{a,-\sigma} + \\
& \sum_{k,\sigma} (V_{ak} \, c_{a\sigma}^\dagger \, c_{k\sigma} + V_{ka} \, c_{k\sigma}^\dagger \, c_{a\sigma}) \quad ,
\end{aligned} \tag{A 12}$$

with U and V_{ak} defined as

$$U = <\phi_a(1)\phi_a(2)|g(1,2)|\phi_a(1)\phi_a(2)>$$

$$V_{ak} = <\phi_a(1)|f(1)|\phi_k(1)> \quad .$$

The Hartree-Fock approximation to this Hamiltonian amounts to replacing the two-particle interaction $U \, n_{a,-\sigma} \, n_{a\sigma}$ by the average repulsion term $U <n_{a,-\sigma}> n_{a\sigma}$, which is a one-particle operator:

$$H_{HF}^{A} = (\epsilon_a + U \langle n_{a,-\sigma} \rangle) \, n_{a\sigma} + \sum_{k} \epsilon_k \, n_{k\sigma} +$$

$$\sum_{k} (V_{ak} \, c_{a\sigma}^{\dagger} \, c_{k\sigma} + V_{ka} \, c_{k\sigma}^{\dagger} \, c_{a\sigma}) \quad . \tag{A 13}$$

2. The Hubbard Hamiltonian

This second approximate Hamiltonian has originally been introduced to examine electron repulsion effects in narrow energy bands [4]. The orthonormal basis consists of the atomic orbitals $\phi_p = \phi(\vec{r} - \vec{R}_p)$ localized on the various sites in the crystal. Electron repulsions are only taken into account for both electrons occupying the same atomic orbital, so that the Hamiltonian reads:

$$H^{H} = \sum_{p,q} \sum_{\sigma} T_{pq} \, c_{p\sigma}^{\dagger} \, c_{q\sigma} + \tfrac{1}{2} I \sum_{p,\sigma} n_{p\sigma} \, n_{p,-\sigma} \tag{A 14}$$

with

$$T_{pq} = \langle \phi_p(1) | f(1) | \phi_q(1) \rangle$$

$$I = \langle \phi_p(1) \phi_p(2) | g(1,2) | \phi_p(1) \phi_p(2) \rangle \quad .$$

In the Hartree-Fock approximation:

$$H_{HF}^{H} = \sum_{p,q} T_{pq} \, c_{p\sigma}^{\dagger} \, c_{q\sigma} + I \sum_{p} n_{p\sigma} \langle n_{p,-\sigma} \rangle \quad . \tag{A 15}$$

In order to study adsorption, the Hamiltonian (A 14) must be extended by the extra terms:

$$\sum_{\sigma} \epsilon_a \, n_{a\sigma} + \tfrac{1}{2} U \sum_{\sigma} n_{a\sigma} \, n_{a,-\sigma} +$$

$$\sum_{p,\sigma} (V_{ap} \, c_{a\sigma}^{\dagger} \, c_{p\sigma} + V_{pa} \, c_{p\sigma}^{\dagger} \, c_{a\sigma}) \quad . \tag{A 16}$$

158

References

[1] S. Raimes, *Many-electron Theory* (North-Holland, Amsterdam, 1972).

[2] T.D. Schultz, *Quantum Field Theory and the Many-body Problem* (Gordon and Breach, New York, 1964).

[3] P.W. Anderson, Phys. Rev. $\underline{124}$, 41 (1961).

[4] J. Hubbard, Proc. R. Soc. Lond. A $\underline{276}$, 238 (1963).

SUMMARY

This thesis deals with a theoretical investigation of the
electronic properties of solid surfaces and the phenomena involved in
chemisorption. We have paid particular attention to the adsorption of
(atomic) hydrogen on various surfaces of nickel and copper crystals.
Our intention was to obtain a better understanding of the chemisorption
binding with transition metals and to explain the variations in the
activity of different sites on the surface in the hope of getting more
insight in the processes which occur in heterogeneous catalysis.

We have started (Chapter II) with a review of the recent
theoretical developments. It is shown how the surface and chemisorption
problem is being tackled both by solid-state physicists and by quantum-
chemists. The merits, restrictions, applicability and mutual relation-
ship of the various methods are discussed, as well as a few important
concepts in chemisorption theory (virtual and split-off states, in-
direct interaction between adsorbed particles). In Chapter III we have
described a numerical resolvent procedure suitable to study realistic
models for transition metals and semiconductors by accounting for the
existence of multiple bands. Finite periodic layer crystals are con-
sidered, which may be conceived as an intermediate case between the
semi-infinite crystal models used in solid-state techniques and the
cluster models originating from the molecular approach. The results of
our Extended Hückel molecular orbital calculations on the adsorption
of hydrogen monolayers on finite periodic nickel crystals and of single
hydrogen atoms on nickel or copper clusters have been presented in
Chapter IV. We were able to draw conclusions about the rôle of d- and
conduction electrons in the adsorption bonding and the dissociative
chemisorption on transition-metal surfaces. Since Chapter III and
Chapter IV (mainly) consist of reprinted articles, we refer to the
respective summaries for further concise information about our resolvent
technique, about the systems investigated and the computational results.

Dit proefschrift handelt over een theoretisch onderzoek naar de elektronische eigenschappen van vaste stof oppervlakken en de verschijnselen die optreden bij chemisorptie. In het bijzonder hebben we aandacht besteed aan de adsorptie van (atomaire) waterstof op verschillende oppervlakken van nikkel en koper kristallen. Hierbij was het de bedoeling om het mechanisme van de chemisorptiebinding met overgangsmetalen beter te begrijpen en om de variaties te verklaren in de aktiviteit van de verschillende oppervlakken, hetgeen kan leiden tot een beter inzicht in de processen die plaatsvinden bij heterogene katalyse.

We zijn begonnen (Hoofdstuk II) met een overzicht van de recente theoretische ontwikkelingen. We laten zien hoe het oppervlakte- en chemisorptievraagstuk zowel door vaste stof fysici als door kwantumchemici wordt aangepakt. De verdiensten, beperkingen, toepasbaarheid en het onderlinge verband van de verschillende methodes worden besproken, evenals enkele belangrijke begrippen uit de chemisorptietheorie (virtuele en uit de energieband afgescheiden toestanden, indirekte wisselwerking tussen geadsorbeerde deeltjes). In Hoofdstuk III hebben we een numerieke resolvent procedure beschreven welke geschikt is om realistische modellen voor overgangsmetalen en halfgeleiders te bestuderen, doordat rekening wordt gehouden met het voorkomen van meervoudige banden. Hierbij worden eindige periodieke laagkristallen bekeken, die kunnen worden opgevat als een overgangsgeval tussen de halfoneindige kristalmodellen in de vaste stof technieken en de klustermodellen afkomstig uit de molekulaire aanpak. De resultaten van onze Extended Hückel molecular orbital berekeningen aan de adsorptie van enkelvoudige waterstoflagen op eindige periodieke nikkel kristallen en van geïsoleerde waterstofatomen op nikkel of koper klusters zijn gepresenteerd in Hoofdstuk IV. We waren in staat om konklusies te trekken aangaande de rol van d- en geleidingselektronen in de adsorptiebinding en de dissociatieve chemisorptie op overgangsmetaal-

oppervlakken. Omdat Hoofdstuk III en Hoofdstuk IV (voornamelijk) be-
staan uit reeds gepubliceerde artikelen, verwijzen we naar de res-
pektievelijke samenvattingen voor verdere beknopte informatie over
onze resolvent techniek, de onderzochte systemen en de rekenresul-
taten.

DANKBETUIGING

CURRICULUM VITAE

De schrijver van dit proefschrift werd op 3 september 1946 te Nijmegen geboren. Na het doorlopen van het gymnasium-β aan het Canisius College aldaar, begon hij in september 1964 met zijn scheikundestudie aan de Katholieke Universiteit. In februari 1970 studeerde hij cum laude af met als hoofdvak fysische chemie en als bijvakken capita uit de wiskunde en uit de natuurkunde. Sindsdien is hij als wetenschappelijk medewerker verbonden aan het Instituut voor Theoretische Chemie van de K.U. Nijmegen.

STELLINGEN

I

De verklaring van Kunz et al voor het verschillende katalytische gedrag van nikkel en koper bij "supported catalysts" en de manier waarop de trend in de aktiviteit van de metalen uit de tweede overgangsreeks hieruit wordt afgeleid, zijn aanvechtbaar

A B Kunz, M P Guse and R J Blint, Chem Phys Lett 37, 512 (1976)

II

De verwachting dat een sterk geparametriseerde semi-empirische methode als MINDO/3 kan dienen als een praktisch chemisch instrument op terreinen die (momenteel) ontoegankelijk zijn voor eksperimenteel onderzoek, is illusoir

R C Bingham, M J S Dewar and D H Lo, J Am Chem Soc 97, 1285 (1975)

III

Brush maakt zijn bewering dat de golftheorie van de warmte van belang is geweest voor de ontdekking van "de wet van behoud van energie", onvoldoende waar

S G Brush, The British Journal for the History of Science 5, 145 (1970)

IV

Ons kennisverwerven van de natuur geschiedt niet objektief, omdat het wordt bemiddeld door een waarnemend subjekt De praktische aktiviteit van het met de natuur in wisselwerking tredende subjekt vindt niet onafhankelijk van de maatschappelijke kontekst plaats Hierdoor is de natuurwetenschap niet waardevrij, maar bezit zij een ideologische komponent, die onder meer tot uiting komt in haar keuze van te verzamelen feiten, uit te voeren eksperimenten en theoretische interpretatiekaders

V

Binnen de natuurwetenschappelijke opleiding behoort een permanente re-
flektie plaats te vinden over de relatie tussen natuurwetenschap en maat
schappij Zonodig dienen praktische konsekwenties hieruit getrokken te
worden, zowel wat betreft inhoud en organisatie van de opleiding en het
wetenschappelijk onderzoek als wat betreft het maatschappelijk handelen
Centrale doelstelling hierbij moet zijn de bevrijding van uitbuiting en onder-
drukking en een toenemende beheersing van de natuur ten behoeve van en
door de mensheid in haar totaliteit

VI

Vanwege de samenhang die bestaat tussen milieuproblematiek en maat-
schappelijke struktuur, moet de aan de fakulteit W & N in Nijmegen op te
richten afdeling milieukunde uitgaan van een projektgewijze en interdisci-
plinaire aanpak Dit betekent dat zowel de natuurwetenschappelijke als
maatschappelijke aspekten   geïntegreerd   aan bod dienen te komen Bo-
vendien moet een dergelijke afdeling een ondersteuning vormen voor de
praktische aktiviteiten van milieu-aktiegroepen

VII

De visie dat de wetenschap van nature progressief is en daarom een natuur-
lijke bondgenoot vormt in de strijd voor het socialisme, gaat uit van een zich
autonoom ontwikkelende wetenschap, aldus de wisselwerking tussen weten-
schap en maatschappelijke verhoudingen veronachtzamend Verder hangt
deze visie samen met een objektivering in het marxisme, waarbij de dialek
tiek van een bewust en aktief in de maatschappelijke werkelijkheid ingrij-
pende mens vervangen is door een interpretatie van de wereld als een vanzelf
volgens objektieve wetten veranderende wereld

VIII

Wanneer Fisher de energiekrisis in de V S aan het begin van de zeventiger
jaren in belangrijke mate wijt aan de milieubeweging, gaat hij eraan voorbij
dat zowel energiekrisis als milieuproblematiek hun oorzaak vinden in de
wijze waarop in een kapitalistische maatschappij de produktie georganiseerd
is

J C Fisher, Physics Today december 1973 blz 40

Het feit dat Van den Doel zijn inaugurale rede voorziet van een citaat uit Engels' *Der Ursprung der Familie, des Privateigentums und des Staats* dat uit zijn verband is gerukt en verkeerd is weergegeven, wijst op een gebrek aan inzicht in het marxisme, waarvan Van den Doel een groot kenner beweert te zijn, ofwel er is sprake van citaatvervalsing

> F Engels *Der Ursprung der Familie, des Privateigentums und des Staats* (Duitse uitgave Dietz, Berlin, 1973 blz 198/199, Nederland-se uitgave Pegasus Amsterdam, 1973, blz 217)
> J van den Doel, *Ekonomie en demokratie in het staatsbestuur* (Kluwer Deventer, 1973 blz 3)
> Vrij Nederland, 30 augustus 1975, blz 9

De "Berufsverbote" in de BRD, welke een fundamentele aantasting vormen van de demokratische rechtsorde, zijn uitdrukking van een toenemende politieke onderdrukking Wanneer de ekonomische krisis blijft voortduren en er een verscherping van de maatschappelijke tegenstellingen plaatsvindt, kan deze repressie gemakkelijk de wegbereider worden voor een hernieuwd fascisme, doordat zij potentieel verzet daartegen van zijn basis heeft beroofd

Nijmegen, 13 mei 1976   D J M Fassaert